Interdisciplinary Studies on Contemporary Research Practices in Engineering- VII

Editor: Assist. Prof. Dr. Murat Metehan TÜRKOĞLU

ÖZGÜR PRESS

Interdisciplinary Studies on Contemporary Research Practices in Engineering- VII

Editör:

Assist. Prof. Dr. Murat Metehan TÜRKOĞLU

ÖZGÜR PRESS

Published by
Özgür Yayın-Dağıtım Co. Ltd.
Certificate Number: 45503

15 Temmuz Mah. 148136. Sk. No: 9 Şehitkamil/Gaziantep
+90.850 260 09 97
+90.532 289 82 15
www.ozguryayınlari.com
info@ozguryayinlari.com

Interdisciplinary Studies on Contemporary Research Practices in Engineering- VII

Editor: Assist. Prof. Dr. Murat Metehan TÜRKOĞLU

Language: Turkish-English
Publication Date: 2024
Cover design by Mehmet Çakır
Cover design and image licensed under CC BY-NC 4.0
Print and digital versions typeset by Çizgi Medya Co. Ltd.

ISBN (PDF): 978-625-95529-3-4

DOI: https://doi.org/10.58830/ozgur.pub575

Suggested citation:
Türkoğlu, M. M. (ed) (2024). *Interdisciplinary Studies on Contemporary Research Practices in Engineering- VII.* Özgür Publications. DOI: https://doi.org/10.58830/ozgur.pub575. License: CC-BY-NC 4.0

The full text of this book has been peer-reviewed to ensure high academic standards. For full review policies, see https://www.ozguryayinlari.com/

Preface

This book focuses on both theoretical and experimental studies regarding the research and development of materials used in industries that are highly dependent on technological input (such as aerospace, automotive, construction, medicine, security, and energy), including composite materials, carbon nanotubes-boron nanotubes, Al-Cu-Si, and Al-5Cu-5Si-5Mg-5Zn-1Zr alloys. At the same time, it conceptually examines the impact of artificial intelligence on complex operational processes such as evaluation, autonomous navigation, environmental sensing, data analysis, and decision-making, not only in these industries but also in security/military applications (e.g., UAVs).

Önsöz

Bu kitap, bir yandan teknolojik girdiye son derece bağımlı endüstrilerde (havacılık, otomotiv, inşaat, tıp, güvenlik ve enerji gibi) kullanılan malzemelerin (kompozit malzemeler, karbon nanotüpler-Bor nanotüpler, Al-Cu-Si ve Al-5Cu-5Si-5Mg-5Zn-1Zr tipli alaşımlar) araştırılması ve geliştirilmesine dair teorik ve deneysel çalışmalara bir yandan da yapay zekanın, bu tür endüstrilere ek olarak güvenlik/askeri uygulamalarda (İHA) karmaşık operasyonel süreçlerin değerlendirilmesi, otonom navigasyon, çevresel algılama, veri analizi ve karar alma gibi süreçlere olan etkisini kavramsal düzeyde inceleyen çalışmalara odaklanmıştır.

Contents

Chapter 1

Explainable Artificial Intelligence Methods Applied to Unmanned Aerial Vehicles: A Conceptual Framework

Mustafa Meliksah Ozmen[1]

Bekir Aksoy[2]

Abstract

The study examined the use of explainable artificial intelligence (XAI) methods for unmanned aerial vehicles (UAVs). The aim of the study is to make the artificial intelligence decision processes in the autonomous systems of UAVs more understandable and transparent. This requirement has gained importance as UAVs are used in increasingly complex tasks. In order to increase the reliability of UAVs especially in areas such as security, military operations and agriculture, and to reinforce users' trust in these systems, the integration of XAI methods has become critical.

In the study, both model-based and post-hoc explanation methods were used. Model-based methods such as decision trees and explainable neural networks were preferred to ensure transparency of UAVs' decision-making processes. Post-hoc methods such as Local Intrepretable Model - Adnogtics Explanations (LIME) and SHapley Additive Explanations (SHAP) were used to increase the explainability of deep learning models . In the study, these techniques were evaluated to understand why UAVs make certain decisions in their complex operational processes.

As a result of the study, it was observed that the integration of Explainable Artificial Intelligence (XAI) methods into UAV systems made decision processes more transparent and thus increased the reliability of UAVs. It was emphasized that this transparency, especially in terms of public safety and ethical practices, plays a critical role in expanding the use of UAVs and making them safer.

1 PhD, Isparta University of Applied Sciences, cadet.2045@gmail.com Isparta, 0000-0003-3585-0518

2 Associate Professor, Isparta University of Applied Sciences, bekiraksoy@isparta.edu.tr Isparta, 0000-0001-8052-9411

https://doi.org/10.58830/ozgur.pub575.c2358

1. INTRODUCTION

With the rapid development of technology today, the use of Unmanned Aerial Vehicles (UAVs) has become widespread. UAVs are frequently used in many important areas such as facilitating social life and performing tasks that are harmful to human health. One of the most important advantages of UAVs is their high success rates in performing tasks. These success rates also minimize possible human-related errors.

UAVs in the realized book section A conceptual framework study based on academic literature has been carried out on the use of Artificial Intelligence (AI) technologies, which are one of the frequently used technologies together with AI technologies. The structure of the study has been examined by considering the general usage areas and importance of UAVs, AI and UAVs, Explainable artificial intelligence (XAI) structure, and the use of XAI in UAVs in the introduction section. The second section , XAI methods and algorithms, has been discussed under two main headings as model-based and post-hoc based methods. Under the title of model-based method, decision trees and explainable neural network models have been examined. In post-hoc based methods, LIME, SHAP models were discussed in detail . In the third part of the study, academic literature-based reviews of UAVs' XAI applications were conducted. In the final stage, the results of the study were discussed in detail.

1.1. General Areas of Use and Importance of Unmanned Aerial Vehicles (UAVs)

With the advancement of technology, the use of UAVs has also begun to be used frequently in social life. UAVs are frequently used especially in military and civilian life. (Thiels et al., 2015). It is possible to define UAVs as vehicles that can be remotely controlled and have the ability to perform autonomous flight. In addition to their high maneuverability due to their small size, their low cost makes the use of UAVs more widespread and effective (Shadiev & Yi , 2023).

of UAVs is in military areas. UAVs have successfully performed many tasks such as reconnaissance, surveillance, intelligence gathering and attack in military operations. In particular, UAVs are of great importance in terms of reducing loss of life and cost effectiveness since they do not require a pilot (Santos et al., 2023).

UAVs have a wide range of applications in civilian areas, from agriculture to mapping and environmental monitoring. (Muhmad Kamarulzaman et al., 2023). It has been determined that UAVs used in the agricultural sector

provide great efficiency in areas such as crop monitoring, spraying and water management and reduce the workload of farmers (Istiak et al., 2023). In addition, the use of UAVs in environmental monitoring and natural disaster management allows for fast and effective interventions. The rapid data collection capacity of UAVs in disasters such as forest fires and floods has great advantages in many points such as the importance of saving human lives (Devoto et al., 2020). Another area of use of UAVs is cargo transportation and logistics. One of the important advantages of UAVs is that they provide fast delivery services, especially in regions where road transportation is difficult, and are used in vital tasks such as the transportation of emergency medical supplies (Çorbacı & Doğan, 2023). As can be understood from the examples given above, it is an inevitable fact that UAVs are an important technological tool not only for military operations but also in all areas of civilian life.

As a result, the advantages offered by UAV technologies in a wide range increase the strategic importance of UAVs day by day. The economic and operational efficiency provided by UAVs in both military and civilian applications causes this technology to become widespread at the global level.

1.2. Artificial Intelligence and UAVs

AI is a branch of science and technology that creates the characteristics and abilities of human intelligence through computer programs (PK, 1984). AI enables machines to perform human-like tasks by modeling the complex functions of the human mind, such as learning, reasoning, problem solving, and language understanding.

UAVs have evolved significantly in recent years thanks to the integration of AI technologies. Its application to UAVs has increased the ability of these vehicles to move autonomously, perceive their environment and adapt to dynamic conditions. This integration has allowed UAVs to perform more complex and sensitive missions in military, civil and commercial areas (Thiels et al., 2015).

AI's One of the most obvious examples of its use in UAVs is autonomous navigation. While traditional UAV systems are dependent on pre-programmed routes, AI-supported UAVs can avoid obstacles and reach their targets in the most effective way by performing real-time data analysis (Talwandi et al., 2024). For example, image processing systems developed using deep learning algorithms can It helps them perceive their environment better and respond quickly to sudden changes (Pandey et al., 2024).

Additionally, AI-based object recognition and tracking systems allow UAVs to detect specific objects or people in search and rescue operations or security applications (Devoto et al., 2020). This offers great advantages, especially in critical missions such as finding missing persons in natural disasters or ensuring border security.

Swarm technology is also used in AI It is another important area of use in UAVs . Due to AI algorithms, multiple UAVs can act in a coordinated manner without a central control mechanism (Campion et al., 2018). This technology enables fast and effective scanning of large areas or large-scale data collection.

AI technologies with UAVs has significantly expanded the capabilities and application areas of these vehicles. AI-supported UAVs are shaping the technological developments of the future by offering innovative solutions in many areas, from agriculture to logistics, from security to environmental monitoring.

1.3. What is Explainable Artificial Intelligence (XAI)?

XAI refers to a set of methods and techniques designed to make the decision-making processes of AI systems transparent and understandable to humans (Adadi & Berrada , 2018). Unlike traditional "black box" models that offer little insight into how inputs are transformed into outputs, XAI provides clear explanations of how and why an AI system reached a particular decision. The importance of XAI lies in its ability to build trust between users and AI systems, facilitate compliance with regulatory standards that require accountability, and enable the identification and reduction of biases within models (Gunning et al., 2019). By making AI models interpretable, XAI improves ethical decision-making and supports the responsible deployment of AI technologies in critical areas such as healthcare, finance, and autonomous vehicles (Doshi-Velez & Kim, 2017).

1.4. XAI's Importance and Necessity of Use in UAVs

XAI has become increasingly critical in the development and deployment of UAVs as these systems grow in complexity and autonomy. UAVs , commonly known as drones , have advanced significantly through the integration of AI, particularly in the areas of autonomous navigation, surveillance, and data analysis (Floreano & Wood , 2015). However, the complexity of AI algorithms often causes them to operate as "black boxes," where decision-making processes are not transparent or easily understood

(Lipton, 2018). This lack of transparency raises concerns about safety, ethical concerns, and trust among users and regulators.

XAI's Integrating into UAVs addresses these challenges by making AI systems more transparent and interpretable (Keneni, 2018). By providing clear explanations of how AI systems reach certain decisions, XAI increases the reliability and safety of UAV operations. This transparency is essential for operators and stakeholders to trust the actions of UAVs , especially in applications involving public safety and security (Adadi & Berrada , 2018).

Safety is a top concern in UAV operations; failures or errors can lead to property damage or loss of life. XAI facilitates the detection of potential errors and biases in AI algorithms, contributing to the development of more robust and reliable UAV systems (Keneni, 2018). By making decision-making processes transparent, engineers can more effectively diagnose errors and quickly implement corrective measures. This capability is especially important in complex environments where UAVs must make instantaneous decisions based on real-time data.

Incorporating explainable AI into UAVs is both important and necessary for the safe, ethical, and effective deployment of these technologies. XAI increases transparency, security, and compliance with regulatory and ethical standards—critical factors for the continued growth and acceptance of UAV applications. By making AI systems in UAVs understandable, we not only improve their functionality, but also build the trust necessary for their integration into various aspects of society.

2. EXPLAINABLE ARTIFICIAL INTELLIGENCE METHODS AND ALGORITHMS

Internet technology and the ability to make sense of the large data sets that increase due to internet technology have been one of the main factors in the rapid development of AI technologies. However, investigating the reasons for the results obtained from AI training has also been a phenomenon that has developed together with AI technologies. For this reason, the concept of XAI has emerged as the meaning of the results obtained from AI training. XAI is a field of research that aims to make the internal workings and decision-making processes of machine learning models understandable to humans (Gunning , 2017).

The history of explainable AI has followed a parallel course with the general developments in the field of AI. Since the first AI systems were built on symbolic structures and rule-based models, the decision-making processes of the models could be easily understood by humans (Russell &

Norvig , 2010). Since the internal workings and logic of the systems were transparent in this period, explainability became a natural feature. However, in the late 1990s and early 2000s, rapid developments in machine learning and especially deep learning significantly increased the complexity of AI models (LeCun , Bengio & Hinton , 2015). These models, which showed high performance on large data sets, became "black boxes" whose internal structures and decision-making mechanisms were difficult to understand by humans . This has raised concerns about the reliability and accountability of models. Traditional "black box" models, despite their high performance, have made it difficult to understand the logic behind their decisions due to the complexity they contain (LeCun , Bengio , & Hinton , 2015). This leads to reliability and accountability problems in many fields, especially in medicine, finance, and law. Therefore, explainable AI addresses these problems by explaining how and why the predictions obtained with models reach certain results and can be considered to provide transparency for AI technology (Ribbon , Singh, & Guestrin , 2016). Explainability is an ethical and legal obligation, beyond a technical requirement. The European Union's General Data Protection Regulation (GDPR) emphasizes the importance of explainability in automated decision-making processes (Wachter , Mittelstadt , & Floridi , 2017). In this context, explainable AI aims to prevent possible risks and misunderstandings while increasing the social acceptance of AI systems. For this purpose, the US Defense Advanced Research Projects Agency (DARPA) first initiated the XAI program in 2016 to encourage research in this field (Gunning , 2017). The program aimed for AI systems to both demonstrate high performance and ensure that their decisions were understandable by humans. The decisions of AI systems can profoundly affect the lives of individuals. For this reason, explainability is considered an ethical imperative, beyond being a technical need. For example, in medical diagnostic systems, the explainability of decisions ensures that doctors and patients trust these decisions (Doshi-Velez & Kim, 2017). Similarly, explainability is of critical importance in financial decision support tools in terms of detecting and correcting errors.

2.1. Model-Based Methods

In the field of XAI, model-based methods involve using models that are directly understandable and interpretable. Since these models are transparent in nature, decision-making processes can be easily followed by humans. Examples of model-based methods include models such as decision trees and explainable neural networks (Molnar , 2019). The advantage of model-based methods is that they integrate explainability into the design of the

model. However, when working with complex data or high-dimensional data sets, their performance may be lower than that of deep learning models, so in some cases a balance may need to be established between explainability and performance (Rudin , 2019).

2.1.1. Decision Trees

Decision trees are models that are frequently used in the field of AI and machine learning and are naturally explainable due to their internal structures. These models perform classification or regression tasks by branching the data according to certain features (Quinlan , 1986). The explainability of decision trees stems from the fact that their structures are easily understandable by humans; each node and branch explains the logic behind the decisions taken by the model (Hastie , Tibshirani , & Friedman, 2009). Since decision trees are an internally interpretable model, they can be considered a model-based model (Molnar , 2019). In these models, since the decision processes and the features used are clearly visible, it is understandable why the model reached a certain conclusion (Breiman , Friedman, Olshen , & Stone, 1984). For example, a decision tree model can use features such as income level, credit score, and existing debts to approve a customer's loan application, and the effect of each of these features on the decision can be read directly from the structure of the tree (Rokach & Maimon , 2005).

Decision trees are frequently preferred in applications requiring explainability in health, finance, marketing and many other areas (Witten , Frank, Hall & Pal, 2016). Especially in sectors where ethical and legal regulations are important, it is critical that the models are transparent and the justifications for the decisions are understandable (Murthy , 1998). The advantages of decision trees are listed below.

- Easy Understandability: Decision trees can be understood even by non-experts thanks to their visually representable structures (Quinlan , 1986).
- Feature Selection: It can be easily seen from the structure of the tree which features the model attaches more importance to (Breiman , Friedman, Olshen & Stone, 1984).
- Fast Computation: Decision trees can generally be trained and predicted quickly, making them practical when working with large data sets (Witten , Frank, Hall & Pal, 2016).

In addition to the advantages mentioned above, decision trees also have some limitations. In particular, the overfitting problem can cause the model to adapt too much to the data it was trained on and to perform poorly on new data (Rudin , 2019). Pruning techniques are used to reduce this problem (Hastie , Tibshirani & Friedman, 2009). In addition, decision trees can have performance problems in complex data structures and high-dimensional data sets (Murthy , 1998).

To overcome these limitations, ensemble methods such as Random Forests and Gradient Boosting Trees have been developed (Rokach & Maimon , 2005). These methods offer higher accuracy and generalization ability by combining multiple decision trees. However, the explainability of these ensemble models is lower than a single decision tree (Molnar , 2019). In this case, it may be necessary to use additional techniques and tools for explainability (Breiman , Friedman, Olshen , & Stone, 1984).

2.1.2. Explainable Neural Networks

Explainable neural networks are approaches that prioritize explainability when designing the structure of the model and the learning process (Zhang & Zhu, 2018). These models aim to present decision-making processes and the information they represent internally in a human-understandable form. Some approaches aim to increase explainability by simplifying the architecture of neural networks or by imposing certain restrictions. For example, linear functions are used as activation functions in Linear Neural Networks to make the behavior of the model more understandable (Kawaguchi , 2016). In model-based methods, certain layers or activation functions of neural networks can be designed with explainability in mind. For example, ReLU (Rectified Linear Unit) activation function can be used instead of more explainable activation functions (Maas , Hannun & Ng, 2013). In addition, the explainability of the model is increased by showing which features it focuses on with attention mechanisms (Bahdanau , Cho & Bengio , 2015). Embedded explanation layers can be added to make the information in the neural networks more understandable. These layers ensure that the intermediate outputs of the model are interpretable by humans (Alain & Bengio , 2017). Prototype-based neural networks provide justifications for their decisions using prototype examples for each class while classifying (Li , Liu , Chen & Rudin , 2018). Explainable neural networks are frequently used in important fields such as medicine and autonomous driving. In the field of medical image analysis, explaining why neural networks make a certain diagnosis allows doctors to trust these decisions (Esteva et al., 2017). Similarly, in autonomous vehicles,

the explainability of decisions is very important in terms of safety and legal responsibilities (Kim & Canny , 2017). Explainable neural networks provide reliability and accountability by making the internal workings of the models more understandable (Montavon , Samek & Müller, 2018). However, while increasing explainability, the performance of the model may be compromised (Chen et al., 2019). Therefore, establishing a balance between explainability and performance is also very important.

2.2. Post-Hoc Methods

Post-hoc methods are one of the important techniques used in the field of XAI to explain the decisions and predictions of complex and often difficult-to-understand models (e.g. deep neural networks). These methods are applied after the model has been trained and aim to understand its outputs and decision processes without changing the internal structure of the model (Lipton, 2016).

Modern machine learning methods, and especially deep learning-based approaches, are characterized as "black boxes" due to their inherent complexity, even though they achieve successful results with high accuracy rates (Guidotti et al., 2018). This reduces the confidence in the results obtained from the models and can lead to critical problems, especially in fields such as medicine, finance and law (Doshi-Velez & Kim, 2017). Post-hoc methods increase the reliability and accountability feature by making the decisions of complex models more understandable (Samek , Wiegand & Müller, 2017).

The biggest advantage of post-hoc methods is that they help understand the decisions of high-performance but unexplainable models (Guidotti et al., 2018). Since these methods can be applied without changing the internal structure of the model, they can be used on existing models without any additional effort (Alvarez -Melis & Jaakkola , 2018). However, post-hoc explanations may not always fully reflect the real decision processes of the model and can sometimes be misleading (Rudin , 2019). Therefore, these explanations should be interpreted carefully. The LIME and SHAP methods, which are frequently used post-hoc methods, are discussed in detail below.

2.2.1. LIME (Local Interpretable Model - Agnostic Explanations)

As the complexity of AI and machine learning models increases, it becomes increasingly difficult to understand the decision-making processes of the models (Samek , Wiegand , & Müller, 2017). In particular, the "black box" nature of deep learning models makes it difficult for users and developers

to understand how XAI models work and why they make certain decisions (Adadi & Berrada , 2018). In this context, the field of XAI has emerged as a research area that aims to make the inner workings and decision-making mechanisms of AI models compatible with human understanding (Gilpin et al., 2018).

LIME method is a prominent technique in the XAI field that can produce local explanations independent of the model (Molnar , 2019). First developed by Ribeiro et al. in 2016, LIME aims to explain the individual predictions of any machine learning model using a simple and understandable model (Ribeiro , Singh & Guestrin , 2016). This method is an effective tool for interpreting the decisions of especially complex and difficult-to-understand models.

of LIME starts by creating synthetic data samples around the data point of interest (Garreau & Luxburg , 2020). These synthetic samples are data that are similar to the original data point but show variations in certain features. The black-box model makes predictions on these synthetic data and is trained with a simple model such as linear regression to examine the relationship between these predictions and the synthetic data (Lundberg & Lee, 2017). Thus, the trained simple model approximately represents the behavior of the black-box model locally and determines the extent to which the decision is affected by which features (Arras et al., 2017).

One of the most important advantages of LIME is that it is model-agnostic (Guidotti et al., 2018). This means that LIME can be used with any machine learning model. Therefore, it is effectively used in explaining AI models such as deep neural networks, random forests or support vector machines (Ribbon , Singh & Guestrin , 2018).

LIME, which has a wide range of applications, has been successfully applied in different areas such as text classification (Hendricks et al., 2016), image recognition (Selvaraju et al., 2017), medical diagnosis (Tjoa & Guan , 2020) and financial forecasting (Chen et al., 2018). For example, in the field of medical diagnosis, LIME can be used to understand how a model reveals a certain diagnosis, and thus doctors can better evaluate the model's decisions (Holzinger et al., 2019). Similarly, in financial forecasting models, risk assessment can be made more transparent with LIME (Bussmann et al., 2020).

The explainability of AI models (Miller, 2019). It plays an important role in complying with ethical, legal and practical requirements by making the decisions of the models more understandable and increasing the trust of

users in these models (Barredo In the future, with the further development of LIME and similar methods, it is expected that AI applications will become more transparent and accountable (Gunning & Aha, 2019).

2.2.2. Shapley Additive exPlanations

Another important method in the field of XAI is SHAP method (Lundberg & Lee, 2017). First proposed by Lundberg and Lee in 2017, this method aims to calculate the contribution of each feature to the model's prediction in a fair and consistent way (Lundberg & Lee, 2017). The working principle of SHAP is based on the Shapley values used in cooperative game theory [51,52]. The Shapley value is used to fairly determine the marginal contribution of each player to the total gain in a game (Roth, 1988). SHAP adapts this concept to AI models and calculates the contribution of each feature to the model (Štrumbelj & Kononenko, 2014). In this way, it can be understood to what extent which features are effective in the decision-making process of the model (Sundararajan & Najmi , 2019).

SHAP method is used to determine the marginal contribution of each feature to the model's prediction by considering all possible feature combinations (Janzing, Minorics & Bloebaum, 2020). However, in practice, since computing all combinations is computationally costly, SHAP calculations are performed with different approximation methods (Chen et al., 2018). In particular, its variants such as Kernel SHAP and Tree SHAP optimize the calculations for different model types (Lundberg, Erion & Lee, 2020).

SHAP is that it can provide both local and global explanations (Kumar et al., 2020). While local explanations show the contribution of features to the model for a single data point, global explanations reveal the behavior and trends of the model in general (Lundberg & Lee, 2017). In addition, the mathematical foundations of SHAP ensure the consistency and fairness of the explanations (Sundararajan, Taly, & Yan, 2017). The SHAP method has been applied in different disciplines such as medicine (Lundberg et al., 2018), finance (Bussmann et al., 2020), energy (Dong et al., 2019), and social sciences (Štrumbelj & Kononenko, 2014). For example, in medical diagnostic models, SHAP can identify the factors that contribute most to disease risk, which helps in the development of clinical decision support systems (Tonekaboni et al., 2019). In financial models, which factors are more effective in credit risk assessments can be analyzed with SHAP (Chen et al., 2018).

In conclusion, the SHAP method is a powerful and flexible tool for improving the explainability of AI models (Gunning & Aha, 2019). It increases the transparency and reliability of models by calculating the contribution of features to the model in a fair and consistent manner (Miller, 2019). In the future, with the further development of SHAP and similar methods, it is expected that AI applications will better comply with ethical and legal requirements (Barredo (Arrieta et al., 2020).

3. LITERATURE REVIEW: STUDIES ON THE USE OF XAI IN UAVS

In the study titled "Assuring Safe and Efficient Operation of UAV Using Explainable Machine Learning" by Alharbi et al. (2023), a demand and capacity management system based on explainable machine learning was developed to ensure the safe and efficient operation of UAVs. In the study, a model was created to predict airspace capacity and determine congestion levels to enable UAVs to operate safely in the airspace. The model aimed to balance performance and explainability by combining deep learning techniques with fuzzy rule-based systems. The system helps UAVs choose the most optimal routes by analyzing air traffic. As a result of testing the developed system in a simulation environment, an increase of over 23% in airspace availability was observed. Additionally, the system's maximum capacity increase was identified as 65%, while the minimum safety gain was found to be 35%. The system's 70% explainability aids UTM (Unmanned Traffic Management) authorities in making more effective decisions (Alharbi , Petrunin & Panagiotakopoulos , 2023)

In the study by Ekramul Haque and colleagues, a solution was proposed using Zero Trust Architecture (ZTA) and Deep Learning (DL) methods to enhance UAV security. The study aimed to detect and classify UAVs using radio frequency signals. Moreover, the model's transparency and explainability were ensured using XAI tools such as SHAP and LIME. The method achieved an accuracy rate of 84.59% using RF signals. As a result, it was demonstrated that ZTA could enhance UAV security, and the integration of DL and XAI provided both security and explainability (Haque et al., 2024).

In the study by Goyal et al. (2024), an XAI-based security solution was developed to enhance the security of 5G-supported UAV networks. In the study, network traffic was monitored and analyzed using XAI to detect nodes attacking UAV networks. The research results showed that the proposed method detected attacking nodes with an accuracy rate of 98.4%.

The method performed better compared to AI/DL-based methods. The results provide a reliable security solution to enhance data transfer security in 5G-based UAV networks (Goyal et al., 2024).

In the study by Zhu et al. (2024), an XAI-based edge computing framework was developed to monitor the safety of UAVs during air surveillance in extreme conditions and to process large-scale image data. In the study, an alert system was designed using the random forest algorithm to monitor drone health and identify security concerns, and a MapReduce-based image processing module was proposed for large-scale image classification and object detection. The research increased the transparency of traditional AI systems using SHAP and provided an effective mechanism for monitoring the operational safety of drones. Experimental results show that the model achieved high accuracy (99.21%) in drone health monitoring and object detection (Zhu et al., 2024).

In the study by Javeed et al. (2024), an Intrusion Detection System (IDS) for UAVs was developed. The system was designed using advanced deep learning techniques to defend UAVs against cyber threats. The method employed the Hierarchical Attention-based Long Short-Term Memory (H-LSTM) architecture, which can model complex temporal dependencies in UAV data. The H-LSTM architecture was effective in detecting short-term anomalies and long-term deviations, and explainability was provided through the SHAP mechanism. SHAP values made it possible to understand the decisions of the IDS transparently, enabling security analysts to explain the system's decisions. Experiments were conducted using the N-BaIoT dataset, and the proposed system achieved high accuracy and low false positive rates in threat detection. The study provided an explainable and efficient cybersecurity solution to enhance UAV security (Javeed et al., 2024).

In the study by Hong and Yoo (2024), a model was developed to detect multiple attacks on the Control Area Network (CAN) protocol of UAVs. In the study, a heterogeneous model capable of detecting multiple types of attacks simultaneously was proposed, and explainability was provided using the SHAP method. The model was used to detect attacks such as DoS and GPS signal spoofing. In the study, feature importance measures were used to distinguish between attack and normal data, thereby improving the model's accuracy. Experimental results showed that the model was successful in detecting attacks with an accuracy rate of 97% (Hong & Yoo , 2024).

In the study by Souripalli et al. (2024), a model was developed for the autonomous navigation of UAVs in dense fog environments using the

Explainable Deep Reinforcement Learning (DRL) method. In the study, Twin Delayed DDPG (TD3) and Proximal Policy Optimization (PPO) algorithms were trained in the AirSim simulation environment, and an image adaptation module optimizing navigation in foggy environments was integrated. Image adaptation used a deep learning-based defogging technique to recover image details lost due to fog. The TD3 algorithm performed better than the PPO algorithm, with a high success rate (77%) and a low collision rate (16%). Additionally, the explainability of the model was ensured using SHAP and LIME. Thus, the transparency of the model's decision-making processes was increased, and it was observed that performance in foggy environments was significantly improved (Sayed , Souripalli & Chiddarwar , 2024).

4. CONCLUSION

Nowadays, the concept of AI, which is one of the concepts that entered our lives with the Industry 4.0 revolution, is. AI is frequently used in many areas such as health, agriculture, security and engineering. With the development of AI technologies , the reliability and transparency of the results obtained from AI models are very important in critically important cases such as medicine and security. In the study, a conceptual study was carried out on UAV technologies, which is one of the areas where AI technologies are frequently used. In the study, a study was carried out on the use of XAI methods, which are a frequently used method in determining the reliability and transparency of UAV and AI .

integrated use of AI technologies has become increasingly important, especially as autonomy and complexity increase. The use of AI in UAVs provides great advantages in critical areas such as autonomous navigation, environmental perception and data analysis. However, with this integration, transparency and security issues have also come to the fore. XAI plays a critical role in making the decision-making processes of AI systems understandable by addressing reliability and transparency issues. The reliability of UAVs is particularly important in terms of public safety and ethical applications. XAI Its use in UAVs increases operators' confidence in these vehicles, while also facilitating the fulfillment of regulatory requirements and the establishment of social acceptance. Therefore, XAI stands out as an important technological development that will contribute to the safer, more accountable and widespread use of UAV technologies in the future. The study was carried out using UAV and XAI methods based on academic literature, and a conceptual study was carried out for applications.

5. References

Adadi , A., & Berrada , M. (2018). Peeking inside the black-box : a survey on explainable artificial intelligence (XAI). IEEE access , 6, 52138-52160.

Alain, G., & Bengio , Y. (2017). Understanding Intermediate Layers Using Linear Classifier Probes . In Proceedings of the International Conference on Learning Representations .

Alharbi , A., Petrunin , I., & Panagiotakopoulos , D. (2023). assuring Safe and Efficient Operation of UAV Using Explainable Machine Learning. Drones , 7(5), 327.

Alvarez -Melis, D., & Jaakkola , T. S. (2018). on the Robustness of Interpretability Methods .arXiv preprint arXiv:1806.08049.

Arras , L., Horn , F., Montavon , G., Müller, KR, & Samek , W. (2017). " What is relevant in a text document ?: An interpretable machine learning approach . PloS one , 12(8), e0181142.

Bahdanau , D., Cho , K., & Bengio , Y. (2015). Neural Machine Translation by Jointly Learning to Align and Translate . In Proceedings of the International Conference on Learning Representations .

Barredo Arrieta , A., et al. (2020). Explainable artificial intelligence (XAI): Concepts , taxonomies , opportunities and challenges about responsible AI. Information Fusion , 58, 82-115.

Breiman , L., Friedman, J., Olshen , R., & Stone, C. (1984). Classification and Regression Trees. Wadsworth .

Bussmann , N., Giudici , P., Marinelli , D., & Papenbrock , J. (2020). Explainable AI in fintech risk management . Frontiers in Artificial Intelligence, 3, 26.

Campion , M., Ranganathan , P., & Faruque , S. (2018). UAV swarm communication and control architectures : a review . Journal of Unmanned Vehicle Systems , 7(2), 93-106.

Chen, C., Li , O., Tao, D., Barnett, A., Rudin , C., & Su, J. K. (2019). this Looks Like That : Deep Learning for Interpretable Image Recognition . Of Advances in Neural Information Processing Systems (pp . 8930–8941).

Chen, H., et al. (2018). explaining neural networks semantically and quantitatively .arXiv preprint arXiv:1806.04220.

Chen, J., Song , L., Wainwright , M. J., & Jordan, M. I. (2018). Learning to explain : An information-theoretic perspective on model interpretation . In International Conference on Machine Learning (pp . 883-892). PMLR.

Çorbacı, FK, & Doğan, YE (2023). An Approach to Preliminary Design of a Quadrotor Cargo UAV. International Journal of Aviation Science and Technol. , 4(02), 63-74.

Devoto , S., Macovaz , V., Mantovani , M., Soldati , M., & Furlani , S. (2020). Advantages of using UAV digital photogrammetry in the study of slow moving Coastal landslides . Remote Sensing , 12(21), 3566.

Dong, Y., et al. (2019). SHAP- based feature importance ranking for time series forecasting In 2019 IEEE International Conference on Big Data (pp . 3785-3791). IEEE.

Doshi-Velez , F., & Kim, B. (2017). Towards a rigorous science of interpretable machine learning .arXiv preprint arXiv:1702.08608.

Esteva , A., Kuprel , B., Novoa , RA, et al. (2017). Dermatologist -Level Classification of Skin Cancer with Deep Neural Networks. Nature, 542(7639), 115–118.

Floreano , D., & Wood , R. J. (2015). science , technology and the future of small autonomous drones . nature , 521(7553), 460-466.

Garreau , D., & Luxburg , U.V. (2020). explaining the explainer : A first theoretical analysis of LIME. In International Conference on Artificial Intelligence and Statistics (pp . 1287-1296). PMLR.

Gilpin , L.H., et al. (2018). explaining explanations : An overview of interpretability of machine learning In 2018 IEEE 5th International Conference on data science and advanced analysis (DSAA) (pp . 80-89). IEEE.

Goyal , SB, Rajawat , AS, Solank , RK, Patil, D., & Potgantwar , A. A Trustable Security Solutions Using XAI for 5G-Enabled UAV.

Guidotti , R., et al. (2018). A survey of methods for explaining Black box models . ACM Computing Surveys (CSUR), 51(5), 93.

Guidotti , R., Monreale , A., Ruggieri , S., Turini , F., Giannotti , F., & Pedreschi , D. (2018). A Survey of Methods for Explaining Black Box Models . ACM Computing Surveys , 51(5), 93.

Gunning , D. (2017). Explainable Artificial Intelligence (XAI). DARPA.

Gunning , D., & Aha, D. W. (2019). DARPA's explainable artificial intelligence (XAI) program. AI Magazine, 40(2), 44-58.

Gunning , D., Stefik , M., Choi , J., Miller, T., Stumpf , S., & Yang, G. Z. (2019). XAI—Explainable artificial intelligence . Science robotics , 4(37), eaay7120.

Haque , E., Hasan, K., Ahmed, I., Alam, MS, & Islam , T. (2024). Enhancing UAV Security Through Zero Trust Architecture: An Advanced Deep Learning and Explainable AI Analysis. arXiv preprint arXiv:2403.17093.

Hastie , T., Tibshirani , R., & Friedman, J. (2009). the Elements of Statistical Learning. Springer .

Hendricks , L.A., et al. (2016). generating visual explanations . In European Conference on Computer Vision (pp . 3-19). Springer .

Holzinger , A., et al. (2019). causability and explainability of artificial intelligence in medicine . Wiley Interdisciplinary Reviews : Data Mining and Knowledge Discovery , 9(4), e1312.

Hong, Y. W., & Yoo , D. Y. (2024). Multiple Intrusion Detection Using Shapley Additive Explanations and a Heterogeneous Ensemble Model in an Unmanned Aerial Vehicle's Controller Area Network. Applied Sciences , 14(13), 5487.

Istiak , MA, Syeed , MM, Hossain , MS, Uddin , MF, Hasan, M., Khan , RH, & Azad, NS (2023). Adoption of Unmanned Aerial Vehicle (UAV) imagery in agricultural management : A systematic literature review . Ecological Informatics , 102305.

Janzing , D., Minorics , L., & Bloebaum , P. (2020). Feature Relevance Quantification in explainable AI: A causal problem. In International Conference on Artificial Intelligence and Statistics (pp . 2907-2916). PMLR.

Javeed , D., Gao , T., Kumar, P., Shoukat , S., Ahmad , I., & Kumar, R. (2024, June). An Intelligent and Interpretable Intrusion Detection System for Unmanned Aerial Vehicles . In ICC 2024-IEEE International Conference on Communications (pp . 1951-1956). IEEE.

Kawaguchi , K. (2016). without Deep Learning Poor Local Minimum . In Advances in Neural Information Processing Systems (pp . 586–594).

Keneni, B. M. (2018). Evolving Rule Based Explainable Artificial Intelligence for Decision Support System of Unmanned Aerial Vehicles (Master's thesis , University of Toledo).

Kim, J., & Canny , J. (2017). Interpretable Learning for Self- Driving Cars by Visualizing Causal Attention . In Proceedings of the IEEE International Conference on Computer Vision (pp . 2942–2950).

Kumar, I.E., Venkatasubramanian , S., Scheidegger , C., & Friedler , S.A. (2020). problems with Shapley-value-based Explanations as featured importance measures . In International Conference on Machine Learning (pp . 5491-5500). PMLR.

LeCun , Y., Bengio , Y., & Hinton , G. (2015). Deep learning Nature, 521(7553), 436-444.

Li , O., Liu , H., Chen, C., & Rudin , C. (2018). Deep Learning for Case- Based Reasoning Through Prototypes : A Neural Network That Explains Its Predictions . In Proceedings of the AAAI Conference on Artificial Intelligence (pp . 3530–3537).

Lipton, Z. C. (2016). The Mythos of Model Interpretability . arXiv preprint arXiv:1606.03490.

Lipton, Z. C. (2018). The mythos of model interpretability : In machine learning , the concept of interpretability is both important and slippery . Queue, 16(3), 31-57.

Lundberg , S. M., & Lee, S. I. (2017). A unified approach to interpreting model predictions . Of Advances in Neural Information Processing Systems (pp . 4765-4774).

Lundberg , S. M., Erion , G., & Lee, S. I. (2020). From local explanations to global understanding with explainable AI for trees . Nature Machine Intelligence, 2(1), 56-67.

Lundberg , S.M., et al. (2018). Explainable machine learning predictions for the Prevention of hypoxemia during surgery . Nature Biomedical Engineering , 2(10), 749-760.

Maas , AL, Hannun , AY, & Ng, AY (2013). Rectifier Nonlinearities Improve Neural Network Acoustics Models . In Proceedings of the 30th International Conference on Machine Learning.

Miller, T. (2019). Explanation in artificial intelligence : Insights from the social sciences . Artificial Intelligence, 267, 1-38.

Molnar , C. (2019). Interpretable Machine Learning. https://christophm.github.io/interpretable-ml-book/

Molnar , C. (2019). Interpretable Machine Learning. leanpub .

Montavon , G., Samek , W., & Müller, K.-R. (2018). methods for Interpreting and Understanding Deep Neural Networks.Digital Signal Processing , 73, 1–15.

Muhammad Kamarulzaman , AM, Wan Mohd Jaafar , W.S., Mohd Said, MN, Saad , SNM, & Mohan , M. (2023). UAV Implementations in Urban Planning and Related Sectors of Rapidly Developing Nations: A Review and Future Perspectives for Malaysia . Remote Sensing , 15(11), 2845.

Murthy , S. K. (1998). Automatic Construction of Decision Trees from Data: A Multi- Disciplinary Survey . Data Mining and Knowledge Discovery , 2(4), 345–389.

Pandey , B.K., Pandey , D., & Sahani , S.K. (2024). autopilot control unmanned aerial vehicle system for sewage defect Detection using deep learning . Engineering Reports , e12852.

PK, FA (1984). What is Artificial Intelligence? Success is no accident It is hard work , perseverance , learning , studying , sacrifice and most of all , love of what You are doing or learning to do, 65.

Quinlan , J. R. (1986). Induction of Decision Trees. Machine Learning, 1(1), 81–106.

Ribeiro , M.T., Singh, S., & Guestrin , C. (2016). " Why I should trust "you ?": Explaining the predictions of any classifier . In Proceedings of the 22nd ACM SIGKDD International Conference on Knowledge Discovery and Data Mining (pp . 1135-1144). ACM.

Ribeiro , M.T., Singh, S., & Guestrin , C. (2018). Anchors : High- precision model -agnostic explanations . In Proceedings of the AAAI Conference on Artificial Intelligence (Vol . 32, No. 1).

Rokach , L., & Maimon , O. (2005). Decision Trees. In Data Mining and Knowledge Discovery Handbook (pp . 165–192). Springer .

Roth , A. E. (1988). The Shapley value : Essays in honor of Lloyd S. Shapley . CambridgeUniversity Press .

Rudin , C. (2019). Stop Explaining Black Box Machine Learning Models for High -Stakes Decisions and Use Interpretable Models Instead . Nature Machine Intelligence, 1(5), 206–215.

Russell, S., & Norvig , P. (2010). Artificial Intelligence: A Modern Approach . prentice Hall .

Samek , W., Wiegand , T., & Müller, K.-R. (2017). Explainable Artificial Intelligence: Understanding , Visualizing and Interpreting Deep Learning Models .arXiv preprint arXiv:1708.08296.

Santos, NP, Rodrigues , VB, Pinto , AB, & Damas , B. (2023, April). automatic Detection of Civilians and Military Personnel in Reconnaissance Missions using a UAV. In 2023 IEEE International Conference on Autonomous Robot Systems and Competitions (ICARSC) (pp . 157-162). IEEE.

Sayed , L.J., Souripalli , PK, & Chiddarwar , SS (2024, June). autonomous Navigation of Drones Using Explainable Deep Reinforcement Learning in Foggy Environment. In 2024 IEEE Students Conference on Engineering and Systems (SCES) (pp . 1-6). IEEE.

Selvaraju , R.R., et al. (2017). Grad -CAM: Visual explanations from deep networks via gradient-based localization . In Proceedings of the IEEE International Conference on Computer Vision (pp . 618-626).

Shadiev , R., & Yi , S. (2023). A systematic review of UAV applications to education Interactive Learning Environments , 31(10), 6165-6194.

Shapley , L. S. (1953). A value for n- person games . In Contributions to the Theory of Games (pp . 307-317). Princeton University Press .

Štrumbelj , E., & Kononenko , I. (2014). explaining prediction Models and individual predictions with feature contributions . Knowledge and Information Systems , 41(3), 647-665.

Sundararajan , M., & Najmi , A. (2019). the many Shapley values for model explanation . In International Conference on Machine Learning (pp . 9269-9278). PMLR.

Sundararajan , M., Taly , A., & Yan, Q. (2017). Axiomatic attribution for deep networks . In International Conference on Machine Learning (pp . 3319-3328). PMLR.

Talwandi , N.S., Thakur , P., & Khare , S. (2024, February). An Automatic Navigation System for New Technical Advanced Drones for Different Alpplications . In 2024 IEEE International Conference on Computing, Power and Communication Technologies (IC2PCT) (Vol . 5, pp . 736–741). IEEE.

Thiels , C.A., Aho , J.M., Zietlow , S.P., & Jenkins, D.H. (2015). Use of unmanned aerial Vehicles for medical product transport.Air medical Journal , 34(2), 104-108.

Tjoa , E., & Guan , C. (2020). A survey on explainable artificial intelligence (XAI): Towards medical IEEE Transactions on Neural Networks and Learning Systems , 32(11), 4793-4813.

Tonekaboni , S., et al. (2019). What clinicians want : Contextualizing explainable machine learning for clinical end use . In Machine Learning for Healthcare Conference (pp . 359-380). PMLR.

Wachter , S., Mittelstadt , B., & Floridi , L. (2017). Why a right to explanation of automated decision making Does not exist in the General Data Protection Regulation . International Data Privacy Law , 7(2), 76-99.

Witten , IH, Frank, E., Hall , M.A., & Pal, C.J. (2016). Data Mining : Practical Machine Learning Tools and Techniques . Morgan Kaufmann.

Zhang, Q. S., & Zhu, S. C. (2018). Visual Interpretability for Deep Learning: A Survey . Frontiers of Information Technology & Electronic Engineering , 19(1), 27–39.

Zhu, H., Demirbaga , U., Aujla , GS, Shi , L., & Zhang, P. (2024). Explainable Edge AI Framework for IoD-Assisted Aerial Surveillance in Extreme Scenarios . IEEE Internet of Things Journal .

Bölüm 2

Kararsız Hal Isı Akışı Rejiminde Serbest Katılaştırılan Al-5Cu-5Si-5Mg-5Zn-1Zr Alaşımının Mikroyapısal Evrimi ve Faz Oluşumu[1]

Hasan Kaya[2]

Emin Çadırlı[3]

Uğur Büyük[4]

Erkan Üstün[5]

Özet

Bu çalışmada, kararsız hal ısı akışı rejimi altında serbest katılaştırılan Al-5Cu-5Si-5Mg-5Zn-1Zr çok bileşenli alüminyum alaşımının mikroyapısal evrimi ve faz oluşumu üzerine soğuma hızının etkisi incelenmiştir. Katılaştırma deneyleri, numune boyunca farklı soğuma hızları elde etmek için özel olarak tasarlanmış bir deney düzeneği kullanılarak gerçekleştirilmiştir. Katılaştırılmış alaşımın mikroyapısı ve faz bileşimi optik mikroskobu, taramalı elektron mikroskobu (SEM), enerji dağılımlı x-ışını spektroskopisi (EDS) ve X-ışını kırınımı (XRD) kullanılarak kapsamlı bir şekilde karakterize edilmiştir. Sonuçlar, soğuma hızının mikroyapı ve intermetalik faz oluşumu üzerinde önemli bir etkiye sahip olduğunu göstermiştir. Soğuma hızı arttıkça dendritik yapılar incelmiş ve ötektik mesafeler azalmıştır. Ayrıca, soğuma hızına bağlı olarak α-Al matris fazı içinde Al_2Cu, Mg_2Si, $MgZn_2$ ve Al_3Zr gibi farklı intermetalik fazların oluştuğu gözlemlenmiştir. Yüksek soğuma hızlarında,

1 Bu çalışma Erciyes Üniversitesi Bilimsel Araştırma Projeleri Koordinasyon Birimi tarafından FBA-2023-12765 numaralı proje ile desteklenmiştir.

2 Prof. Dr., Erciyes Üniversitesi, Eğitim Fakültesi, Matematik ve Fen Bilimleri Eğitimi Bölümü, Kayseri, Türkiye, hasankaya@erciyes.edu.tr, ORCID: 0000-0003-3529-9762

3 Prof. Dr., Niğde Ömer Halisdemir Üniversitesi, Fen Fakültesi, Fizik Bölümü, Niğde, Türkiye, ecadirli@gmail.com, ORCID: 0000-0002-8085-9733

4 Prof. Dr., Erciyes Üniversitesi, Eğitim Fakültesi, Matematik ve Fen Bilimleri Eğitimi Bölümü, Kayseri, Türkiye, buyuk@erciyes.edu.tr, ORCID: 0000-0002-6830-8349

5 Dr., Niğde Ömer Halisdemir Üniversitesi, Fen Bilimleri Enstitüsü, Fizik Anabilim Dalı, Niğde, Türkiye, erkanustun_07@hotmail.com, ORCID: 0000-0002-7745-396X

https://doi.org/10.58830/ozgur.pub575.c2359

intermetalik fazlar daha ince ve daha homojen bir şekilde dağılırken, düşük soğuma hızlarında daha kaba ve düzensiz bir dağılım gözlemlenmiştir. Bu bulgular, kararsız hal ısı akışı rejiminde katılaştırmanın çok bileşenli alüminyum alaşımlarının mikroyapısını ve dolayısıyla mekanik özelliklerini kontrol etmek için etkili bir yöntem olduğunu göstermektedir. Bu çalışma sonuçları, yeni çok bileşenli alüminyum alaşımlarının geliştirilmesi ve mevcut alaşımların performansının iyileştirilmesi için yol gösterici olabilir.

1. GİRİŞ

Alüminyum alaşımları, günümüz mühendislik uygulamalarında vazgeçilmez bir rol oynamaktadır. Hafiflikleri, yüksek dayanım/ağırlık oranları, iyi korozyon dirençleri ve mükemmel dökülebilirlikleri; onları otomotiv, havacılık, inşaat ve ambalaj gibi birçok sektörde popüler malzemeler haline getirmiştir [1-3]. Özellikle son yıllarda, çok bileşenli alüminyum alaşımları, geleneksel alaşımlara göre daha üstün mekanik ve fiziksel özellikler sergileme potansiyelleri nedeniyle yoğun bir araştırma konusu olmuştur [4-6]. Bu alaşımların, daha yüksek mukavemet, gelişmiş süneklik, artırılmış aşınma direnci ve iyileştirilmiş yüksek sıcaklık özellikleri gibi bir dizi avantajlar sunabileceği gösterilmiştir.

Çok bileşenli alüminyum alaşımlarının performansları, karmaşık mikro yapıları tarafından belirlenir, bu ise dendritik yapı, tane boyutu, ikinci fazların dağılımı ve intermetalik bileşiklerin oluşumu gibi çeşitli faktörlerden etkilenir. Bu mikro yapısal özellikler, katılaştırma koşulları tarafından büyük ölçüde etkilenir. Bu durum malzemelerin özelliklerini hassas bir şekilde ayarlamak için bir yol sunar.

Katılaştırma hızı, alüminyum alaşımlarının mikroyapısal özelliklerini şekillendiren kritik parametrelerden biridir. Hızlı soğuma, daha ince taneli ve daha homojen bir mikro yapıya yol açarken, yavaş soğuma genellikle daha kaba taneli ve heterojen bir mikro yapı ile sonuçlanır. Bu ise malzemenin mekanik özelliklerini, örneğin dayanım, sertlik ve sünekliğini önemli ölçüde etkiler.

Kararsız hal ısı akışı rejimi, eriyik metallerin kontrollü bir şekilde soğutulmasını ve farklı soğuma hızlarında katılaşmasını içeren bir tekniktir. Bu teknik, dendritik yapı, tane boyutu ve ikinci faz dağılımı gibi mikroyapısal özellikleri kontrol etmek için etkili bir yöntemdir [7-9]. Kararsız hal rejiminde katılaştırma, katılaşma cephesindeki sıcaklık gradyantını ve hızını değiştirerek malzemenin mikro yapısı üzerinde hassas bir kontrol sağlar ve bu durum istenen özelliklere sahip malzemelerin üretilmesine olanak tanır.

Bu çalışma, Al-5Cu-5Si-5Mg-5Zn-1Zr (% ağırlıkça) bileşimine sahip çok bileşenli alüminyum alaşımının kararsız hal ısı akışı rejimi altında serbest katılaştırılması üzerine odaklanmaktadır. Bu özel alaşım, otomotiv ve havacılık sektörlerinde potansiyel uygulamalar için umut vadeden bir adaydır. Bu çalışmada, farklı soğuma hızlarının dendritik yapı, ötektik mesafe ve intermetalik fazların oluşumu üzerindeki etkisini incelemeyi ve bu mikroyapısal özelliklerin malzemenin genel performansını nasıl etkilediğini anlamayı amaçlamaktadır. Optik mikroskobu (OM), taramalı elektron mikroskobu (SEM), enerji dağılımlı X-ışını spektroskopisi (EDS) ve X-ışını kırınımı (XRD) gibi gelişmiş karakterizasyon teknikleri, katılaşmış mikroyapıyı detaylı bir şekilde analiz etmek ve farklı soğuma hızlarının etkisini ortaya çıkarmak için kullanılacaktır. Bu çalışmadan elde edilen bulguların, çok bileşenli alüminyum alaşımlarının katılaşma davranışının daha iyi anlaşılmasına ve bu malzemelerin özelliklerinin belirli mühendislik uygulamaları için özelleştirilmesine katkı sağlaması beklenmektedir.

2. DENEYSEL YÖNTEM

Bu çalışmada, Al-5Cu-5Si-5Mg-5Zn-1Zr (% ağırlıkça) bileşimine sahip çok bileşenli alüminyum alaşımı, vakumlu indüksiyon eritme yöntemi kullanılarak yüksek saflıkta elementlerden (%99.99) üretilmiştir. Alaşımın homojen bir bileşimini sağlamak için, hassas bir eritme ve döküm protokolü izlenmiştir. Belirlenen ağırlık oranlarındaki alaşım elementleri öncelikle grafit pota içine yerleştirilmiş ve vakumlu indüksiyon eritme fırını kullanılarak eritilmiştir. Erime işlemi, 1073 K sıcaklıkta gerçekleştirilmiş ve eriyik alaşım 30 dakika boyunca bu sıcaklıkta tutularak, elementlerin homojen bir şekilde karışması sağlanmıştır. Eriyik alaşım, homojenizasyon işleminden sonra, önceden ısıtılmış grafit kalıplara dökülmüş ve oda sıcaklığında soğumaya bırakılarak ana (master) alaşım üretilmiştir.

Master alaşım numuneleri, daha sonra kararsız hal ısı akış rejimi altında serbest katılaştırma deneylerine tabi tutulmuştur. Bu deneyler, Şekil 1'de şematik olarak gösterilen özel olarak tasarlanmış bir deney düzeneği kullanılarak gerçekleştirilmiştir. Deney düzeneği; kontrollü katılaştırma fırını, güç ünitesi, hassas bir sıcaklık kontrol ünitesi, sıcaklık verilerini kaydetmek için bir veri kaydedici, soğutma suyu sirkülasyonunu sağlayan bir sistem, numune tutucu ve kontrollü bir argon atmosferi sağlamak için bir gaz akış sisteminden oluşmaktadır.

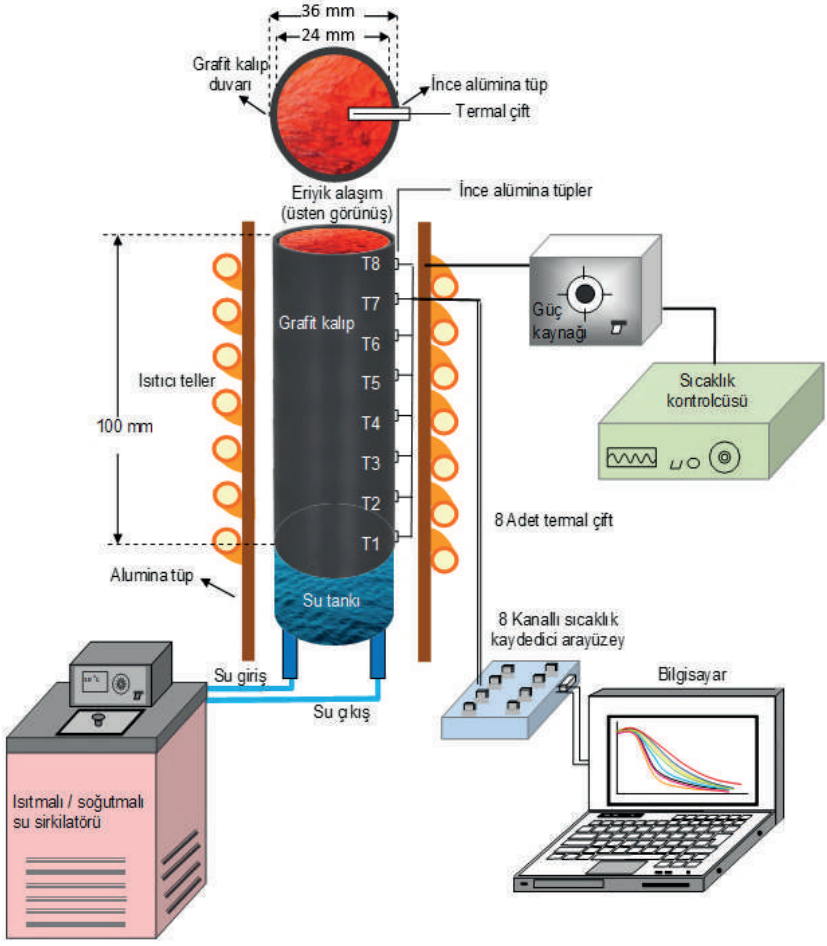

Şekil 1. Kararsız hal ısı akışı rejiminde serbest katılaştırma deney düzeneğinin şematik gösterimi

Master alaşım numunesi, deney düzeneğinde 22 mm iç çapa ve 120 mm boya sahip silindirik bir grafit pota içine yerleştirilmiştir. Grafit pota, homojen bir ısı dağılımı sağlamak ve numune boyunca kontrollü bir soğuma hızı elde etmek için seçilmiştir. Daha sonra, grafit pota tabanından itibaren 1 cm aralıklarla 8 adet kılcal alümina tüp, pota duvarına dik olarak, pota merkezine yakın bir konuma kadar uzanacak şekilde yerleştirilmiştir. Bu alümina tüpler, alaşım eriyik ile temas etmelerini önlemek ve doğru sıcaklık ölçümleri sağlamak için termal çiftleri izole etmek amacıyla kullanılmıştır. K tipi termal çiftler daha sonra bu alümina tüplerin içine yerleştirilmiş ve her biri, numune boyunca farklı konumlardaki sıcaklığı doğru bir

şekilde kaydetmek üzere veri kaydedici (Data logger, TC-08) arayüzüne bağlanmıştır. Veri kaydedici, katılaşma işlemi boyunca sıcaklık verilerini gerçek zamanlı olarak kaydetmeyi ve görselleştirmeyi sağlamaktadır. Deney sistemi, istenmeyen oksidasyonu ve kontaminasyonu önlemek için kontrollü bir argon atmosferinde çalıştırılmıştır. Master alaşım numunesi, grafit pota içinde yaklaşık 960 K sıcaklığa kadar ısıtılmış ve bu sıcaklıkta 1 saat bekletilerek homojen bir sıcaklık dağılımı sağlanmıştır. Daha sonra, fırın kapatılmış ve soğutma suyu sirkülasyon sistemi devreye alınarak numunenin soğutulma süreci başlatılmıştır. Serbest doğrusal katılaşma, soğutma suyunun grafit pota tabanını soğutması ile başlamıştır. Katılaşma işlemi boyunca, termal çiftler ile numune boyunca farklı konumlardaki sıcaklıklar hassas bir şekilde izlenmiş ve kaydedilmiştir. Sıcaklık ölçümleri, yüksek bir veri toplama hızı olan saniyede 10 ölçüm alınarak gerçekleştirilmiştir. Bu, katılaşma sürecinin ayrıntılı bir şekilde anlaşılmasını ve soğuma hızı profillerinin doğru bir şekilde belirlenmesini sağlamıştır. Elde edilen sıcaklık verileri, numunenin farklı konumlarındaki soğuma hızlarını hesaplamak için kullanılmıştır. Bu soğuma hızı profilleri, mikro yapısal evrim ve faz oluşumu üzerindeki soğuma hızının etkisini analiz etmek için önemli bir girdi sağlamıştır.

3. DENEYSEL SONUÇLAR

Kararsız hal ısı akışı rejimi altında serbest katılaştırılan Al-5Cu-5Si-5Mg-5Zn-1Zr alaşım numunelerinin mikro yapısı ve faz bileşimi, ileri karakterizasyon teknikleri kullanılarak kapsamlı bir şekilde incelenmiştir. Deneysel sonuçlar aşağıda detaylı olarak verilmiştir.

Kararsız ısı akış rejiminde kontrollü katılaştırma fırınında alaşım eridikten sonra fırının güç kaynağı kapatılmış ve soğutma suyu açılarak Şekil 2'de görüldüğü gibi numune alt kısımdan başlayarak katılaşmaya başlamış ve belli bir süre sonra katılaşma tamamlanmıştır. Şekil 2'de soğuma hızının makro ve mikroyapıya etkisi görülmektedir.

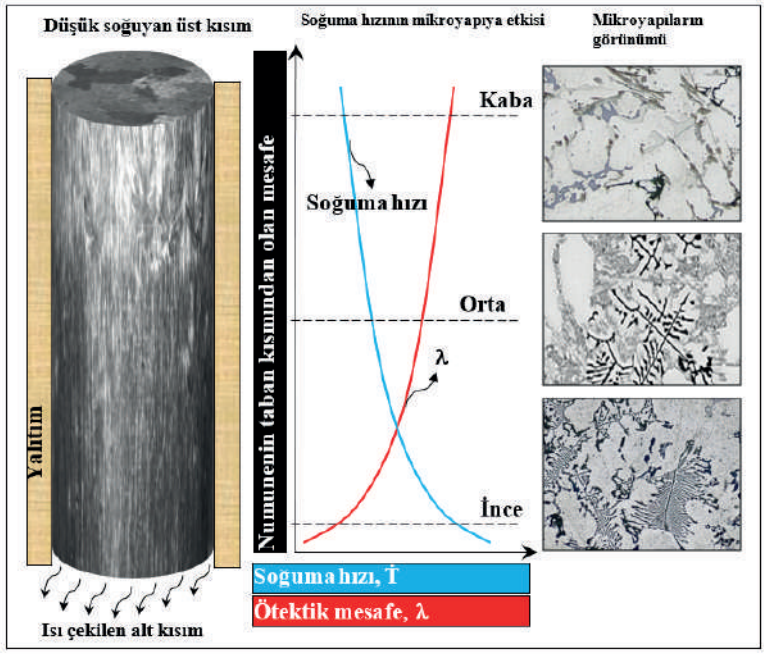

Şekil 2. Kararsız ısı akış rejiminde katılaştırılan numunede makro ve mikroyapı değişimi

Numunenin üst kısmına doğru soğuma hızlarının giderek düşüş gösterdiği tespit edilmiştir. Makroyapı numunenin üst kısmında daha kaba yapı sergilerken alt kısma yaklaşırken daha ince bir tane yapısı gözlemlenmiştir. Aynı durum mikroyapı içinde söylenebilir. Elde edilen soğuma eğrilerinde herhangi bir kusur gözlenmemiştir. Şekil 3'de kararsız ısı akış rejiminde katılaştırılan numuneden alınan soğuma eğrileri görülmektedir.

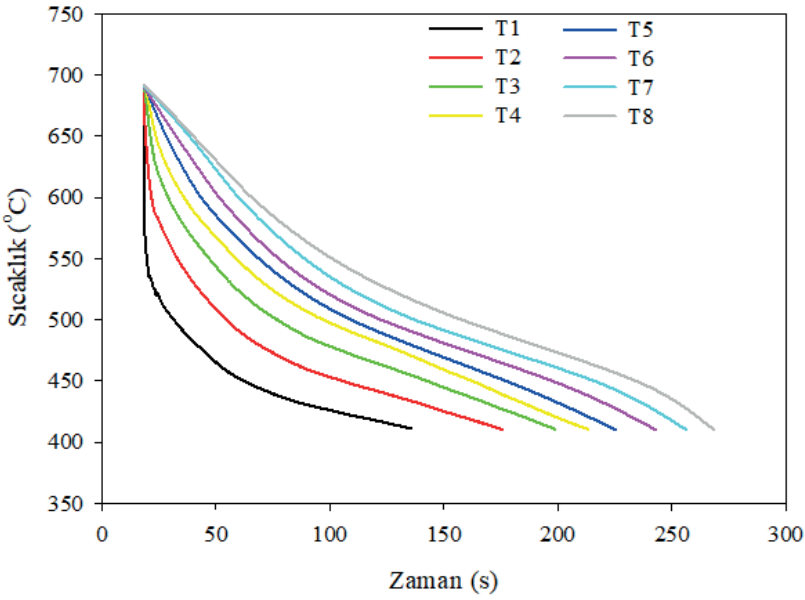

Şekil 3. Numune içine yerleştirilen termal çiftler vasıtasıyla elde edilen soğuma eğrileri

Bu eğride 8 adet soğuma hızı görülmektedir. T1 numunenin en alt kısmında yerleştirilen (tabandan itibaren 1cm) soğuma eğrisini gösterirken diğer termal çiftler kademeli olarak 1'er cm yukarıya doğru konumlandırılmış ve son olarak T8 numunenin en üst kısmına yerleştirilmiş (tabandan itibaren 8cm) soğuma eğrisini temsil etmektedir.

Alaşım içinde yer alan faz bileşenlerinin erime sıcaklıkları da göz önüne alınarak belirlenen sıcaklık aralığında soğuma hızları, bu soğuma eğrileri vasıtasıyla tespit edilmiş ve Tablo 1'de bu değerler verilmiştir. Şekil 4'de ise yarım silindir biçimli uzun numune ve dilimlenmiş 8 bölge görülmektedir.

Tablo 1. Numune içine yerleştirilen termal çiftlerin ölçtüğü ortalama soğuma hızları

Numune tabanından olan mesafeler, P (cm)	1	2	3	4	5	6	7	8
Soğuma hızları, $\dot{T}$ (°C/s)	$\dot{T}_1$	$\dot{T}_2$	$\dot{T}_3$	$\dot{T}_4$	$\dot{T}_5$	$\dot{T}_6$	$\dot{T}_7$	$\dot{T}_8$
	2.77	1.80	1.41	1.18	1.09	1.01	0.95	0.88

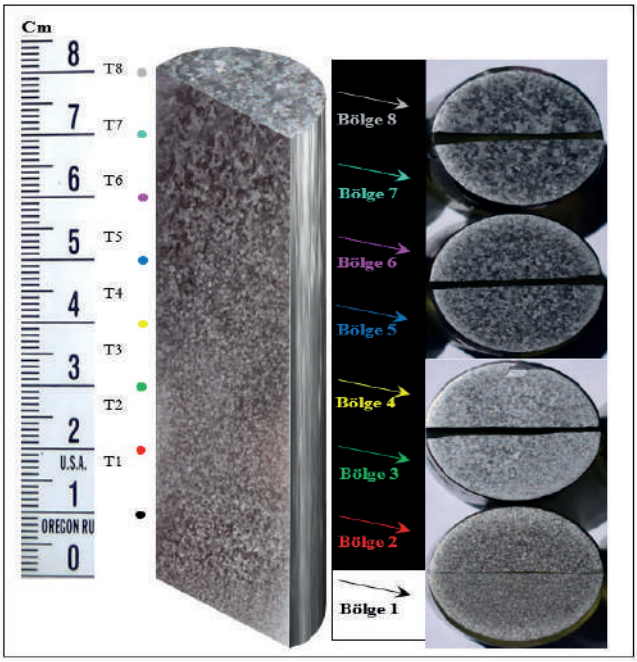

Şekil 4. Boyuna ve enine dilimlenmiş numunenin makroyapıları

Tablo 1 ve Şekil 4'den de görüldüğü gibi uzun numunenin üst kısmı 0.88 ^{o}C/s ile soğurken, en alt kısım 2.77 ^{o}C/s soğuma hızıyla serbest katılaşmıştır. Soğutma kazanına yakın kısmın soğuma hızı üst kısmın soğutma hızından yaklaşık üç kat daha fazladır. Hem boyuna hem de enine kesit göz önüne alındığında Bu soğuma hızlarındaki farklılıktan dolayı uzun numunenin üst kısmı ve 8 numaralı dilim (Bölge 8) daha kaba tane yapısına sahip olarak katılaşmışken uzun numunenin alt kısmı ve 1 numaralı dilim (Bölge 1) daha ince tane yapısına sahip olarak katılaşmıştır. Bu durum makroyapılardan açık olarak görülmektedir.

Şekil 5'de soğuma hızına göre mikroyapılar verilmiştir. Dilimlenmiş numuneler üzerinde yapılan incelemelerde genellikle kabalaşmış ve gelişigüzel yönelmiş dendritik kalıntıların (α-Al katı çözeltisi) yanısıra genellikle tane sınırları üzerinde çöken intermetalikler tespit edilmiştir. Katılaşma sırasında, α-Al katı çözeltisinin ve intermetaliklerin dağılımı eşit oluşmamış ve genellikle bileşim ayrışması da meydana gelmiştir. Ayrıca soğutma hızı, sıcaklık, safsızlık, kimyasal elementin içeriği de homojen olmayan mikroyapılara ve özelliklere neden olabilmektedir. Bu mikroyapılar kararsız hal ısı akış rejiminden dolayı düzenli büyümediği için mikro yapı içinde gelişigüzel olarak dağılmış düzensiz kaba dendrit yapılar ve intermetalik

oluşumlar içinde düzenli olarak bilinen yer yer $Al+Al_2Cu$ ötektik yapılar görülmektedir. Şekil 5'de de görüldüğü gibi numunenin alt kısmına doğru yaklaştıkça soğuma hızının daha yüksek olmasından dolayı daha ince bir ötektik tane yapısı görülmektedir. Bölgesel olarak düzenli olmalarından dolayı bu ötektik (lamelsel) yapılardan ölçüm alınmış ve ötektik mesafelerin soğuma hızına göre nasıl bir değişim gösterdiği tespit edilmiştir. Şekil 6'da numunenin tabanından olan mesafenin bir fonksiyonu olarak soğuma hızlarının değişimi verilmiştir.

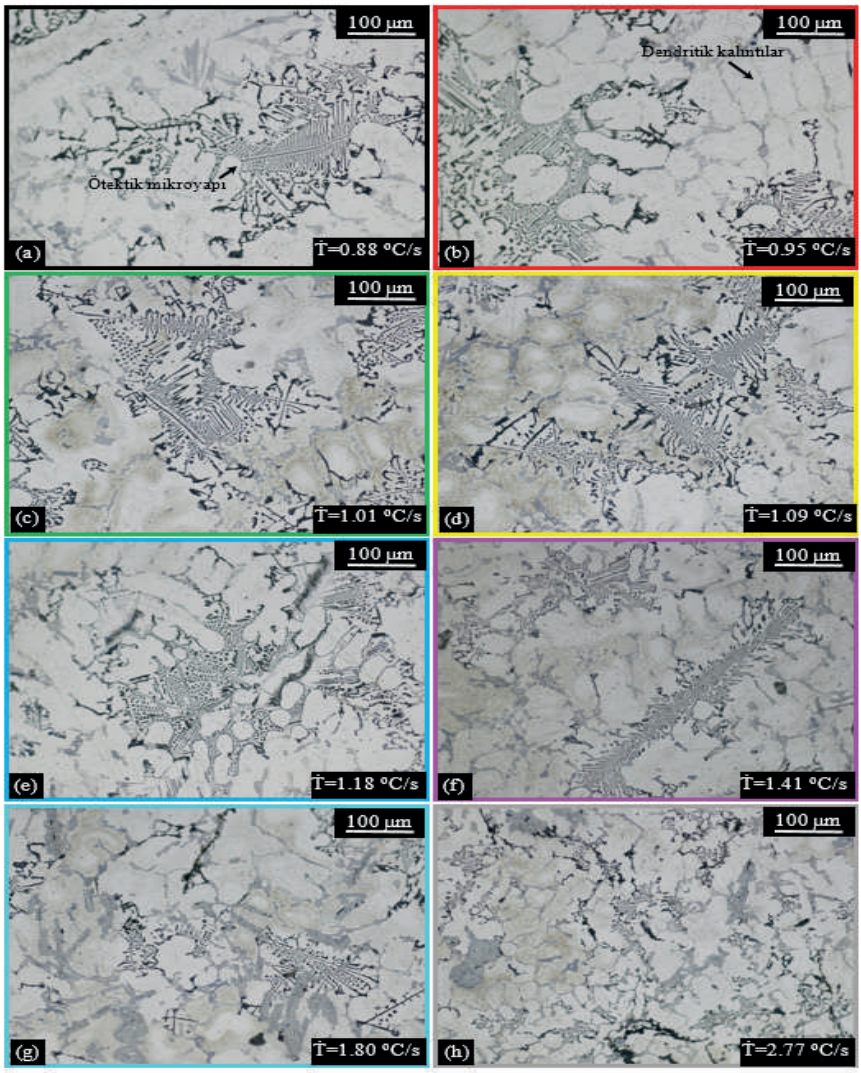

Şekil 5. Numunelerin mikroyapıları (a) Bölge 1 (b) Bölge 2 (c) Bölge 3 (d) Bölge 4 (e) Bölge 5 (f) Bölge 6 (g) Bölge 7 (h) Bölge 8

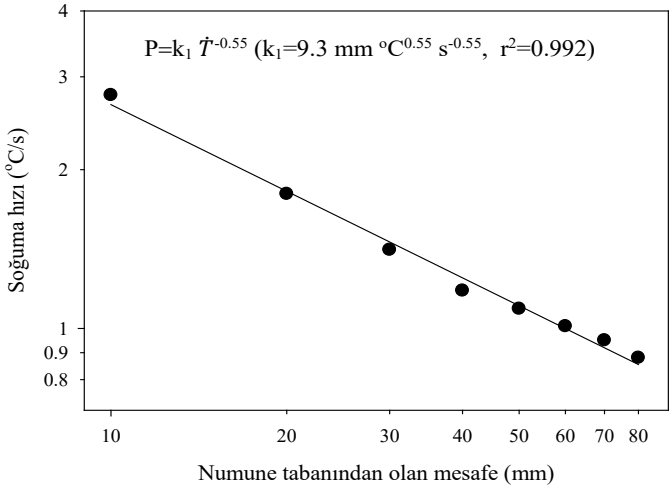

Şekil 6. Soğuma hızının mesafeye göre değişimi

Şekil 6'da görüldüğü gibi numune tabanından yukarıya doğru gidildikçe soğuma hızı yaklaşık üçte biri değerine düşmüştür. Ṫ ile P arasındaki bağıntıdan P'nin Ṫ'nin 0.55 üstel değeri ile ters orantılı olarak değişim gösterdiği görülmektedir. Şekil 7'de numune içinde ölçümü yapılmış ötektik mesafenin sırasıyla numune tabanından olan mesafe ve soğuma hızına göre değişimleri verilmiştir.

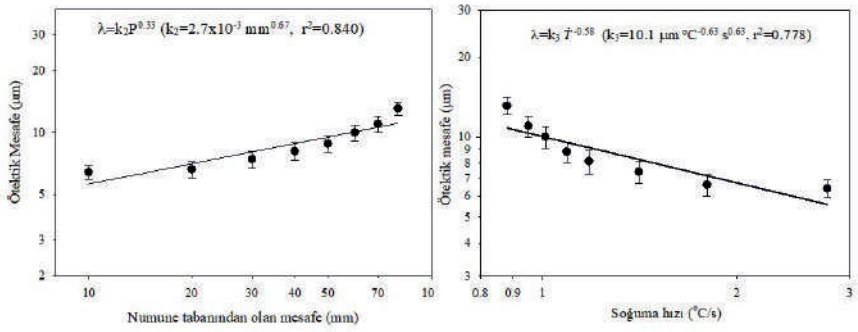

Şekil 7. Ötektik mesafenin numune tabanından olan uzaklığa göre ve soğuma hızına göre değişimi

Şekil 7. Ötektik mesafenin numune tabanından olan uzaklığa göre ve soğuma hızına göre değişimi

Daha sonra üretilen alaşımın kimyasal bileşim analizi çalışmaları yürütülmüştür. Bunun için katılaştırılan numunenin en alt (Bölge 1), orta (Bölge 4) ve en üst (Bölge 8) kısımlarından alınan yaklaşık 1 mm kalınlıktaki hacimli örnekler hazırlanmış Panalytical-Axios Advanced model cihaz kullanılarak WDXRF (Wavelength Dispersive X-ray Fluorescence) kimyasal bileşim analizi yapılmıştır. Analiz sonuçları Şekil 8'de verilmiştir.

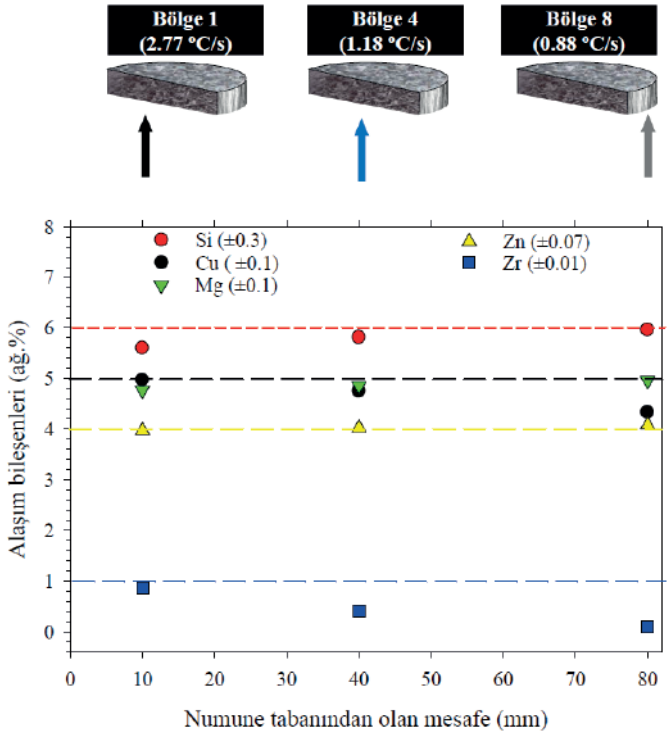

Şekil 8. Farklı bölgelerdeki WDXRF yöntemi ile yapılan kimyasal bileşim analizi

Şekil 8'dan görüldüğü üzere numunenin en alt kısmında (Bölge 1) Si nominal bileşimin üzerinde dağılım göstermişken Zn biraz altındadır, diğer bileşenler (Cu, Mg ve Zr) nominal değerlere yakındır. Numunenin orta kısmı (Bölge 4) ve üst kısmında (Bölge 8) ise Si, Mg ve Zn değerleri kısmen artış göstermiş, Cu ve Zr ise yine kısmen azalış göstermiştir. Tablo 2'de kimyasal bileşim analizi sonucu elde edilen değerler verilmiştir. Taban kısmında Cu ve Zr miktarının diğer bölgelere göre kısmen fazla olması diğer bileşenlere göre ağır metal olmasından dolayı konveksiyonun etkisi görülmektedir. Zn'nin nominal bileşimin biraz altında çıkması buharlaşma

sıcaklığının diğer bileşenlere göre düşük olmasından dolayı biraz kütle kaybı oluşmuş olabileceğini düşündürmektedir.

Tablo 2. Çalışmada kullanılan alaşımın bileşim analizi (WDXRD)

Bölge	Al (ağ.%)	Cu (ağ.%)	Si (ağ.%)	Mg (ağ.%)	Zn (ağ.%)	Zr (ağ.%)
En alt kısım (Bölge 1)	79.83±0.5	4.97±0.1	5.60±0.3	4.77±0.1	3.97±0.07	0.86±0.02
Orta kısım (Bölge 4)	80.15±0.5	4.75±0.1	5.81±0.3	4.86±0.1	4.02±0.07	0.41±0.15
En üst kısım (Bölge 8)	80.57±0.5	4.33±0.1	5.96±0.3	4.96±0.1	4.08±0.07	0.10±0.01

Alaşımın çok bileşenli olmasından dolayı mikroyapıda α–Al matris fazı içinde ve özelliklede primer dendrit kalıntılarının kolları arasında ve tane sınırlarında çeşitli intermetalik bileşikler oluşmuştur. Bunların cinsi ve kompozisyon analizi SEM/EDS analizleri yapılarak spekrumları elde edilmiştir. Bu ana faz içinde Al_2Cu, Mg_2Si, $MgZn_2$, Al_3Zr ve Si ötektik fazlar tespit edilmiştir. Elde edilen spekrumlar Şekil 9'da verilmiştir. Üretilen alaşım için analiz edilen numunelerde gözlemlenen mikroyapılar, esas olarak ana faz ve intermetalik bileşikler içeren ikincil fazlardan oluşmaktadır. Şekil 9(a)'dan görülebileceği gibi, irileşmiş dendrit kolları arasında daha sık düzenli Al-Al_2Cu ötektik yapılar gözlenirken (b), (c) ve (d)'de sırasıyla yer yer karışık biçimli Mg_2Si, düzensiz formda Si fleykler ve blok biçimli Al_3Zr intermetalik oluşumlar gözlenmiştir. Mg ve Cu'nun başlıca görevi Mg_2Si ve Al_2Cu sertleşme çökeltilerini oluşturmaktır. Silikon, tek başına alüminyum döküm alaşımlarının mukavemetine çok az katkıda bulunur, ancak magnezyumla birleşerek Mg_2Si'yi oluşturmak için kullanıldığında çok etkili bir güçlendirme düzeyi sağlar Zirkonyum katkılanması yeniden kristalleşmeyi engeller. Bu tespitler bazı araştırmacılar tarafından desteklenmektedir. Al-Si-Cu-Mg alaşımlarının karmaşık mikroyapılar geliştirdiği iyi bilinen bir gerçektir ve çeşitli çalışmalarda yayımlanmıştır [10-14]. Dökme haldeki yapı α-Al, ötektik silikon, farklı morfolojilere sahip bakır alüminüt (Al_2Cu), Magnezyum silisit (Mg_2Si), ve Q fazı ($Al_5Cu_2Mg_8Si_6$) gibi intermetalik fazlar içerir.

Şekil 10 ve 11'de verilen EDS/mapping spektrumda (haritalama analizinde) her bir Al, Mg, Si, Zn, Cu ve Zr elementinin en alt (Bölge 1) ve en üst (Bölge 8) kısımlardaki dağılımı farklı renklerle elde edilmiştir. Şekil 10'de verilen EDS spektrumundan görüldüğü gibi, numunenin en alt kısmı için ağırlıkça 82.95 Al, 3.45 Mg, 3.98 Si, 5.20 Cu, 3.19 Zn ve 1.26 Zr bileşim değerleri belirlenmiştir. Cu ve Zr miktarları nominal bileşim değerlerinden biraz yüksek çıkarken diğer Si, Mg ve Zn değerleri biraz düşük çıkmıştır. Benzer şekilde Şekil 11'de verilen EDS spektrumundan görüldüğü

gibi, numunenin en üst kısmı için ağırlıkça 80.81 Al, 5.12 Mg, 6.15 Si, 3.95 Cu, 3.58 Zn ve 0.39 Zr bileşim değerleri belirlenmiştir. Bu spektrumda da Mg ve Si miktarları nominal değerden biraz yüksek çıkarken özellikle Cu ve Zr değerleri biraz düşük çıkmıştır. Bu durum muhtemelen daha önce bahsedildiği gibi konveksiyon ve buharlaşmanın etkisinden kaynaklanabilir.

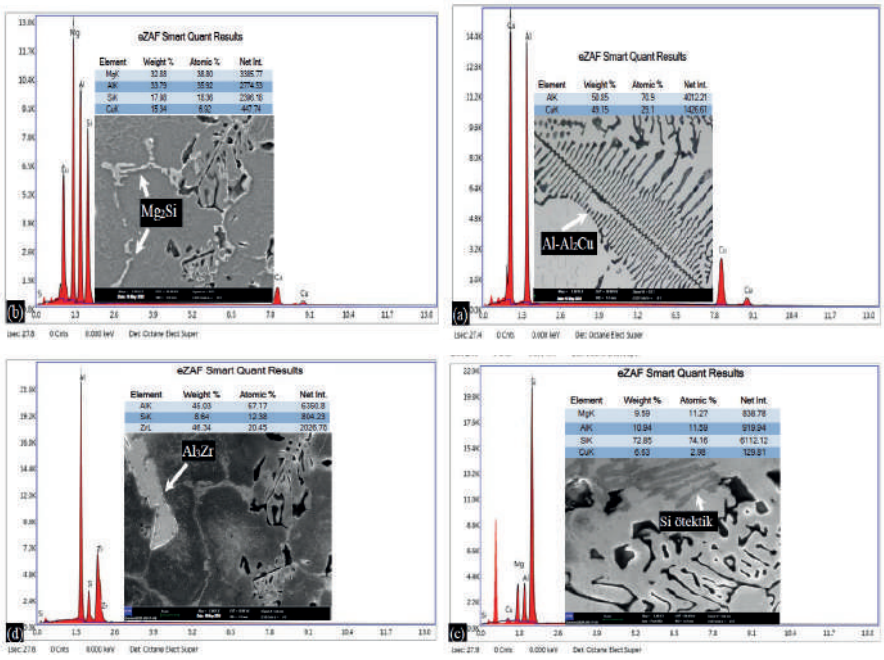

Şekil 9. *α–Al matrisi içinde oluşmuş Si ötektik ve intermetalik fazların EDS spektrumları (a) Al_2Cu (b) Mg_2Si (c) Si Ötektik fazı (d) Al_3Zr*

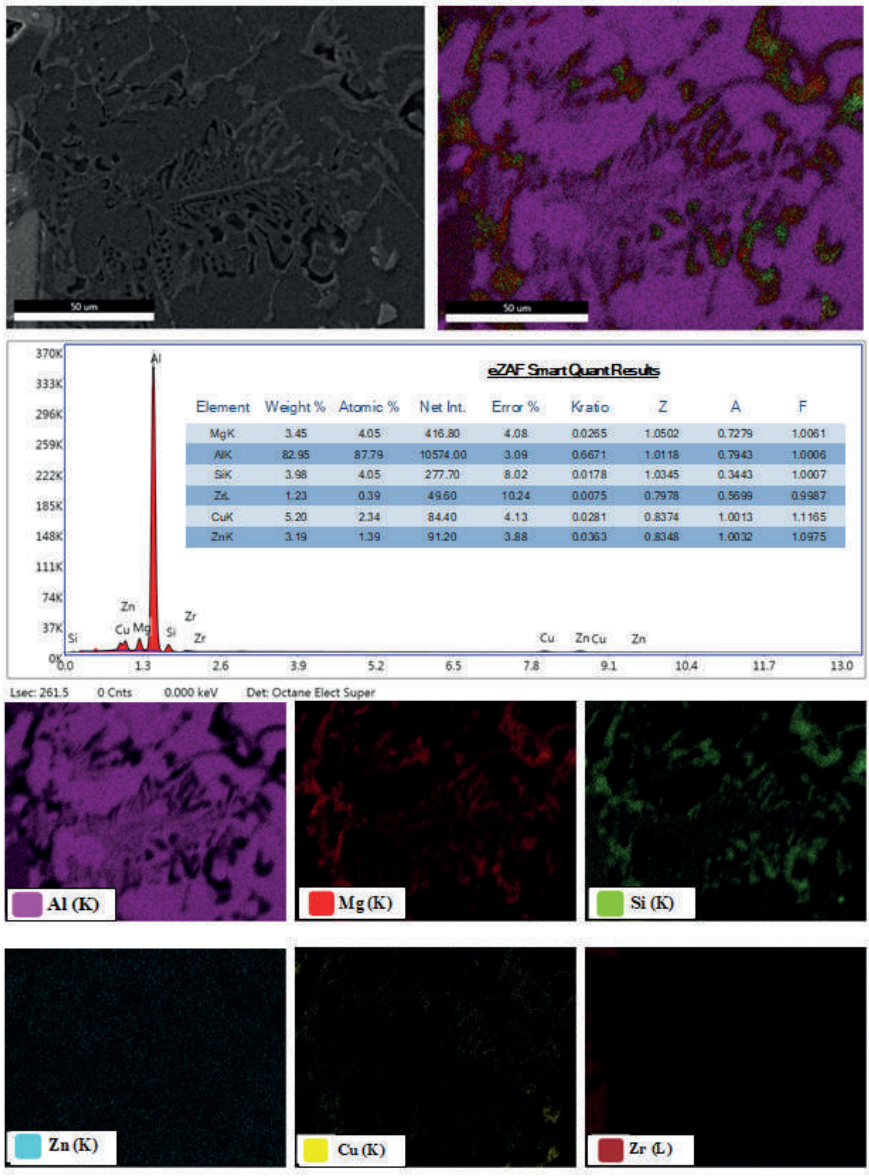

Şekil 10. Al-5Cu-5Si-5Mg-5Zn-1Zr alaşımının en alt kısmı (bölge 1) için EDS spektrumu ve elementel haritalama analizi

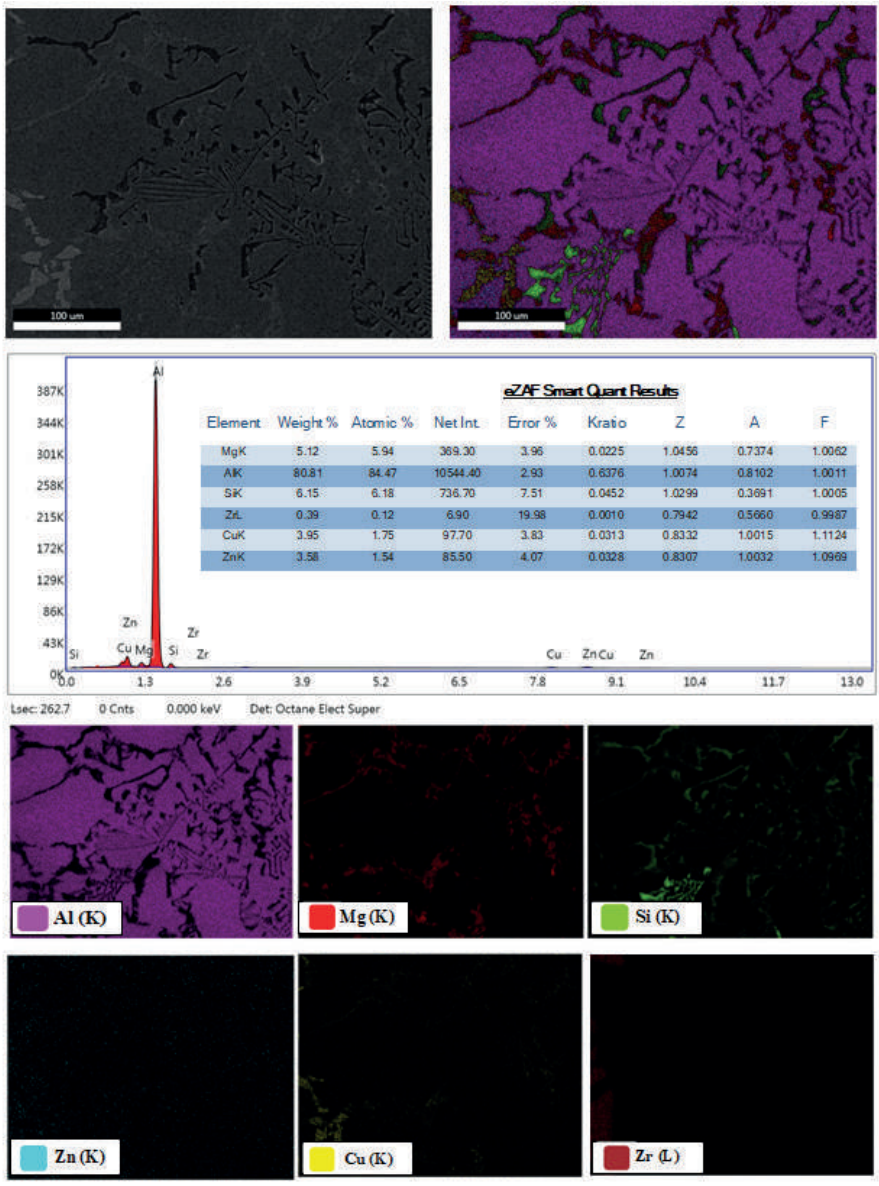

Şekil 11. Al-5Cu-5Si-5Mg-5Zn-1Zr alaşımının en üst kısmı için (bölge 8) için EDS spektrumu ve elementel haritalama analizi

Çalışılan alaşımın en alt ($\dot{T}$=2.77 °C/s) ve en üst ($\dot{T}$=0.88 °C/s) kısımları için ana matris ve içinde oluşan fazlar, XRD analizi ile de belirlenmiştir. 2.77 °C/s ve 0.88 °C/s soğuma hızlarında katılaşan bölgeler için elde edilen XRD desenleri Şekil 12'de gösterilmektedir. Bu fazlar Şekil 13'de verilen SEM görüntüsü üzerinde tanımlanmıştır.

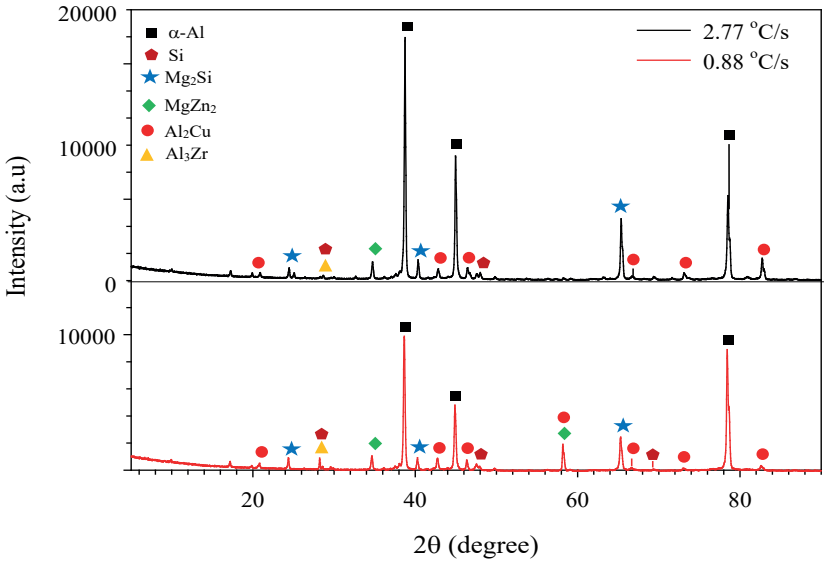

Şekil 12. 2.77 °C/s ve 0.88 °C/s soğuma hızlarında katılaşan bölgeler için XRD desenleri

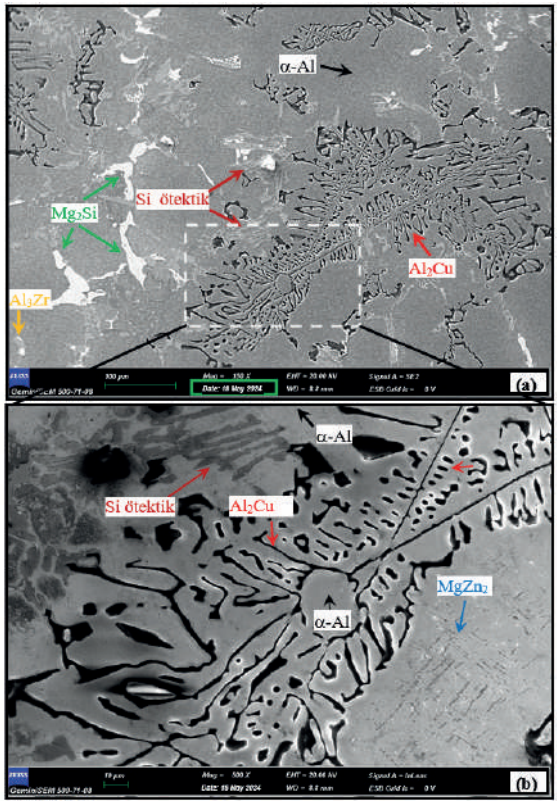

Şekil 13. Ana matris fazı (α-Al) içinde yer alan intermetalik fazların SEM görüntüsü

Belirtildiği gibi, α–Al (matris fazı), Al_2Cu, Mg_2Si, $MgZn_2$, Si ötektik fazı ve Al_3Zr fazı, karşılık gelen yüksek sayıda piklerle doğrulanmıştır. Hem EDS analizleri hem de XRD analizi, çalışılan alaşım için α-Al ve Si ötektik fazlarına ilaveten Al_2Cu, Mg_2Si, $MgZn_2$, ve Al_3Zr intermetalik fazların mevcut olduğunu göstermektedir. Bazı pikler diğer piklerden daha şiddetlidir. 38.4°, 44.4° ve 78°'deki oluşan pikler (siyah kareler) α-Al fazına, 65.2°'de oluşan pik (mavi yıldız) Mg_2Si fazına, 58.1°'de oluşan pik (kırmızı daire ve yeşil baklava dilimi) Al_2Cu ve $MgZn_2$ intermetalik fazlarına karşılık gelmektedir. Diğer fazların pikleri daha zayıf şiddetli olarak ortaya çıkmıştır.

4. TARTIŞMA VE SONUÇ

Bu çalışma, Al-5Cu-5Si-5Mg-5Zn-1Zr çok bileşenli alüminyum alaşımının kararsız hal ısı akışı rejimi altında serbest katılaştırılmasının mikroyapısal özellikleri ve faz oluşumu üzerindeki etkilerini araştırmıştır. Serbest katılaştırma deneyleri, numune boyunca farklı soğuma hızları oluşturmak için özenle tasarlanmış bir deney düzeneği kullanılarak gerçekleştirilmiştir. Optik mikroskopi, taramalı elektron mikroskobu, enerji dağılımlı X-ışını spektroskopisi ve X-ışını kırınımı gibi bir dizi ileri karakterizasyon tekniği, katılaşmış alaşımın farklı bölgelerdeki mikro yapısını ve faz bileşimini analiz etmek için kullanılmıştır.

Çalışmanın temel bulguları aşağıdaki gibi özetlenebilir:

Soğuma Hızının Dendritik Yapı ve Ötektik Mesafe Üzerine Etkisi

Soğuma hızı, katılaşan alaşımların mikro yapısını şekillendiren en önemli faktörlerden biridir. Bu çalışmada, soğuma hızının artmasıyla, dendritik yapıda belirgin bir incelme gözlemlenmiştir. Düşük soğuma hızlarında, dendrit kolları daha kalın ve daha uzun olup daha kaba bir dendritik ağ oluşturur. Soğuma hızı arttıkça, dendrit kolları giderek incelir ve kısalır, bu da daha ince taneli bir mikro yapı ile sonuçlanır. Bu gözlem, yüksek soğuma hızlarında çekirdeklenme (nükleasyon) hızının artması ile açıklanabilir. Hızlı soğuma, eriyik içinde daha fazla nükleasyon bölgesi yaratır ve bu da daha fazla dendritin aynı anda büyümesine yol açar, bu da daha ince bir dendritik yapı ile sonuçlanır.

Benzer şekilde, ötektik mesafe, soğuma hızının artmasıyla azalmıştır. Ötektik mesafe, ötektik yapıyı oluşturan iki komşu faz arasındaki mesafedir ve katılaşma hızı ile ters orantılı olarak değişmektedir. Yavaş soğuma, ötektik fazların büyümesi için daha fazla zaman sağlar ve daha büyük ötektik mesafelere yol açar. Hızlı soğuma ise ötektik büyümesini kısıtlar ve daha ince ve daha sık dağılmış bir ötektik yapı ile sonuçlanır. Bu çalışmada, ötektik mesafe ile soğuma hızı arasındaki ilişki, $\lambda = A\dot{T}^{-n}$ denklemi ile nicelendirilmiş

ve n değeri 0.53 olarak bulunmuştur. Bu değer, literatürde yer alan Al-Cu esaslı alaşımlar için bulunan değerlerle uyumludur [15-17].

İntermetalik Fazların Oluşumu ve Dağılımı

Al-5Cu-5Si-5Mg-5Zn-1Zr alaşımı, katılaştırma sırasında α-Al matris fazı içinde farklı intermetalik fazlar oluşturmuştur. SEM-EDS ve XRD analizleri, Al_2Cu, Mg_2Si, $MgZn_2$ ve Al_3Zr fazlarının varlığını doğrulamıştır. Bu intermetalik fazlar, alüminyum alaşımlarında yaygın olarak bulunan ve mukavemet, sertlik ve korozyon direnci gibi özellikleri etkilediği bilinen fazlardır.

Soğuma hızının artması, intermetalik fazların morfolojisi ve dağılımında da değişikliklere neden olmuştur. Yüksek soğuma hızlarında, intermetalik fazlar daha ince ve daha homojen bir şekilde dağılmış olarak gözlemlenirken, düşük soğuma hızlarında daha kaba ve düzensiz bir dağılım gözlemlenmiştir. Bu gözlem, hızlı soğumanın ikinci fazların nükleasyonunu hızlandırması ve büyümeleri için daha az zaman bırakması ile açıklanabilir [18]. Sonuç olarak, yüksek soğuma hızlarında daha ince ve daha homojen dağılmış intermetalik fazlar oluşur.

Sonuç

Bu çalışma, kararsız hal ısı akışı rejimi altında serbest katılaştırma yoluyla Al-5Cu-5Si-5Mg-5Zn-1Zr çok bileşenli alüminyum alaşımının mikro yapısının ve faz bileşiminin etkin bir şekilde kontrol edilebileceğini göstermiştir. Soğuma hızını değiştirerek, dendritik yapı, ötektik mesafe ve intermetalik fazların oluşumu ayarlanabilir, bu da malzemenin nihai özelliklerini optimize etmek için kullanılabilir. Bu bulgular, çok bileşenli alüminyum alaşımlarının geliştirilmesi ve belirli mühendislik uygulamaları için malzemelerin özelliklerinin özelleştirilmesi için önemli etkilere sahiptir.

Örneğin, otomotiv ve havacılık endüstrileri, hafif ve yüksek mukavemetli malzemeler talep etmektedir. Bu çalışmada incelenen Al-5Cu-5Si-5Mg-5Zn-1Zr alaşımı, bu sektörler için potansiyel bir adaydır. Kararsız hal katılaştırma tekniği kullanılarak, alaşımın mikroyapısı ve dolayısıyla mekanik özellikleri, belirli uygulama gereksinimlerini karşılayacak şekilde ayarlanabilir.

Bu çalışmanın sonuçları, yeni çok bileşenli alüminyum alaşımlarının geliştirilmesi ve mevcut alaşımların performansının iyileştirilmesi için yol gösterici olabilir. Ayrıca, kararsız hal katılaştırma tekniğinin, malzemelerin özelliklerini kontrol etmek için kullanılabileceği diğer alaşım sistemlerine de uygulanabilir.

Gelecekteki Araştırma Önerileri

Bu çalışma, kararsız hal ısı akışı rejiminin çok bileşenli alüminyum alaşımlarının mikroyapısını kontrol etmek için etkili bir yöntem olduğunu göstermiştir. Elde edilen sonuçlar, gelecekteki araştırmalar için aşağıdaki gibi çeşitli öneriler sunmaktadır:

- **Mekanik Özelliklerin İncelenmesi:** Farklı soğuma hızlarında katılaştırılan Al-5Cu-5Si-5Mg-5Zn-1Zr alaşımının mekanik özellikleri (sertlik, çekme dayanımı, yorulma dayanımı, aşınma direnci) detaylı bir şekilde incelenebilir. Bu, mikroyapı ile mekanik özellikler arasındaki ilişkiyi daha iyi anlamamıza yardımcı olacaktır.
- **Isıl İşlem Etkilerinin Araştırılması:** Farklı ısıl işlem parametrelerinin (çözündürme sıcaklığı ve süresi, yaşlandırma sıcaklığı ve süresi) mikroyapı ve mekanik özellikler üzerindeki etkileri araştırılabilir. Bu, alaşımın özelliklerini optimize etmek için uygun ısıl işlem koşullarının belirlenmesini sağlayacaktır.
- **Katılaşma Modelleri:** Bu çalışmada elde edilen deneysel veriler, kararsız hal ısı akışı rejimi altında çok bileşenli alüminyum alaşımlarının katılaşma davranışını modellemek için kullanılabilir. Geliştirilen modeller, farklı katılaştırma koşullarında alaşımın mikroyapısını tahmin etmek için kullanılabilir.
- **Diğer Alaşım Sistemleri:** Bu çalışmada kullanılan yöntem ve analizler, diğer çok bileşenli alüminyum alaşımları ve hatta farklı metalik sistemler için de uygulanabilir. Bu, farklı alaşım sistemlerinin katılaşma davranışını anlamamıza ve özelliklerini kontrol etmek için yeni yöntemler geliştirmemize yardımcı olacaktır.

TEŞEKKÜR

Bu çalışma Erciyes Üniversitesi Bilimsel Araştırma Projeleri Koordinasyon Birimi tarafından FBA-2023-12765 numaralı proje ile desteklenmiştir. Yazarlar finansal destek için Erciyes Üniversitesi'ne teşekkür eder.

Kaynaklar

1. ASM International. (1996). *ASM specialty handbook: Aluminum and aluminum alloys*.
2. Davis, J. R. (2001). *Aluminum and aluminum alloys*. ASM International.
3. Fakıoğlu, A., Özyürek, D., & Yılmaz, R. (2012). Effects of different heat treatment conditions on fatigue behavior of AA7075 alloy. *High Temperature Materials and Processes, 32*(4), 345-351.
4. Yılmaz, R., Özyürek, D., & Kibar, E. (2012). The effect of retrogression parameters on hardness and wear behaviours of 7075 aluminium alloys. *Journal of the Faculty of Engineering and Architecture of Gazi University, 27*(2), 429-438.
5. Baek, E. J., Ahn, T. Y., Jung, J. G., Lee, J. M., Cho, Y. R., & Euh, K. (2017). Effects of ultrasonic melt treatment and solution treatment on the microstructure and mechanical properties of low-density multicomponent Al70Mg10Si10Cu5Zn5 alloy. *Journal of Alloys and Compounds, 696*, 450-459.
6. Ibrahim, M. F., Samuel, E., Samuel, A. M., & Al-Ahmari, A. M. A. (2011). Metallurgical parameters controlling the microstructure and hardness of Al–Si–Cu–Mg base alloys. *Materials & Design, 32*(5), 2130-2142.
7. Stefanescu, D. M. (2015). *Science and engineering of casting solidification* (2nd ed.). Springer.
8. Campbell, J. (2008). *Complete casting handbook: Metal casting processes, metallurgy, techniques and design*. Butterworth-Heinemann.
9. Kurz, W., & Fisher, D. J. (1998). *Fundamentals of solidification* (4th ed.). Trans Tech Publications.
10. Sandoval, J. H., Elizondo, G. H. G., Samuel, A. M., Valtiierra, S., & Samuel, F. H. (2014). The ambient and high temperature deformation behavior of Al–Si–Cu–Mg alloy with minor Ti, Zr, Ni additions. *Materials & Design, 58*, 89–101.
11. Hernan, G. E. G. (2016). *Effect of Ni, Mn, Zr and Sc additions on the performance of Al-Si-Cu-Mg alloys* [Doctoral dissertation, Université du Québec à Chicoutimi].
12. Shaha, S. K. (2015). *Development and characterization of cast modified Al-Si-Cu-Mg alloys for heat resistant power train applications* [Doctoral dissertation, Ryerson University].
13. Mohamed, A., & Samuel, F. (2013). Microstructure, tensile properties and fracture behavior of high temperature Al–Si–Mg–Cu cast alloys. *Materials Science and Engineering: A, 577*, 64-72.

14. Lasa, L., & Ibabe, J. R. (2004). Evolution of the main intermetallic phases in Al-Si-Cu-Mg casting alloys during solution treatment. *Journal of Materials Science, 39*, 1343-1355.

15. Rosso, E., Santos, C. A., & Garcia, A. (2022). Microstructure, hardness, tensile strength, and sliding wear of hypoeutectic Al–Si cast alloys with small Cr additions and Fe-impurity content. *Advanced Engineering Materials, 24*, Article 2001552.

16. Araujo, R. L. M., Kikuchi, R. H. L., Barros, A. S., Gomes, L. G., Moutinho, D. J. C., Gonçalves, F. A., Moreira, A. L. S., & Rocha, O. F. L. (2016). Influence of upward and horizontal growth direction on microstructure and microhardness of an unsteady-state directionally solidified Al-Cu-Si alloy. *Revista Matéria, 21*, 261–269.

17. Shaha, S. K., Czerwinski, F., Chen, D. L., & Kasprzak, W. (2015). Dislocation slip distance during compression of Al–Si–Cu–Mg alloy with additions of Ti–Zr–V. *Materials Science and Technology, 31*(1), 63-72.

18. Callister, W. D., & Rethwisch, D. G. (2018). *Materials science and engineering: An introduction* (10th ed.). Wiley.

Chapter 3

CNTs and BNNTs in Aerospace Enginnering

Murat Metehan Türkoğlu[1]

Abstract

The continuous efforts to enhance performance and efficiency in the aerospace industry necessitate the development of advanced materials with improved thermal stability and mechanical strength. In this section, the potential applications of Carbon (CNTs), Boron Nitride Nanotubes (BNNTs) in the aerospace sector are examined. In this context, their advantages in key areas such as thermal and mechanical properties and weight reduction of aircraft are analyzed. Composite materials like CNTs and BNNTs have the potential to significantly improve the strength-to-weight ratio of structural components of aircraft, thereby enhancing fuel efficiency and considerably reducing carbon emissions. This study discusses the advantages of nanocomposite structures such as CNTs and BNNTs in reshaping aerospace architecture in terms of energy efficiency and strength.

1. INTRODUCTION

Starke and Staley (1996) showed that the strength/weight ratio was important in material selection fort he first aircraft and they noted that nanocomposite materials were crucial for the aviation industry. Over time, due to the problems encountered in the aviation industry, it has been showed that composite materials have interesting additional properties. Throughout the 1990s, when aircraft fleets were examined, the need for composite materials with corrosion and damage resistance was indicated [1]. This evolution in requirements led to the development of advanced composite materials to address these challenges. With the static and dynamic strength calculations used in today's modern aircraft designs, the lifespan of aircraft has been extended to 70 years, and it has been reported that some bomber aircraft remain in the inventory for nearly 40 years due to their low

1 İstanbul Gelişim Üniversitesi Uçak Mühendisliği (İngilizce)-İstanbul Teknik Üniversitesi Savunma Teknolojileri Programı, mmturkoglu@gelisim.edu.tr, mmturkoglu@itu.edu.tr ORCID ID 0000-0002-2857-866X

https://doi.org/10.58830/ozgur.pub575.c2360

frequency of use [2]. The prolonged service life of these aircraft illustrates the effectiveness of these material innovations. The use of composite materials allows fewer parts to be used at each stage. As the number of parts decreases, the number of spare parts and the budget allocated for them also decrease, which is very important for the continuity of the system [3]. For example, materials such as titanium have high corrosion resistance but are quite expensive [4]. Thus, the cost-effectiveness of composites over metals like titanium has also boosted their adoption. Carbon nanotubes usually have high aspect ratios, but their small lengths make them challenging to process. The difficulty of processing is demonstrated by the fact that, while Zheng et al. (2004) [5] has succeeded in synthesizing CNTs several centimeters long, mass production of long nanotubes is still not feasible, which is a significant barrier to their widespread application in aerospace. Further research by Kyoung et al. (2011) [6] produced micrometer-thick, free-standing CNTs using highly oriented multi-walled carbon nanotube airgel sheets, potentially enhancing the commercial manufacturability of CNT-based terahertz polarizers. Similarly, Okawa et al. (2007) reported on JAXA's development of a propulsion system using CNT field emission cathodes, highlighting the versatile applications of CNTs in both terrestrial and extraterrestrial technologies. [7] Unlike conventional filled polymers, Polymer Nanocomposites (PNCs) require relatively low dispersant loadings, making them an important candidate for aerospace applications .[8] Regarding aerospace applicability, thermal electrical and mechanical properties of PNCs were experimentally and theoretically investigated by Njuguna et al. and results were shown to be superior to other aerospace materials. [9] Moreover, Bellucci et al. (2005) focused on enhancing the mechanical properties of CNT-based nanocomposites by improving the synthesis methods and ensuring uniform dispersion of CNTs in epoxy resin matrices. Their research highlights the resistance to compression and stability against buckling. These findings underscore the significant potential of CNT composites in aerospace. [10] The challenges of dispersion and alignment in nanocomposites lead to randomly oriented PNCs, which are often used in low volumes because their morphology cannot be controlled. However, the modulus and electrical conductivity of carbon nanotube (CNT) composites aligned with controlled morphology are maximum along the CNT axis. It has been determined that aligned CNTs have higher strength and electrical conductivity [11] The development and integration of CNTs into spacecraft structures, notably for the Juno spacecraft, as detailed by Rawal et al. (2011), not only enhance electrostatic dissipation and shielding but also improve overall spacecraft performance in terms of mechanical properties,

thermal and electrical conductivity, and fracture toughness. These advances underscore the broad applicability and potential of nanocomposites in high-stress environments. [12]

Recent developments and reduced production costs of BNNTs have reawakened interest in these nanomaterials in the aviation industry due to their transformative potential for aviation technology. Essentially, BNNTs are nanotubes made up of boron and nitrogen atoms arranged in a hexagonal lattice, forming robust covalent bonds, similar to CNTs. This structural similarity to CNTs provides a basis for comparison, yet it is their unique properties that distinguish BNNTs in aerospace applications. The unique molecular configuration of BNNTs provides numerous advantages to their application as a nanomaterial. For instance, BNNTs exhibit remarkable tensile strength, enabling them to be resistant to deformation and enduring mechanical stress. Moreover, the bond between boron and nitrogen demonstrates exceptional thermal stability, allowing it to maintain its structural integrity even under extremely elevated temperatures. Furthermore, BNNTs not only display chemically inert behavior but also, unlike CNTs, act as electrical insulation. This characteristic is due to boron nitride's large energy bandgap (5-6 eV), which makes BNNTs an excellent choice for electrical insulation applications such as aerospace and electronic components. Overall, further exploration of the application of BNNTs has uncovered their distinctive characteristics, including their improved tensile strength, thermal stability, chemical resistance, and corrosion resistance. These properties make the BNNT-based nanocomposites suitable for a range of aerospace uses, particularly in situations where materials need to endure extreme temperatures, harsh environments, and mechanical strains. Thibeault et al (2016) [13] demonstrated that hydrogen-containing BNNTs effectively protect against cosmic radiation and neutrons over a broad energy range. Additionally, Yamaguchi et al. (2012) [14] explored that nanohybrid BNNT/aluminum matrix composites could withstand at least nine times higher stresses compared to no-armed Al metal. It has been reported that this pioneering work could be a step towards the production of ultra-light and super-strong structural materials for aerospace applications. Zhang et al. (2009) [15] contribute to this area by developing heteronanotubes that combine carbon and boron nitride elements, potentially combining the best properties of CNTs and BNNTs. These heteronanotubes indicated that the stability of C-BN heteronanotubes (C-BNNTs) was comparable to carbon nanotubes, and they were found to be direct gap semiconductors with varying band gaps.

2. AEROSPACE APPLICATIONS

2.1. Fundamental problems in Aerospace Industry

Fundamental problems in use of structural aerospace are divided into categories as follows;

a) **The Cost and Repairability**

Applications of advanced materials in aviation and space have become an advanced industry. Global aircraft production is worth approximately US$200 billion annually [16] and accounts for approximately half of annual sales in aerospace and defense. In addition, the cost of raw material production is estimated to be 12 billion US dollars annually. [17] Material selection is critical for structural applications to define the aspects of the life cycle, ease of production, and service conditions. With the proper evaluation of material properties, safer, more durable, and cost-effective structures can be obtained through well-defined selection and optimization processes. Especially, in aerospace structures, the selection of materials is a prominent factor for designing structures that can carry loads without adding unnecessary weight. Lighter structures are better for aircraft because every extra kilogram added to structures plays a key role in earning less revenue from cargo, requiring more fuel to carry it. Although both higher strength-to-weight ratios, referred to as specific strength, and strength-to-cost ratios are desirable properties, higher specific strength increases the strength-to-cost ratio, which means materials with higher specific strength are more expensive. The main problem with costs is that no manufacturer will continue to produce large quantities because the materials may cause another problem while they are under development or the materials may encounter a new problem and therefore prices cannot fall to acceptable levels.

Table 1. Prices and physical properties of composite materials and metal alloys used in aircraft [18]

	Graphite Composite (aerospace grade)	Graphite Composite (commercial grade)	Fiberglass Composite	Aluminum 6061 T-6	Steel, Mild
Cost $/kg	$44-$550+	$10-$45	$3.5-6.5	$6.5	$0.65
Strength (MPa)	620-1400	350-620	140-240	240	410
Stiffness (GPa)	70-350	55-70	7-10	70	210
Density (kg/m^3)	1400	1400	1500	2800	8300

b) **The Preparation Phase for Technological Breakthroughs**

Although the history of composite materials dates back fifty years, the technology required for their mass production does not exist. For example, due to the high strength of composite material, it is extremely difficult to cut it to the appropriate size for a required application [19]. The time it takes to bring the materials used in the aviation industry to the market, the properties of nanomaterials, or the patent process can be evaluated as technical difficulties.

c) **Weight Budget**

In order to ensure that flights in the aerospace industry are safe, efficient and economical, care is taken to select the right structural materials for the design of aircraft and their components. Structural materials must be resistant to abrasion and puncture (hardness), have the ability to resist deformation (strength), have the ability to bend or twist without breaking (ductility), and have the ability to return to their original size. They must also have the properties of being flexible and good conductors of heat or electricity. Steel alloys, aluminum alloys, composite materials, plastics, rubber, fabrics and wooden materials are used in aircraft for reasons such as the amount of load, exposure to various environmental factors such as stress, excessive heat and fire, and the purpose of the aircraft (subsonic or supersonic).

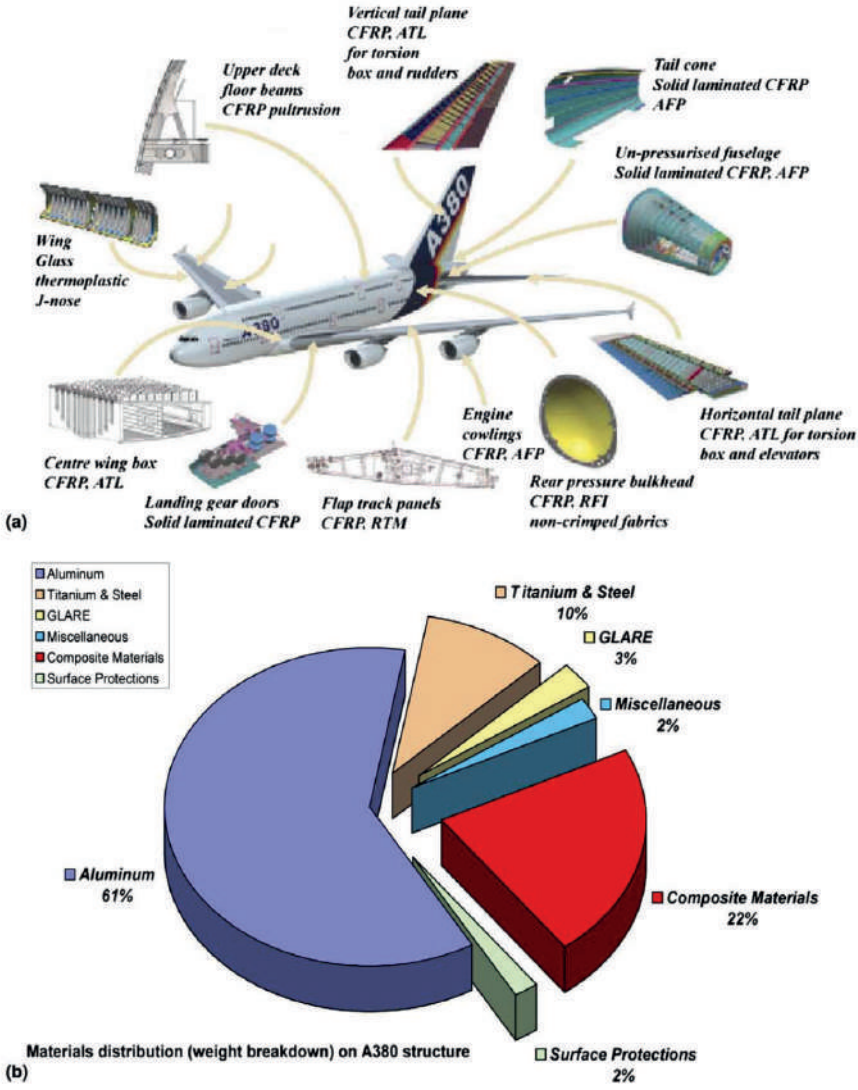

Figure 1. (a) Composite materials and thermoplastics used in the A380 and (b) their distribution on the architecture [20]

The strength coupled with the low density provides conceptual design objectives for aerospace structures hence, aluminum alloys (mainly aluminum-copper (2XXX series), and aluminum-zinc (7XXX series) have been widely used since the 1930s. However, aluminum alloys have major flaws. The absence of an strength limit and their susceptibility to corrosion restrict their areas of application. The vibrations produced by engines lead to crack formation and propagation, which is a major issue for aircraft

structures. Steel alloys have higher strength compared to aluminum and can better withstand cyclic loads and fatigue below the endurance limit. On the other hand, steel is 2.5 times denser than aluminum, increasing the weight of the aircraft and leading to higher fuel consumption. Their specific strength is the same as aluminum. Titanium alloys, on the other hand, have a good fatigue strength/tensile strength ratio and corrosion resistance but are disadvantageous due to their high density. For such reasons, composite materials with strong fibers embedded in a matrix have emerged.

In modern aircraft such as the Boeing 787 Dreamliner, more than 50% composite materials are used. Due to their high strength-to-weight and stiffness-to-weight ratios, they provide a 10-15% weight savings in the manufacturer's empty mass (MEM), thus being extensively used in civil aircraft and between 15-25% in military aircraft.

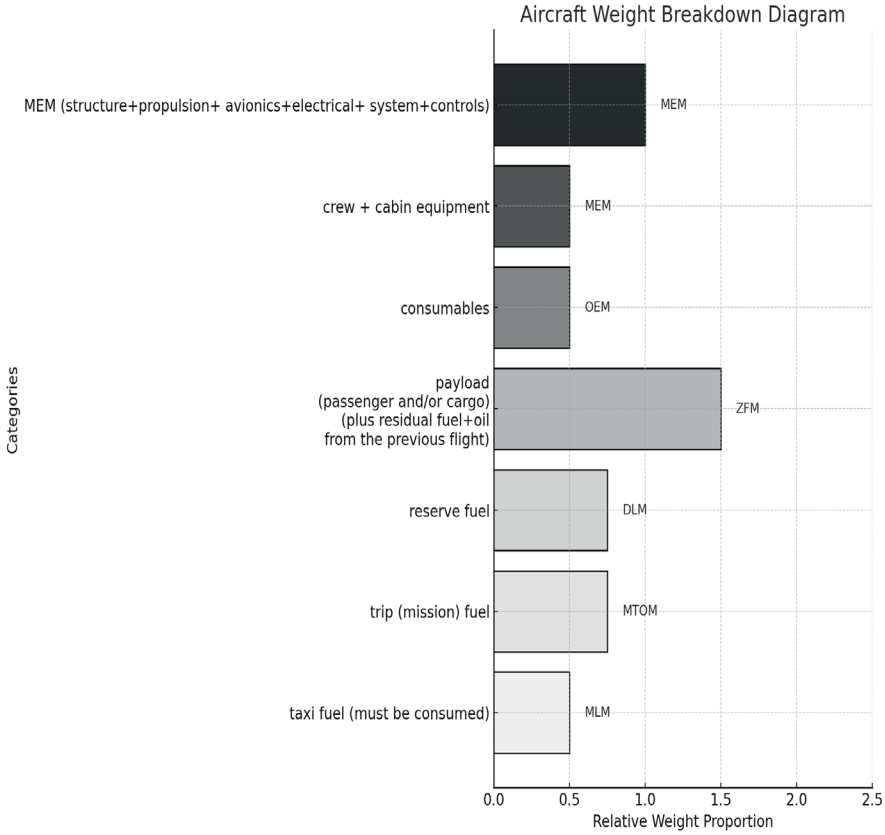

Figure 2. The aircraft weights diagram

Naturally, lightweight design is highly important for Airbus, which is planned to carry 35% more passengers (555 people) than the current aircraft with the highest passenger capacity. Thanks to the composite materials planned for use in Airbus, it is estimated that it will consume 20% less fuel per passenger.

d) **Sustainability and Service Life**

Sustainability is key issue in the aerospace industry. In this context, the Advisory Council for Aeronautical Research in Europe was established in Paris. Among the main goals that the institution plans to achieve by 2050 are a reduction of up to 75% in CO2 emissions, up to 90% in NOx emissions, and a 65% reduction in noise pollution. Therefore, researching new technologies is of utmost critical importance [21]

Table 2: Comparison of structures used in modern aircraft in terms of mass percentage. [22]

Material	Boeing 747	Boeing 777	Boeing 787	Difference
Aluminum alloys	81	70	20	↘
Steel alloys	13	11	10	↘
Titanium alloys	4	7	15	↖
Composites (various types)	1	11	50	↖

In order to quantify the danger, nanoparticles used in aircraft are defined as particles with a length/diameter greater than 3. This criterion has been established for the hazard assessment of natural and artificial mineral fibers. [23]

Turkish Air Forces Command launched the Özgür Project on 15 December 2010 for the modernization of F-16 aircraft that were not modernized within the scope of the CCIP project (Common Configuration Implementation Program, US Air Force was prepared for F-16 aircraft). Another aim of this study is to present practical concrete alternatives regarding modernization and evaluate their possible consequences. With the implementation of the Özgür project, new technologies will be adapted to aging warplanes but repair costs are expected to increase since old warplanes will be used. However, it is envisaged to become less dependent on foreign sources compared to producing new aircraft.

Gasses containing composite materials can cause risks. The fire-resistant composites in aircraft are shown in detail and their effects are discussed [24].

Air pollution in aircraft cabins was examined in the 1950s [25]. The effects of cabin air pollution on aircraft crews have been recorded [26]. Aerotoxic Syndrome, which describes exposure to pollutants, was introduced in 2000 [27].

e) **Airworthiness certification**

Authorities that monitor airworthiness evaluate the design of aviation materials according to qualification procedures. For example, patent processes progress faster due to the existing database of metals that has been accumulated over many years and material properties that have already been approved within the scope of airworthiness [28]. However, quality-patent processes are quite complex due to the characteristics of composites, the versatility of weaving, multiple production processes, production environment, and testing methods. Moreover, it is very difficult to obtain patents until additional tests are performed after the manufacture of complex composite parts [29]. Due to the complex nature of composite material properties, it is necessary to spend a lot of time and budget on qualification procedures.

Due to difficulty and risk, the patent procedures for the aviation and space industry are quite expensive and require long periods of time, as well as being uncertain and constantly renewing dynamic processes. For example, the FAA's regulations have over 1,000 pages and are constantly being developed to include new technologies. Additionally, the certification process is quite expensive: According to a study by the AIA, the average cost of certifying in the United States is approximately $1 billion, with the average time being approximately seven years. Finally, certification in the aerospace industry requires a high level of technique and expertise. Startups are therefore forced to rely on consultants or partners for certification [30].

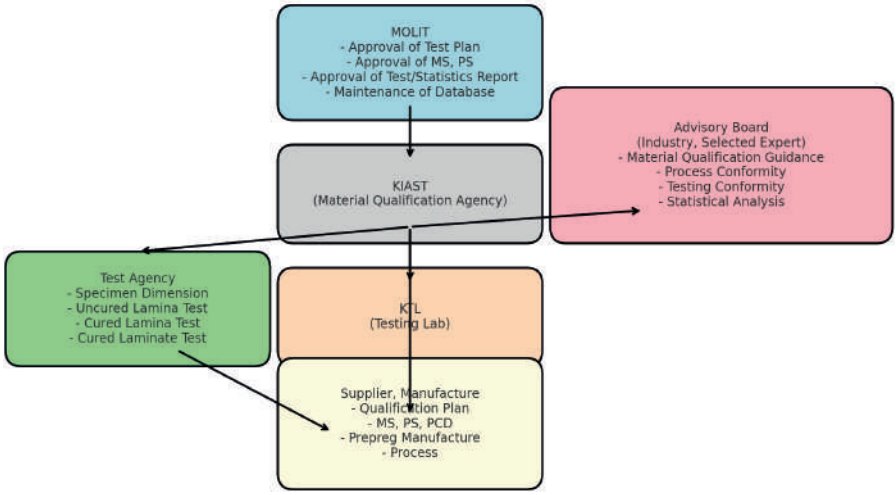

Figure 3. Composite Material Qualification System

f) **Fast Prototyping**

New approaches in the aerospace industry may provide solutions to existing problems, but they also come with significant risks and costs that require investment in technology. Long time periods are therefore needed to reduce risk. Adaptive wings or wingtips, reducing turbulent friction resistance, etc. are processes that require a long time [31]. For example, the problem of increasing cruising speed (Mach number) and the intense drag increase that occurs due to the presence of intense and strong shocks are both theoretical and very complex processes to produce materials resistant to these strong shocks.

Although composite materials have significant advantages, they also have some disadvantages, for example relatively low interlayer strength, poor durability, and brittleness due to exposure to ultraviolet radiation [32]. Therefore, new types of material studies are vital. In addition, topics such as cost trends and long-term maintenance and repairability are decisive for composite selection and determine the usability limit of the material. The aerospace industry must keep the design process long due to aerodynamic heating and thermal management, structural integrity and material limitations, propulsion and engine design challenges, thermal stress analysis, structural design optimization, hypersonic experiment constraints, etc.

2.2. Nanomaterials

CNTs are cylindrical structures with diameters typically ranging from 3 nanometers, formed by the arrangement of carbon atoms in a hexagonal lattice [33]. CNTs have a Young's modulus of approximately 1 terapascal (TPa) and a strength 10-100 times higher than that of steel due to their sp^2 hybrid covalent bonds [34]. Furthermore, they have electrical conductivity ranging from 10^5 to 10^7 S m^{-1} [35]. CNTs have a high aspect ratio, enabling them to convert an insulating polymer into a conductive composite even at very low loadings [36]. Following the pioneering work by Iijima and colleagues on carbon nanotubes, there has been great interest in nanomaterials [37]. For instance, boron nitride nanotubes (BNNTs) are structural analogs of carbon nanotubes, but instead of a carbon-carbon pair, they are arranged by substituting a boron-nitrogen pair [38]. Moreover, there are differences in electron density distributions between BNNTs and CNTs [39]. BNNTs have an elastic modulus of 1 TPa and a tensile strength of 60 GPa and their excellent flexibility makes them very suitable for composite applications. They exhibit excellent thermal conductivity (~350 $Wm^{-1}K^{-1}$) and maintain stability even at high temperatures such as 900 °C and above 1000 °C in an oxygen-rich environment [40]. BNNTs exhibit superior thermo-oxidative stability compared to CNTs, making them suitable materials for harsh environments. BNNTs, especially in conjunction with the 10B isotope, have a significant neutron absorption and scattering cross-section, making them highly potential candidates for radiation shielding. It is conceivable that they could be used to protect satellites in low Earth orbit from radiation. Furthermore, BNNTs not only exhibit chemically inert behavior but also serve as electrical insulation, unlike CNTs. This characteristic is due to the wide energy bandgap (5-6 eV) of boron nitride, making BNNTs an ideal candidate for electrical insulation applications in aerospace and electronic components.

In the aerospace industry, it is highly critical for a material to simultaneously possess various desired properties. Multifunctional nanocomposites are well-suited for this task. Such composites contribute to simplified production processes, reduced system complexity, cost savings, enhanced product performance, and increased reliability. The ability of BNNTs to bond with CNTs due to their structural similarity has paved the way for the development of advanced composite materials. Zhang et al. (2009) [41] developed hetero-nanotubes that combine carbon and boron nitride elements. These hetero-nanotubes demonstrated that the stability of C-BN hetero-nanotubes (C-BNNTs) is similar to carbon nanotubes and that they are semiconductors.

2.3 CNTs in Aerospace

a) Electrical Applications

CNTs possess exceptional conductivity and high surface area, making them highly efficient materials for electrical applications [42]. Due to their high aspect ratios, CNTs need to be loaded into the matrix at 1.5-4.5% by weight to form conductive pathways, thereby achieving uniform electrical properties. The integration of CNTs into fiber-reinforced polymer composites significantly enhances electrical conductivity, with increases of 10^6 for in-plane and 10^8 for through-thickness directions. This feature makes them suitable for structural health monitoring (SHM) and non-destructive evaluation (NDE), which are of critical importance for space applications. Bellucci et al. (2007) [43] demonstrated that even small changes in CNT content can significantly affect electrical resistivity and mechanical properties. The addition of 0.5% CNTs by weight to composite materials indicates a significant improvement in electrical conductivity. These properties are crucial for electromagnetic interference shielding.

Experimental studies have shown that an increase in current density through the bond reduces resistance and allows for a controlled electric current. However, increasing the density damages the bond. Additionally, it is known that the specific contact resistivity decreases with the amount of nanotubes, and the mechanical integrity of the bond, when measured in terms of shear strength and fatigue resistance, is unaffected by the current. However, high concentrations of MWCNTs reduce bond resistance, which negatively impacts fatigue resistance [44]. Additionally, the experiments showed that the volume resistivity of epoxies decreased with increasing MWCNT aspect ratio, which in turn increased electrical conductivity [45]. CNT-based sensors can facilitate rapid electron transfer, enhancing electrochemical reactivity, and allowing for their use in strain sensors where conductance changes reproducibly with strain or bending, and enabling in-situ monitoring of health (e.g., pilot health). The incorporation of multi-walled carbon nanotubes (MWNTs) into aerospace-grade epoxy resin composites can enhance lightning strike performance. Panels containing 0.1 wt.% MWNTs have been reported to show improved lightning strike performance [46].

b) Mechanical applications

CNTs integrated into glass fibers can function as strain sensors, helping to detect mechanical stresses such as strain, cracks, and delamination in real-time. This feature is highly important for aircraft architecture [42]. The

fracture toughness of alumina composites was increased by 24% with a 10 vol-% loading of multi-walled nanotubes (MWNTs), while the addition of 1 wt-% carbon nanotubes improved the elastic stiffness of polystyrene by 36-42% and resulted in a 25% increase in tensile strength. They have considerable potential for extensive use in the aerospace sector. Tensile and Charpy impact tests confirmed the improved mechanical properties of CNT-reinforced composites. For example, the ultimate tensile strength of epoxy-impregnated CNT buckypaper was measured at 56.6 MPa. Charpy impact tests showed a 42% improvement in Young's modulus and a 10% increase in the ultimate tensile strength for CNT-reinforced composites [39]. The reinforcement of carbon fiber composites by inserting vertically aligned carbon nanotubes (VACNTs) between the layers has increased in-plane strength, which is of critical importance for aerospace applications. These improvements include a 30% increase in bolt-bearing strength, a 10% increase in open-hole compression strength, and a 40% increase in L-shaped laminate bending tests. VACNTs act like nano-stitches, strengthening the interfaces without compromising the structural integrity of the composite, unlike traditional reinforcement techniques [47]. The incorporation of MWCNTs into woven carbon fiber (CF) laminae has been shown to increase the fracture toughness of the cured composite by approximately 50%. Additionally, the flexural modulus of the composite increased by about 5%, indicating an improvement in structural stiffness [48]. Polymer matrix composites reinforced with carbon nanofibers and carbon nanotubes (CNTs) have demonstrated significant improvements in vibration damping. Dynamic mechanical analysis (DMA) revealed that nanocomposite beams with carbon nanopaper sheets exhibited a 200-700% increase in damping ratios at higher frequencies compared to those without sheets. Therefore, such materials hold strong potential for use as structural components in aerospace applications.

c) Thermal applications

Changes in the mechanical resonant frequency of CNTs can be utilized to develop thermal sensors, and the high aspect ratio and large surface area of CNTs can enhance the sensitivity of thermal applications.

d) Coating applications

The application of CNTs as coatings for lightning strike protection is due to their thermal and conductive properties. Additionally, it leads to improvements in strength and durability. CNTs were dispersed into a thermoplastic polyurethane (PU) matrix to be used as de-icing coatings. The integration of 1 wt.-% MWNTs into the PU matrix also enhanced the

tensile strength of the coating. Thermal stability is crucial for aerospace coatings. Thermogravimetric analysis (TGA) has shown that the addition of MWNTs improves the thermal stability of nanocomposites [49]. The volume resistivity decreased from 10^{13} Ω·cm for pure PU to 10^{8} Ω·cm for composites with 0.5 wt.-% MWNTs and to 10^{7} Ω·cm for composites with 3.0 wt.-% MWNTs. This substantial reduction in resistivity protects the structure from electrostatic discharge damage [49] Thermal diffusivity determines the coating's ability to conduct heat. The thermal diffusivity of the nanocomposites showed a 24% improvement compared to pure PU with the addition of 1.0 wt.-% MWNTs. Improved thermal diffusivity at optimal MWNT concentrations enables the coating to manage thermal energy efficiently and helps prevent ice accumulation in aerospace architecture [49].

2.4. BNNTs in Aerospace

BNNTs possess exceptional mechanical strength, thermal conductivity, and electrical insulation properties [50]. Therefore, BNNTs are highly suitable for aerospace applications, particularly for structural reinforcement, thermal management, and electromagnetic shielding.

a) Electrical and Thermal Applications

Semiconducting BNNTs are ideal electrical insulation materials, regardless of chirality or diameter [51]. Due to these functions, they are of great importance for thermal management in aerospace electronics. Materials with low dielectric constant values are used to reduce power consumption in high-frequency circuits [52]. BNNTs possess a low relative dielectric constant range, from 1.0 to 1.1 (50 Hz - 2 MHz) [52]. These properties offer advantages for applications that require high insulation and low energy loss. Huang et al [53] achieved significant improvements in the dielectric properties of BNNT composites compared to pure epoxy resin. Such properties of BNNTs suggest that they may offer a promising solution to the reliability issues commonly encountered in aerospace applications.

b) Mechanical Applications

BNNTs hold a significant place in mechanical applications due to their high thermal stability, mechanical strength, and piezoelectric properties. For example, BNNTs have significantly reinforced aluminum composites. On the other hand, molecular dynamics simulations have shown that BNNT-Al composites exhibit enhanced elastic properties [54]. Another study revealed that ceramic composites containing 1.5% BNNTs showed significant improvements in flexural strength, fracture toughness, and thermal shock resistance [55]. Additionally, similar results were obtained for BNNT-added

Si3N4 ceramic composites [56]. BNNTs have an average Young's modulus of approximately 906.2 GPa. However, it was found that the outer diameter of BNNTs decreases due to impact effects, forming a defective shell and reducing the Young's modulus to approximately 662.9 GPa. Despite this reduction, the modulus remains three times higher than that of steel. These results indicate that BNNTs possess material properties suitable for extreme environments such as space.

c) Shielding Applications

Harrison et al. (2008) conducted research on the synergistic potential of Boron Nitride (BN) composites for enhancing protection against space radiation, such as galactic cosmic rays (GCRs) and solar energetic particles (SPEs) [57]. Thibeault et al. (2016) demonstrated that hydrogen-containing BNNTs provide effective protection against cosmic radiation and neutrons over a broad energy range [13]. Yamamato et al. observed that by applying aligned carbon nanotubes (CNTs) to alumina fiber-reinforced laminates, the thermal and electrical conductivities of the composite increased. Increasing electrical conductivity has been noted to be useful for electrostatic discharge and sensing applications and can be used for both electromagnetic interference (EMI) shielding and deicing. It is envisaged that with this method, fire-resistant structures and the change in electrical or thermal resistance resulting from damage will be minimized [58]. BNNTs have been integrated into CNT-BNNT-CNT nanostructures for the purpose of developing gas sensing applications. Such structures exhibit high sensitivity and selectivity for gases such as NO_2 and O_2 due to the quantum mechanical tunneling process [59].

3. CONCLUSION

The high strength, thermal resistance, and thermal stability, electrical conductivity, chemical stability, and corrosion resistance of CNT (Carbon Nanotubes) and BNNT (Boron Nitride Nanotubes) structures provide versatile benefits across different areas, from aircraft bodies to the internal components of spacecraft. Additionally, they can be used to offer protection against radiation in space environments, contributing to the safety of spacecraft and astronauts. BNNTs are chemically inert and exhibit excellent resistance to many chemical substances, making them highly durable against chemical corrosion and harsh space conditions. CNTs also demonstrate chemical resistance under certain conditions. They are a durable option for aerospace and aviation components that may be exposed to corrosive substances or oxidative environmental conditions. CNTs and BNNTs can

enhance the mechanical, thermal, and electrical properties of composite materials. For example, making aircraft bodies lighter and more durable can lead to energy savings and increased flight safety. Additionally, composites made with these materials offer high impact resistance and durability. Furthermore, CNTs have the ability to absorb radar waves, making them applicable for use in military aircraft and other aerospace applications. This property allows them to reduce radar visibility and align with stealth technology.

References

[1] Starke, Jr. E.A, Staley, J.T. (1996). Progress in Aerospace Sciences,32,131–172. doi:10.1016/ 0376-0421(95)00004-6

[2] Williams J. C. ve Starke, E. A. (2003). Acta Materialia,51, 5775–5799.

[3] Blanchard, B. S., Fabrycky W. J.(2006). Bringing system into being, System Engineering and Analysis (4. Baskı). New Jersey: Pearson Prentice Hall

[4] Boyer, R.R. (1996). Materials Science and Engineering, 213,103–114. doi: 10.1016/0921–5093(96)10233–1

[5] Zheng, L., O'Connell, M., Doorn, S. et al. Nature Mater 3, 673–676 (2004) https://doi.org/10.1038/nmat1216

[6] Jisoo Kyoung, Eui Yun Jang, Márcio D. Lima, Hyeong-Ryeol Park, Raquel Ovalle Robles, Xavier Lepró, Yong Hyup Kim, Ray H. Baughman, and Dai-Sik Kim Nano Letters 2011 (10), 4227-4231 DOI: 10.1021/ nl202214y

[7] Yasushi Okawa, Shoji Kitamura, Satomi Kawamoto, Yasushi Iseki, Kiyoshi Hashimoto, Etsuo Noda, Acta Astronautica,Volume 61, Issues 11–12,2007, Pages 989-994, https://doi.org/10.1016/j.actaastro.2006.12.017. (https://www.sciencedirect.com/science/article/pii/S0094576507001294)

[8] D. M. Lincoln, R. A. Vaia, J. M. Brown, T. H. B. Tolle,IEEE Aerospace Conf. Proc.(Eds: IEEE Aerospace and Electronic Systems Society), IEEE, Big Sky

[9] M. Njuguna, J. and Pielichowski, K. (2004), Adv. Eng. Mater., 6: 204-210. O2000,Vol. 4, p. 183S. *Nature* 1991, 354, 56–5

[10] Bellucci, S., Balasubramanian, C., Mancia, F., Marchetti, M., Regi, M., Tombolini, F., Composite materials based on carbon nanotubes for aerospace applications, Proceedings Volume 5852, Third International Conference on Experimental Mechanics and Third Conference of the Asian Committee on Experimental Mechanics; (2005) https://doi.org/10.1117/12.621441

[11] Hülya Cebeci, Roberto Guzman de Villoria, A. John Hart, Brian L. Wardle, Composites Science and Technology, Volume 69, Issues 15–16, 2009, Pages 2649-2656, ISSN 0266-3538, https://doi.org/10.1016/j.compscitech.2009.08.006

[12] Rawal, Suraj and Ravine, J. and Czerw, Richard (2011), Graphene nanoplatelet membranes for aerospace applications, Volume 1, pages 411-414

[13] Thibeault, S.A., Fay, C.C., Lowther, S.E., Earle, K., Sauti, G., Kang, J.H., Park, C., & McMullen, A.M. (2012). Radiation Shielding Materials Containing Hydrogen, Boron, and Nitrogen: Systematic Computational and Experimental Study. Phase I.

[14] Maho Yamaguchi, Dai-Ming Tang, Chunyi Zhi, Yoshio Bando, Dmitry Shtansky, Dmitri Golberg, Acta Materialia, Volume 60, Issue 17, 2012, Pages 6213-6222, ISSN 1359-6454, https://doi.org/10.1016/j.actamat.2012.07.066.

[15] Zi-Yue Zhang, Zhuhua Zhang, and Wanlin Guo The Journal of Physical Chemistry C 2009 *113* (30), 13108-13114. DOI: 10.1021/jp902246u

[16] 2015 Global Aerospace and Defense Industry Outlook (Deloitte, New York, 2015)

[17] P.C. Zimm , Aerospace Supply Chain & Raw Material Outlook (ICF International, Fairfax, VA , 2014)

[18] Graphite Composite Design Guide," www.performancecomposites.com, June 24, 2005

[19] D. Ginburg: "Abrasive Waterjet Cutting of Aerospace Materials," SME Technical Paper, 1989

[20] L. Ye, Y. Lu, Z. Su, and G. Meng, Compos. Sci. Technol., vol. 65, no. 9, pp. 1436–1446, 2005

[21] Advisory Council for Aeronautics Research in Europe (ACARE) (accessed on 19 March 2021)]. Available online: https://www.acare4europe.org/sria/flightpath-2050-goals/protecting-environment-and-energy-supply-0

[22] "Materials & Minerals Processing:" Materials World News, Feb. 2004.

[23] International Agency for Research on Cancer (IARC), 1988. IARC Monograph on the Evaluation of Carcinogenic Risks to Humans From Man-Made Mineral Fibers, Lyon, France.

[24] Dodds N., Gibson A.G., Dewhurst D., Davies J.M. *Compos. Part A Appl. Sci. Manuf.* 2000;31:689–702. doi: 10.1016/S1359-835X(00)00015-4

[25] Kitzes G. Aviation Medicine. 1956; 27(1): 53-8. PMCID: 13286221.

[26] Bachman G, Santos C, Weiland J, Hon S, Lopez G. *Clin Toxicol.* 2017; 55(7): 773–774. doi: 10.1080/15563650.2017.1348043.

[27] Winder C, Balouet JC, Aerotoxic Syndrome: Adverse Health Effects Following Exposure to Jet Oil Mist During Commercial Flights. 'editor' Eddington I. Towards a Safe and Civil Society: Proceedings of the International Congress on Occupational Health Conference; 2000 4–6 September 2000; Brisbane, Australia: ICOH.

[28] S. H. Bae and E. S. Lee, Proc. of KSAS Autumn Conference 2018, Jeju, Republic of Korea, pp. 759-760, Nov 2018

[29] S. Y. Rhee and J. W. Suh, Journal of Aerospace System Engineering, vol. 7, no. 4, pp. 55-61, Dec 2013.

[30] https://fastercapital.com/content/Certification-and-Startup-Evaluation--Certification-Challenges-in-the-Aerospace-Industry.html

[31] Chernyshev, S.L., Lyapunov, S.V. & Wolkov, *Adv. Aerodyn*. 1, 7 (2019). https://doi.org/10.1186/s42774-019-0007-6

[32] Boyer, R.R., Cotton, J.D., Mohaghegh, M. *et al*. *MRS Bulletin* 40, 1055–1066 (2015). https://doi.org/10.1557/mrs.2015.278

[33] Ramachandran, K., Boopalan, V., Bear, J.C. *et al*. *J Mater Sci* 57, 3923–3953 (2022). https://doi.org/10.1007/s10853-021-06760-x

[34] Thostenson, E.T., Ren, Z. and Chou, T.W. (2001) Composite Science Technology, 61, 1899-1912. http://dx.doi.org/10.1016/S0266-3538(01)00094-X

[35] Kaseem, M., Hamad, K. and Ko, Y.G. (2016). European Polymer Journal, 79, 36-62. https://doi.org/10.1016/j.eurpolymj.2016.04.011

[36] Ashraf R, Kausar A, Siddiq M. *Journal of Plastic Film & Sheeting*. 2014;30(4):412-434. doi:10.1177/8756087914527982

[37] Iijima, S. *Nature* 354, 56–58 (1991). https://doi.org/10.1038/354056a0

[38] Marvin L. Cohen, Alex Zettl; *Physics Today* 1 November 2010; 63 (11) 3438. https://doi.org/10.1063/1.3518210

[39] Michael B. Jakubinek, Behnam Ashrafi, Yadienka Martinez-Rubi, Jingwen Guan, Meysam Rahmat, Keun Su Kim, Stéphane Dénommée, Christopher T. Kingston, Benoit Simard, Chapter 5 - Boron Nitride Nanotube Composites and Applications, Editor(s): Mark J. Schulz, Vesselin Shanov, Zhangzhang Yin, Marc Cahay, In Micro and Nano Technologies, Nanotube Superfiber Materials (Second Edition), William Andrew Publishing, 2019, Pages 91-111, ISBN 9780128126677, https://doi.org/10.1016/B978-0-12-812667-7.00005-7.

[40] Janet Hurst, David Hull, Daniel Gorican. Synthesis of Boron Nitride Nanotubes for Engineering Applications. **2008**, 95-102. https://doi.org/10.1002/9780470291375.ch11

[41] P. Zhao, D.S. Liu, Y. Zhang, Y. Su, H.Y. Liu, S.J. Li, G. Chen, Solid State Communications,Volume 152, Issue 12, 2012, 1061-1066, ISSN 0038-1098, https://doi.org/10.1016/j.ssc.2012.03.018.

[42] Boehle, M., Jiang, Q., Li, L., Lagounov, A., & Lafdi, K. (2012). International Journal of Smart and Nano Materials, 3(2), 162–168. https://doi.org/10.1080/19475411.2011.651509

[43] Bellucci, S., Balasubramanian, C., Micciulla, F., & Rinaldi, G. (2007). Journal of Experimental Nanoscience, 2(3), 193–206. https://doi.org/10.1080/17458080701376348

[44] Iosif D. Rosca, Suong V. Hoa, Composites Science and Technology, Volume 71, Issue 2, 2011, 95-100, ISSN 0266-3538, https://doi.org/10.1016/j.compscitech.2010.10.016

[45] J. Li and J. K. Lumpp; *2007 IEEE Aerospace Conference*, Big Sky, MT, USA, 2007, pp. 1-6, doi: 10.1109/AERO.2007.352642.

[46] Jikui Zhang, Xianglin Zhang, Xiaoquan Cheng, Yanwei Hei, Liying Xing, Zhibao Li, Composites Part B: Engineering, 168, 2019, 342-352, https://doi.org/10.1016/j.compositesb.2019.03.054.

[47] Roberto Guzman de Villoria, Lisa Ydrefors, Per Hallander, Kyoko Ishiguro, Pontus Nordin and Brian Wardle, 2012 https://doi.org/10.2514/6.2012-1566

[48] K.L. Kepple, G.P. Sanborn, P.A. Lacasse, K.M. Gruenberg, W.J. Ready, Carbon, 46, Issue 15, 2008, 2026-2033, https://doi.org/10.1016/j.carbon.2008.08.010.

[49] Zhao, W., Li, M. and Peng, H.-X. (2010), Macromol. Mater. Eng., 295: 838-845. https://doi.org/10.1002/mame.201000080

[50] Chopra NG, Luyken RJ, Cherrey K, Crespi VH, Cohen ML, Louie SG, Zettl A. Science. 1995 Aug 18;269(5226):966-7. doi: 10.1126/science.269.5226.966. PMID: 17807732.

[51] Golberg D, Bando Y, Huang Y, Terao T, Mitome M, Tang C, Zhi C. ACS Nano. 2010 Jun 22;4(6):2979-93. doi: 10.1021/nn1006495. PMID: 20462272.

[52] Hong, X., Wang, D. & Chung, D.D.L. Boron Nitride Nanotube Mat as a Low-*k* Dielectric Material with Relative Dielectric Constant Ranging from 1.0 to 1.1. *J. Electron. Mater.* **45**, 453–461 (2016). https://doi.org/10.1007/s11664-015-4123-8

[53] Huang, X., Zhi, C., Jiang, P., Golberg, D., Bando, Y. and Tanaka, T. (2013), Adv. Funct. Mater., 23: 1824-1831. https://doi.org/10.1002/adfm.201201824

[54] Ziyu Cong, Seungjun Lee, Composite Structures, Volume 194, 2018, 80-86, https://doi.org/10.1016/j.compstruct.2018.03.103.

[55] Akintola, T.M.; Tran, P.; Downes Sweat, R.; Dickens, T. Composites. *J. Compos. Sci.* 2021, *5*, 61. https://doi.org/10.3390/jcs5020061

[56] Wang, S., Wang, G., Wen, D. *et al. Appl Compos Mater* **25**, 415–423 (2018). https://doi.org/10.1007/s10443-017-9627-3

[57] Harrison, C., Weaver, S., Bertelsen, C., Burgett, E., Hertel, N. and Grulke, E. (2008), J. Appl. Polym. Sci., 109: 2529-2538. https://doi.org/10.1002/app.27949

[58] Amiko Yamamoto, Roberto Guzman de Villoria, Brian L. Wardle, Composites Science and Technology, Volume 72, Issue 16, 2012, Pages 2009-2015, ISSN 0266-3538, https://doi.org/10.1016/j.compscitech.2012.09.006.

[59] Seyed Shahim Vedaei, Ebrahim Nadimi, Applied Surface Science, 470, 2019, 933-942, https://doi.org/10.1016/j.apsusc.2018.11.220.

Bölüm 4

Bridgman Yöntemi İle Katılaştırılmış Al-Cu-Si Ötektik Alaşımlarının Karakterizasyonu[1]

Uğur Büyük[2]

Özet

Alüminyum şekillendirme kolaylığı, korozyona ve çevresel etkilere karşı direnci ve yüksek mukavemet/ağırlık oranı nedeniyle gıda endüstrisinden elektrik ve elektronik endüstrisine, otomotiv ve havacılık endüstrilerinden inşaat uygulamalarına kadar birçok sektörde yaygın olarak kullanılmaktadır. Çok bileşenli alüminyum alaşımlarının fiziksel özellikleri; kimyasal bileşime, yani alaşım elementlerine ve alaşım elementlerinin oranına bağlı olarak değişir. Alüminyum esaslı döküm alaşımlarında kullanılan ana alaşım elementleri silikon, bakır ve magnezyum olup, demir ve çinko artık elementler olarak kullanılır. Al-Si-Cu, güç aktarma organları ve şanzımanlarda büyük kullanım oranına sahiptir. Bu çalışmada, Al-26.5Cu-6Si (% ağırlıkça) üçlü ötektik alaşımının fiziksel özellikleri doğrusal katılaştırma yöntemi ile ilişkili olarak incelenmiştir. Alaşım vakumlu ergitme fırınında hazırlanmış ve Bridgman tipi fırın kullanılarak farklı katılaştırma hızlarında doğrusal olarak katılaştırılmıştır. Üretilen numunelerden Vickers mikrosertliği, maksimum çekme dayanımı ve elektriksel özdirenç değerleri ölçülmüş ve katılaştırma hızının bu değerleri önemli ölçüde etkilediği belirlenmiştir. Bu çalışmadaki sonuçlar, ikili Al-Cu ve dörtlü Al-Cu-Si-Fe ötektik alaşımları için elde edilen deneysel sonuçlarla karşılaştırılmıştır.

1. GİRİŞ

Malzemelerin fiziksel özellikleri ve performansları, katılaşma sırasında oluşan mikroyapılar tarafından belirlenir. Mikroyapıların oluşumunu ve nasıl kontrol edileceğini anlamak, malzeme bilimi alanındaki temel zorluklardan biridir (Wilde vd., 2005; Morando vd., 2018). İkili alaşımlar on yıllardır

1 Bu araştırma Türkiye Bilimsel ve Teknik Araştırma Kurumu (TÜBİTAK) tarafından 112T588 numaralı proje ile desteklenmiştir.

2 Prof. Dr., Erciyes Üniversitesi, Eğitim Fakültesi, Matematik ve Fen Bilimleri Eğitimi Bölümü, Kayseri, Türkiye, buyuk@erciyes.edu.tr, ORCID: 0000-0002-6830-8349

https://doi.org/10.58830/ozgur.pub575.c2361

hem teorik (Jackson & Hunt, 1966) hem de deneysel (McCartney, 1980a,b; Himemiya & Umeda, 1999; Himemiya, 1999; Himemiya, 2000) olarak çalışılmış olmasına rağmen, üç veya daha fazla bileşen içeren çok bileşenli alaşımların katılaştırılması sırasında oluşan mikroyapılar daha az araştırılmıştır.

Katılaştırma süreci ve bileşim (Co) malzemelerin mikroyapılarının belirlenmesinde en etkili iki unsurdur. Kontrollü katılaştırma; malzemenin bileşimini, sıcaklık gradyantını (G) ve katılaştırma hızını (V) yönetmek için kullanılabilir. Böylece malzemenin mikroyapısı değişir ve mekanik, elektriksel ve termal özellikler de etkilenir. Otomotiv ve uçak endüstrileri, farklı katılaştırma hızlarının alaşımların mekaniksel özellikleri üzerindeki etkisini ölçmek için genellikle kontrollü katılaştırma sürecini kullanmaktadırlar. Katılaştırma parametrelerinin termo-fiziksel özellikler üzerindeki etkilerini araştırmak için birçok deneysel çalışma yapılmıştır (Çadırlı vd., 1999; Hecht vd. 2004; Gündüz vd., 2004; Böyük & Maraşlı, 2009; Çadırlı vd., 2009; Böyük vd., 2009, 2010, 2011; Engin & Büyük, 2018; Büyük vd., 2020).

Son yıllarda kolay şekillendirilebilirlikleri, düşük özgül ağırlıkları, elektriksel ve termal iletkenlikleri ve yüksek korozyon dirençleri nedeniyle Al-Cu-Si alaşımlarının endüstride kullanımı artmıştır. Bu çalışmada, farklı hızlarda katılaştırılan Al-26.5Cu-6Si (% ağırlıkça) ötektik alaşımının Vickers mikrosertliği (HV), maksimum çekme dayanımı (UTS) ve elektriksel özdirenci (ρ) ölçülmüş ve bu parametrelerin katılaştırma hızı ile ilişkileri doğrusal regresyon analizi ve Hall-Petch denklemi ile araştırılmıştır. Bu çalışmadaki sonuçlar, ayrıca ikili Al-Cu ve dörtlü Al-Cu-Si-Fe ötektik alaşımları için elde edilen deneysel sonuçlarla karşılaştırılmıştır.

2. DENEYSEL SÜREÇ

2.1. Doğrusal katılaştırma ve metalografi

Bu çalışma Al-%26.5Cu-%6Si ötektik alaşımına odaklanmaktadır. Bu alaşım, %99.99 saflıkta alüminyum, %99.98 saflıkta bakır ve %99.97 saflıkta silisyum kullanılarak vakum ortamında eritilmiştir. Alaşım daha sonra 200 mm uzunluğunda, 4 mm iç çapında ve 6.35 mm dış çapında 10 grafit kalıba dökülmüştür. Her bir numune Bridgman fırınına konmuş ve sabit bir sıcaklık gradyantı (G=8.50 K/mm) ve farklı katılaştırma hızlarında (V=8.25-164.80 μm/s) katılaştırılmıştır. Bridgman doğrusal katılaştırma fırınının şematik diyagramı ve detayları Şekil 1'de sunulmuştur.

Ani soğutulan (quench) numuneler, 10 mm uzunluğunda kesilmiş ve grafit kalıptan çıkarılmıştır. Her bir numune bir seri SiC zımpara kâğıdı

ile düzleştirildikten sonra TegraPol-15 Struers parlatma makinesi ile parlatılmıştır. Numunelerin mikroyapılarını gözlemlemek için her biri 10-15 saniyede 95 ml damıtılmış su+5 ml Hidroflorik Asit (HF) çözeltisinde dağlanmıştır.

2.2. Katılaşma parametrelerinin ölçümü

Numunedeki sıcaklık ölçümü üç adet K-tipi 0.25 mm çapında yalıtılmış termalçift kullanılarak gerçekleştirilmiştir. Katılaştırma süreci boyunca soğuma hızları bilgisayar aracılığıyla bir veri kaydedicisiyle kaydedilmiştir. Sıvı fazdaki sıcaklık gradyantı ($G = \Delta T/\Delta X$) ve katılaştırma hızının değeri ($V = \Delta X/\Delta t$) her bir numune için belirlenmiştir.

2.3. Mikrosertlik ve maksimum çekme dayanımının ölçümü

Al-Cu-Si ötektik alaşımı için katılaştırma hızı, mikrosertlik ve maksimum çekme dayanımı arasındaki ilişkileri analiz etmek amacıyla numunelerin yüzeyleri parlatılmıştır. Mikrosertlik ölçümleri, Future Tech FM-700 sertlik test cihazı (50-300 g yük ve 10 s tutma süresi) ile Vickers yöntemi kullanılarak numunelerin enine kesitlerinden yapılmıştır. Her değer, en yüksek ve en düşük değerler hariç olmak üzere en az 10 ayrı ölçümün ortalaması alınarak hesaplanmıştır. Numunelerin maksimum çekme dayanımı, oda sıcaklığında 0.5 mm/dak test hızına sahip bir Shimadzu AG-IS çekme test cihazı ile ölçülmüştür. Çekme numuneleri, çekme ekseni numune büyüme yönüne paralel olacak şekilde 40 mm uzunluğunda ve 4 mm çapında hazırlanmıştır. Tüm çekme testleri, verilerin kararlılığını sağlamak için aynı test koşulları altında üç kez tekrarlanmıştır.

2.4. Elektriksel özdirençlerin ölçümü

Metalik alaşımların önemli fiziksel özelliklerinden biri olan elektrik özdirençleri genellikle dört nokta uç (four point prob) tekniği kullanılarak ölçülür. Bu tekniğe göre, iki uç akım kaynağı oluşturmak için kullanılırken, diğer iki uç voltajı ölçmek için kullanılır (Smiths, 1958; Gise & Blanchard, 1979). Bu çalışmada, akım-gerilim (IV) karakteristikleri Keithley 2400 Akım Uygulayıcı ve Keithley 2700 Multimetre kullanılarak bilgisayar kontrollü bir arayüz kartı aracılığıyla ölçülmüştür. Akım ve potansiyel ucu olarak 0.5 mm çapında platin teller kullanılmıştır. Uygulanan akıma karşı voltaj düşüşü ölçülmüş ve elektrik direnci standart dönüşüm yöntemi kullanılarak hesaplanmıştır.

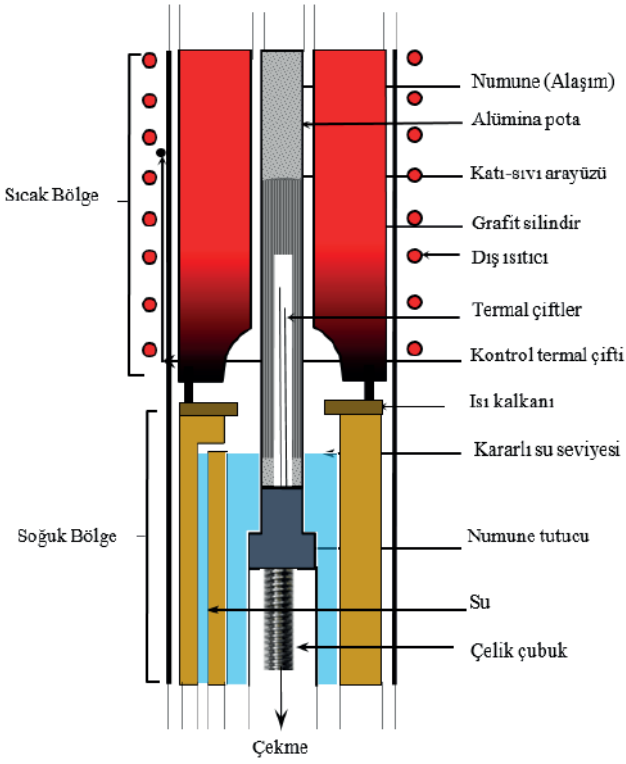

Şekil 1. Bridgman doğrusal katılaştırma fırınının şeması ve detayları

3. BULGULAR VE TARTIŞMA

3.1. Katılaştırma hızının mikrosertlik üzerine etkisi

Katılaştırma hızındaki artış, Al-Cu-Si ötektik alaşımı için mikrosertlikte bir artışa neden olmuştur. Katılaştırma hızı 8,25'ten 164,80 μm/s'ye yükseldikçe, mikrosertlik değerleri 176.80'den 216.00 kg/mm^2'ye yükselmiştir. Tablo 1, mikrosertlik değerlerinin katılaştırma hızıyla değişimini göstermektedir Al-Cu-Si ötektik alaşımı için bu çalışmada elde edilen sonuçlar, Al–Cu ötektik alaşımı (Engin & Büyük, 2018) ve Al-Cu-Si-Fe ötektik alaşımı (Büyük vd., 2020) için elde edilen mikrosertlik değerleri ile karşılaştırılmış ve sonuçlar Şekil 2'de verilmiştir. Bu çalışmada Al-Cu-Si ötektik alaşımı için elde edilen HV değerleri (176.80-216.00 kg/mm^2), Al–Cu ötektik alaşımının HV değerlerinden (143.48-185.19 kg/mm^2) (Engin & Büyük, 2018) daha yüksek ve Al-Cu-Si-Fe ötektik alaşımının HV değerlerine (178.78-214.98 kg/mm^2) (Büyük vd., 2020) oldukça yakındır.

Tablo 1. Doğrusal katılaştırılmış Al-Cu-Si ötektik alaşımı için mikrosertlik, maksimum çekme dayanımı ve elektriksel özdirenç değerleri.

Alaşım (ağ.%.)	Katılaştırma Parametreleri		Mikrosertlik	Maksimum Çekme Dayanımı	Elektriksel Özdirenç
	G (K/mm)	V (μm/s)	HV (kg/mm²)	UTS (MPa)	$\rho \times 10^{-8}$ (Ωm)
Al-26.5Cu-6Si	8.50	8.25	176.80	75.39	6.86
		16.60	184.00	83.07	7.61
		41.65	193.00	87.46	7.83
		90.05	200.00	91.80	8.85
		164.80	216.00	104.00	9.56

Şekil 2, doğrusal katılaştırılmış Al-Cu-Si ötektik alaşımının mikrosertliğinin katılaştırma hızıyla değiştiğini göstermektedir. Mikrosertlik ve katılaştırma hızı arasındaki ilişkiyi belirlemek için doğrusal regresyon analizi kullanılmış ve sonuçlar Tablo 2'de verilmiştir. Regresyon analizi sonucu $HV=154.11(V)^{0.06}$ denklemi hesaplanmıştır. Ek olarak, mikrosertlik ve katılaştırma hızı arasındaki ilişkiyi elde etmek için Hall-Petch tipi korelasyon analizi de kullanılmış ve bu analiz sonucu $HV=143.59+109.64(V)^{0.25}$ denklemi bulunmuştur. Bu değerler, Al-Cu-Si ötektik alaşımının mikrosertliğinin katılaştırma hızına bağlı artma ilişkisini göstermektedir. Üstel değerler 0.06 ve 0.25, farklı üçlü ötektik alaşım sistemleri için çeşitli araştırmacılar tarafından bildirilen üstel değerler ile (0.03-0.11) uyumludur (Çadırlı vd., 1999; Böyük & Maraşlı, 2009; Çadırlı vd., 2009; Böyük vd., 2009, 2010, 2011; Gündüz vd., 2004; Engin & Büyük, 2018; Büyük vd., 2020). Al-Cu-Si ötektik alaşımının mikroyapı değerleri, katılaştırma hızı arttıkça azalır ve bu da mikrosertlikte kayda değer bir artışa neden olur. Ayrıca, numune boyunca intermetalik fazların varlığı, mikrosertliğin değişiminde önemli bir faktördür. Bu çalışmada elementlerin alaşıma eklenmesinin mikrosertlik değeri üzerinde önemli bir etkisi olmuştur. Diğer taraftan Kaygısız ve Maraşlı'nın Al-Cu-Mg alaşımı için elde ettikleri sonuçlar (Kaygısız & Maraşlı, 2017), Al-Cu-Si alaşımı için bu çalışmada elde edilen sonuçlardan çok daha yüksek bir başlangıç mikrosertlik değeri (HVo) göstermiştir. Ötektik Al-Cu-Mg alaşımının katılaştırma hızı arttıkça, ötektik dizi değişmeden kalmış, ancak kolonideki intermetalik fazların aralığı azalmıştır (Kaygısız & Maraşlı, 2017). Alaşımdaki Mg miktarının da mikrosertlik üzerinde önemli bir etkisi olduğu görülmektedir. Bununla birlikte, Al-Cu-Si alaşımının ötektik dizilimi daha yüksek katılaştırma hızlarında bozulduğu görülmüştür.

Tablo 2. Bazı doğrusal katılaştırılmış alaşımlar için katılaştırma hızı ile mikrosertlik, maksimum çekme dayanımı ve elektriksel özdirenç arasındaki ilişkiler.

Alaşım (ağ.%.)	Mikrosertlik	Maksimum Çekme Dayanımı	Elektriksel Özdirenç	Kaynak
Al–33Cu	$HV = 121.74(V)^{0.08}$ $HV = 109.99 + 119.07(V)^{0.25}$	$UTS = 36.36V^{0.10}$ $UTS = 31.51 + 44.99(V)^{0.25}$	$\rho = 3.19 \times 10^{-8}(V)^{0.12}$	(Çadırlı vd., 1999)
Al-26.5Cu-6Si	$HV = 154.11(V)^{0.06}$ $HV = 143.59 + 109.64(V)^{0.25}$	$UTS = 62.00\ V^{0.10}$ $UTS = 53.38 + 76.12\ (V)^{0.25}$	$\rho = 5.52 \times 10^{-8}(V)^{0.10}$	(Bu çalışma)
Al-26.5Cu–6.5Si–0.5Fe	$HV = 156.54(V)^{0.06}$ $HV = 147.33 + 107.93(V)^{0.25}$	$UTS = 69.91\ (V)^{0.06}$ $UTS = 65.56 + 47.98\ (V)^{0.25}$	$\rho = 7.87 \times 10^{-8}(V)^{0.08}$	(Büyük vd., 2020)

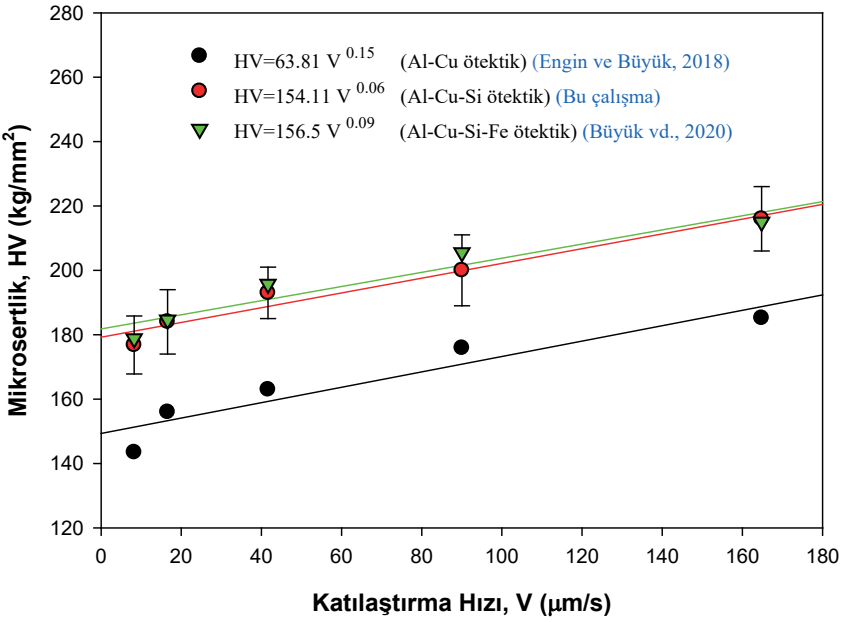

Şekil 2. Doğrusal katılaştırılmış Al-Cu-Si ötektik alaşım için katılaştırma hızının bir fonksiyonu olarak mikrosertliğin değişimi ve bazı deneysel sonuçlarla karşılaştırılması.

3.3. Katılaşma hızının maksimum çekme dayanımı üzerine etkisi

Tablo 1, maksimum çekme dayanımı değerlerinin (UTS) katılaştırma hızı ile değişimini göstermektedir. Katılaştırma hızı 8.25'ten 164.80 µm/s'ye yükseldiğinde, maksimum çekme dayanımının 75.39'dan 104.00 MPa'ya yükseldiği bulunmuştur. Bu çalışmada Al-Cu-Si ötektik alaşımı için elde edilen sonuçlar Al-Cu ötektik alaşımı (Engin & Büyük, 2018) ve Al-Cu-Si-Fe ötektik alaşımı (Büyük vd., 2020) ile karşılaştırılmış ve sonuçlar Şekil 3'te

sunulmuştur. Bu çalışmadan elde edilen UTS değerlerinin (75.39-104.00 MPa), Al-Cu ötektik alaşımı için elde edilen UTS değerlerinden (45.61-59.16 MPa) daha yüksek olduğu (Engin & Büyük, 2018) ve benzer koşullar altında katılaştırılan Al-Cu-Si-Fe ötektik alaşımına (79.34-105.62 MPa) (Büyük vd., 2020) yakın değerde olduğu bulunmuştur.

Şekil 3'ün doğrusal regresyon analizi, Al-Cu-Si ötektik alaşımındaki maksimum çekme dayanımının katılaştırma hızının bir fonksiyonu olarak değişimini göstermektedir. Maksimum çekme dayanımı ve katılaştırma hızı arasındaki ilişkiyi belirlemek için doğrusal regresyon analizi kullanılmış ve sonuçlar Tablo 2'de verilmiştir.

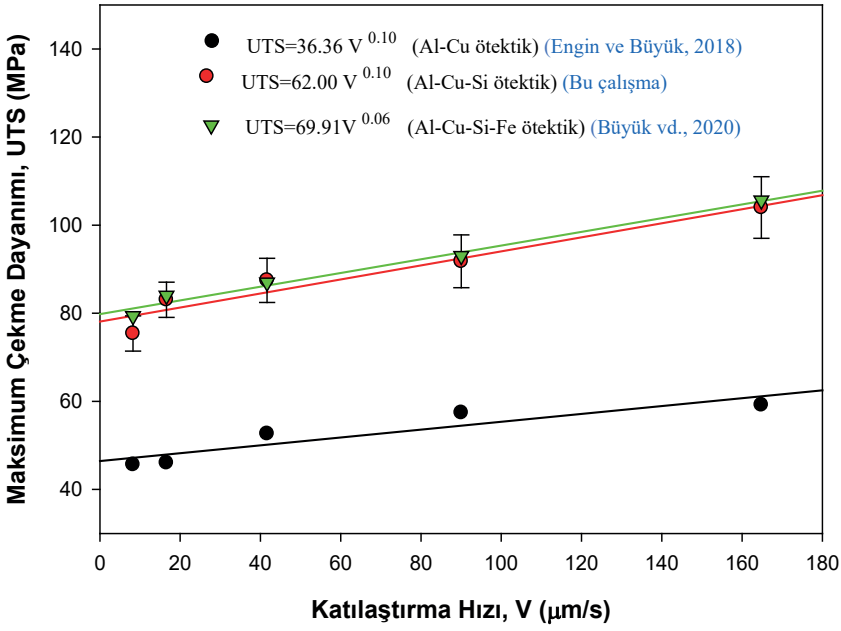

Şekil 3. ***Doğrusal katılaştırılmış Al-Cu-Si ötektik alaşım için katılaştırma hızının bir fonksiyonu olarak maksimum çekme dayanımının değişimi ve bazı deneysel sonuçlarla karşılaştırılması.***

Regresyon analizi sonucu UTS=62.00$(V)^{0.10}$ denklemi hesaplanmıştır. Ek olarak, maksimum çekme dayanımı ve katılaştırma hızı arasındaki ilişkiyi elde etmek için Hall-Petch tipi korelasyon analizi de kullanılmış ve bu analiz sonucu UTS=53.38+76.12$(V)^{0.25}$ denklemi hesaplanmıştır. Erime sıcaklığındaki ilk maksimum çekme dayanımı 53.38 MPa ve katılaştırma hızına göre maksimum çekme dayanımı 76.12 MPa olarak bulunmuştur. Bu çekme dayanım değeri, bildirilen çeşitli alaşımlar için deneysel değerlerle

uyumludur (Engin Büyük, 2018; Büyük vd., 2020). Çekme dayanım değerleri; katılaştırma hızı, mikroyapı, metaller arası fazlar ve alaşımda bulunan elementlerden etkilenebilir.

3.4. Katılaştırma hızının elektriksel özdirenç üzerine etkisi

Bu çalışmada, Al-Cu-Si ötektik alaşımı için katılaştırma hızının elektriksel özdirenci önemli ölçüde etkilediği belirlenmiştir. Katılaştırma hızı 8.25'ten 164.80'e µm/s yükseldikçe, elektriksel özdirencin 6.86×10^{-8}'den 9.56×10^{-8} Ωm'ye yükseldiği bulunmuştur. Bu çalışmada elde edilen sonuçlar Al-Cu ötektik alaşımı (Engin & Büyük, 2018) ve Al-Cu-Si-Fe ötektik alaşımı (Büyük vd., 2020) ile karşılaştırılmış ve Şekil 4'te verilmiştir.

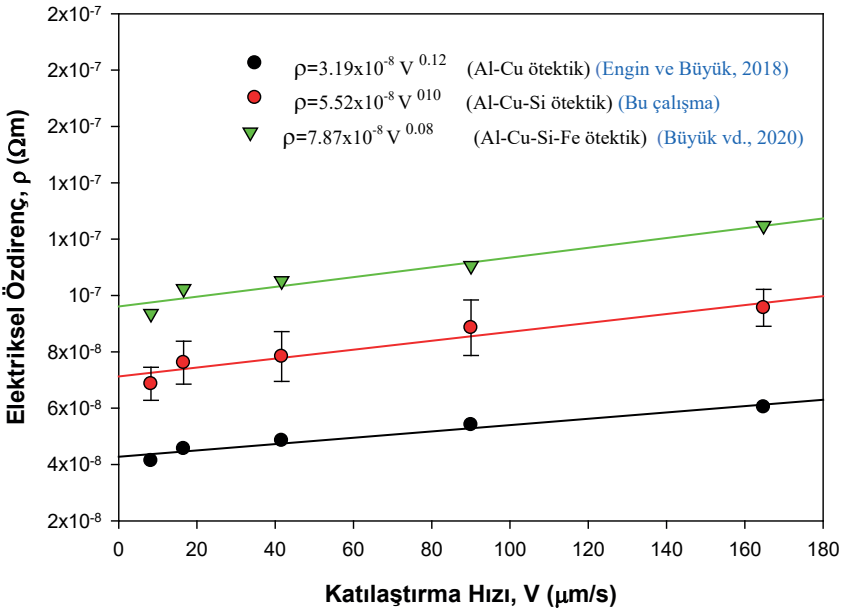

Şekil 4. Doğrusal katılaştırılmış Al-Cu-Si ötektik alaşımı için katılaştırma hızının bir fonksiyonu olarak elektrik özdirencin değişimi ve bazı deneysel sonuçlarla karşılaştırılması.

Mevcut çalışmada elde edilen doğrusal katılaştırılmış Al-Cu-Si ötektik alaşımında farklı katılaştırma hızları (8.25-164.80 µm/s) için ρ değerleri (6.86×10^{-8} – 9.56×10^{-8} Ωm), Al-Cu ötektik alaşımının ρ değerlerinden daha yüksektir (4.13×10^{-8} - 6.03×10^{-8} Ωm) (Engin & Büyük, 2018) ve benzer koşullar altında katılaştırılan Al-Cu-Si-Fe ötektik alaşımının ρ değerlerinden (9.34×10^{-8} - 12.47×10^{-8} Ωm) (Büyük vd., 2020) daha düşüktür. Al-Cu-Si ötektik alaşımının doğrusal regresyon analizi ρ ile alaşımın V'si arasında

$\rho=5.52\times10^{-8}(V)^{0.10}$ şeklinde ifade edilen bir ilişki ortaya çıkarmıştır. Bu çalışmanın sonuçları, üçlü Al-Cu-Si ötektik alaşımının özdirencinin, farklı araştırmacılar tarafından çalışılmış olan Al-Cu-Mg ve Al-Si-Mg üçlü alaşımlarından daha yüksek olduğunu göstermektedir (Kaygısız & Maraşlı, 2015; Kaygısız & Maraşlı, 2017). Benzer deneysel koşullar altında elde edilen elektriksel özdirenç değerlerinin eklenen farklı elementlerin miktarlarından etkilenebileceği açıktır.

4. SONUÇLAR

Bu çalışmada, doğrusal katılaştırılan Al-Cu-Si ötektik alaşımının katılaştırma hızı ile mikrosertlik, maksimum çekme dayanımı ve elektriksel özdirenç değeri arasındaki ilişkileri belirlemek amacıyla deneysel çalışmalar yürütülmüştür. Elde edilen sonuçlar aşağıdaki gibi özetlenebilir. Al-Cu-Si ötektik alaşımı için; katılaştırma hızı 8.25'ten 164.80 μm/s'ye yükseldikçe, mikrosertlik 176.80'den 216.00 kg/mm^2'ye, maksimum çekme dayanımı 75.39'dan 104.00 MPa'ya ve elektriksel özdirenç 6.86×10^{-8}'den 9.56×10^{-8} Ωm'ye yükselmiştir. Regresyon analizi sonucu katılaştırma hızı ile mikrosertlik, maksimum çekme dayanımı ve elektriksel özdirenç değerleri arasındaki ilişkiler: $HV=154.11(V)^{0.06}$, $UTS=62.00\ (V)^{0.10}$, $\rho=5.52\times10^{-8}(V)^{0.10}$olarak hesaplanmıştır. Mikrosertlik ve maksimum çekme dayanımı için Hall-Petch tipi ilişkiler, katılaştırma hızının bir fonksiyonu olarak: $HV=143.59+109.64\ (V)0^{.25}$, $UTS=53.38+76.12(V)^{0.25}$ olarak elde edilmiştir.

TEŞEKKÜR

Bu araştırma Türkiye Bilimsel ve Teknik Araştırma Kurumu (TÜBİTAK) tarafından 112T588 numaralı proje ile desteklenmiştir. Yazar, finansal destekleri için Türkiye Bilimsel ve Teknik Araştırma Kurumu'na teşekkür eder.

Kaynaklar

Böyük, U., Engin, S., Kaya, H., & Maraşlı, N. (2010). Effect of solidification parameters on the microstructure of Sn-3.7Ag-0.9Zn solder. *Materials Characterization, 61*, 1260-1267. https://doi.org/10.1016/j.matchar.2010.08.007

Böyük, U., Engin, S., & Maraşlı, N. (2011). Microstructural characterization of unidirectional solidified eutectic Al-Si-Ni alloy. *Materials Characterization, 62*(9), 844-851. https://doi.org/10.1016/j.matchar.2011.05.010

Böyük, U., & Maraşlı, N. (2009). The microstructure parameters and microhardness of directionally solidified Sn-Ag-Cu eutectic alloy. *Journal of Alloys and Compounds, 485*, 264-269. https://doi.org/10.1016/j.jallcom.2009.06.067

Böyük, U., Maraşlı, N., Kaya, H., Çadırlı, E., & Keşlioğlu, K. (2009). Directional solidification of Al–Cu–Ag alloy. *Applied Physics A, 95*, 923–932. https://doi.org/10.1007/s00339-009-5130-5

Büyük, U., Engin, S., Kaya, H., Çadırlı, E., & Maraşlı, N. (2020). Directionally solidified Al–Cu–Si–Fe quaternary eutectic alloys. *Physics of Metals and Metallography, 121*(1), 78-83. https://doi.org/10.1134/s0031918x20010044

Çadırlı, E., Böyük, U., Kaya, H., Maraşlı, N., Keşlioğlu, K., Akbulut, S., & Ocak, Y. (2009). The effect of growth rate on microstructure and microindentation hardness in the In-Bi-Sn ternary alloy at low melting point. *Journal of Alloys and Compounds, 470*, 150-156. https://doi.org/10.1016/j.jallcom.2008.02.056

Çadırlı, E., Ülgen, A., & Gündüz, M. (1999). Directional solidification of the aluminium-copper eutectic alloy. *Materials Transactions, JIM, 40*(9), 989–996. https://doi.org/10.2320/matertrans1989.40.989

Engin, S., & Büyük, U. (2018). Variations with growth rate of the microstructural, mechanical and electrical properties of directionally solidified the Al-Cu alloy. *Gümüşhane University Journal of Science and Technology Institute, 8*(2), 209-221. https://doi.org/10.17714/gumusfenbil.349996

Gise, P. E., & Blanchard, R. (1979). *Semiconductor and integrated circuit fabrication techniques*. Reston Publishing Company.

Gündüz, M., Kaya, H., Çadırlı, E., & Özmen, A. (2004). Interflake spacings and undercoolings in Al-Si irregular eutectic alloy. *Materials Science and Engineering: A, 369*, 215–229. https://doi.org/10.1016/j.msea.2003.11.020

Hecht, U., Gránásy, L., Pusztai, T., Böttger, B., Apel, M., Witusiewicz, V., Ratke, L., Wilde, J., De, Froyen, L., Camel, D., Drevet, B., Faivre, G., Fries, S. G., Legendre, B., & Rex, S. (2004). Multiphase solidification in multicomponent alloys. *Materials Science and Engineering: R, 46*, 1-49.

Himemiya, T. (1999). Growth models of two-phase eutectic cell in a ternary eutectic system: A phase selection map. *Materials Transactions, JIM, 40*(7), 675-684. https://doi.org/10.2320/matertrans1989.40.675

Himemiya, T. (2000). Extension of cellular/dendritic eutectic growth model to off-monovariant range: Phase selection map of a ternary eutectic alloy. *Materials Transactions, JIM, 41*(3), 437-443. https://doi.org/10.2320/matertrans1989.41.437

Himemiya, T., & Umeda, T. (1999). Three-phase planar eutectic growth models for a ternary eutectic system. *Materials Transactions, JIM, 40*(7), 665-674. https://doi.org/10.2320/matertrans1989.40.665

Jackson, K. A., & Hunt, J. D. (1966). Lamellar and rod eutectic growth. *Transactions of the Metallurgical Society of AIME, 226*, 1129-1142.

Kaygısız, Y., & Maraşlı, N. (2015). Microstructural, mechanical and electrical characterization of directionally solidified Al–Si–Mg eutectic alloy. *Journal of Alloys and Compounds, 618*, 197–203. https://doi.org/10.1016/j.jallcom.2014.08.056

Kaygısız, Y., & Maraşlı, N. (2017). Microstructural, mechanical, and electrical characterization of directionally solidified Al–Cu–Mg eutectic alloy. *Physics of Metals and Metallography, 118*(4), 389–398. https://doi.org/10.1134/s0031918x17040123

McCartney, D. G., Hunt, J. D., & Jordan, R. M. (1980a). The structures expected in a simple ternary eutectic system: Part II. The Al-Ag-Cu ternary system. *Metallurgical Transactions A, 11*(8), 1251-1257. https://doi.org/10.1007/bf02653478

McCartney, D. G., Hunt, J. D., & Jordan, R. M. (1980b). The structures expected in a simple ternary eutectic system: Part 1. Theory. *Metallurgical Transactions A, 11*(8), 1243-1249. https://doi.org/10.1007/bf02653477

Morando, C., & Fornaro, O. (2018). Morphology and phase formation during the solidification of Al-Cu-Si and Al-Ag-Cu ternary eutectic systems. *Materials Research, 21*(2), e20170930. https://doi.org/10.1590/1980-5373-mr-2017-0930

Smiths, F. M. (1958). Measurement of sheet resistivities with the four-point probe. *The Bell System Technical Journal, 37*, 711-718. https://doi.org/10.1002/j.1538-7305.1958.tb03883.x

De Wilde, J., Nagels, E., Lemoisson, F., & Froyen, L. (2005). Unconstrained growth along a ternary eutectic solidification path in Al-Cu-Ag: Preparation of a MAXUS sounding rocket experiment. *Materials Science and Engineering: A, 413–414*, 514–520. https://doi.org/10.1016/j.msea.2005.08.171

Chapter 5

The Foundation of Modern Engineering: Composite Materials

Musa Yılmaz[1]

Mert Can Emre[2]

Abstract

Composite materials are defined as innovative structures that are formed by combining several different materials and that, thanks to this combination, combine properties such as lightness, durability and high performance. These materials have a rapidly growing importance in the field of engineering and technology and offer a wide range of applications. A review of their historical development shows that composites continue to be used in many fields, from building materials to modern engineering applications.

From airframes to wind turbines, medical implants to sports equipment, composites are used in modern engineering to meet the needs for low cost, light weight and high strength. Innovative research is focused on further improving the mechanical, thermal and electrical properties of these materials, continuously expanding the range of uses for composites.

This study presents an in-depth review of the existing literature by addressing the increasing role of composite materials in engineering, their basic properties and their impact from the historical process to the present day. At the same time, it aims to identify new research topics in this field and to provide researchers with a comprehensive perspective.

1. Introduction

Composite materials are defined as substances formed by the amalgamation of at least two distinct traditional materials that do not dissolve into one another. This combination aims to integrate features like lightweight, strength, and corrosion resistance that are absent when the

1 Musa YILMAZ, Yozgat Bozok University, musa.yilmaz@yobu.edu.tr, 0000-0002-3912-5607

2 Mert Can EMRE, Yozgat Bozok University, m.can.emre@yobu.edu.tr, 0000-0002-1445-0358

https://doi.org/10.58830/ozgur.pub575.c2362

materials are utilized separately. The essential characteristics of composite materials are as follows:

• They are constituted by the amalgamation of various materials, devoid of components such as solute and solvent.

• There is no atomic exchange among the components, and they do not chemically influence one another. It typically comprises a primary substance known as a matrix and a more resilient component referred to as a reinforcing element. When the mixture is at the nanoscale scale, these composites are referred to as nanocomposites. Composite materials have been utilized historically since antiquity. Adobe, utilized as a construction material, is among the most renowned and ancient examples. In adobe manufacture, organic fibers like straw and vine branches are incorporated into the clay soil, which possesses a brittle structure, therefore substantially enhancing the material's mechanical strength. These natural reinforcements mitigate the likelihood of cracking and crumbling in adobe, yielding a more resilient building material [1].

Studies indicate that the fibers typically employed to strengthen composites have a remarkably ancient provenance. The manufacture of glass fibers originates from Ancient Egypt. In the 1600s BC, evidence from the XVIII Dynasty suggests the presence of diverse artifacts crafted from fine glass fibers in varied hues, indicating that glass fiber manufacture was extensively practiced during this era. [2].

The early 19th century saw the acquisition of numerous patents for the production of artificial stone slabs using hydraulic bindings and fibrous materials. These patents serve as markers of pioneering revolutionary methodologies in the research and manufacturing processes of composite materials [3].

The initial documentation of glass fiber utilization in industry originates from 1877. Industrial applications have extensively utilized fiber-reinforced synthetic resins since the 1950s. The most recognized category among these materials is glass fiber-reinforced polyester composites [4].

The recent innovative studies have garnered significant attention in the engineering field due to the enhancement of the mechanical, thermal, and electrical properties of composite materials. The applications of these materials are extensive, encompassing aircraft fuselages, wind turbines, sports equipment, and medical implants, all aimed at fulfilling the demands for low cost, lightweight, and high strength [5].

The exceptional characteristics of composite materials, their diverse applications, and their growing significance in engineering have intensified researchers' interest in this domain. In this scenario, compiler studies have become essential to thoroughly assess the possibilities of composite materials. This study seeks to fill a gap in the literature by carefully compiling existing information and pinpointing new research domains.

2. Advantages and Disadvantages of Composite Materials

The extended durability, lightweight composition, exceptional chemical and mechanical resistances, and several other advantageous properties of composite materials render them highly favored. The fabrication of composite materials seeks to integrate one or more of the following characteristics.

- Resistance,
- Lightness,
- Corrosion resistance,
- Electrical conductivity,
- Design flexibility,
- Fatigue resistance,
- Wear resistance,
- Thermal and acoustic performance,
- Applicability to surfaces,
- Economical,
- Aesthetics.

A significant advantage of composite materials is their superior strength-to-weight ratio. This attribute, referred to as specific strength, denotes the load a material can support per unit weight. Composites are favored in industries where weight is critical, such as aerospace, automotive, and sporting goods, owing to their elevated specific strength ratios. Carbon fiber-reinforced composites can offer comparable or superior strength to steel while being lighter [6].

An additional significant attribute of composite materials is their elevated stiffness-to-density ratio, often known as specific stiffness. Specific stiffness denotes the stiffness of a material relative to its weight and is an essential quantity, particularly concerning vibration control, structural integrity, and energy efficiency. Sectors such as aircraft, space, and automotive

extensively utilize composites exhibiting high specific stiffness, as they require lightweight and rigid constructions. For instance, glass and carbon fiber-reinforced polymers exhibit comparable rigidity to conventional metal materials while significantly reducing weight, hence enhancing fuel efficiency and performance [7].

Composite materials provide significant advantages in corrosion resistance, showcasing resilience against damage resulting from chemical interactions. This attribute renders them a favored material even under severe environmental conditions. Polymer matrix composites can preserve their physical integrity even in corrosive environments, including saltwater, moisture, acids, and alkaline solutions. Consequently, sectors such as seafaring, the chemical industry, and infrastructure extensively utilize them [8].

Superior dielectric resistance qualities distinguish composite materials, making them suitable for applications requiring electrical insulation. High dielectric strength signifies that a material has substantial resistance to electrical current, showing its appropriateness for application as an electrical insulation material. Glass fiber reinforced polymer composites are extensively utilized in sectors such as electric vehicles, power transmission lines, and electronic equipment, as these materials reduce electrical conductivity while ensuring mechanical endurance [9].

Composites' exceptional design flexibility makes them stand out and provides engineers with novel options. Design flexibility is the capacity to tailor the material's characteristics to individual tastes by combining various matrix and reinforcement options. Composites can meet precise demands for load-bearing capacity, weight, strength, and thermal resistance due to their adaptability. The aerospace and automotive industries, for instance, can tailor carbon fiber reinforced polymer composites to achieve low weight and high strength goals, while the chemical resistance and electrical insulation of glass fiber reinforced composites can be tailored to specific needs. Engineering designs often choose composites for their adaptability, which helps to optimize performance while keeping costs down [10].

Composite materials exhibit a notable characteristic: high fatigue resistance. Fatigue resistance denotes the capability of a material to preserve its structural integrity over an extended duration when subjected to repeated loading conditions. Composites have the potential to impede the propagation of fatigue cracks, attributed to the load-bearing properties of the fibers and the energy distribution characteristics of the matrix. Carbon and glass fiber-reinforced polymer composites demonstrate significantly enhanced fatigue

performance when compared to metallic materials. This characteristic serves as a primary factor for the extensive application of composites in sectors such as aviation, automotive, and wind turbine industries, where repetitive loading conditions are commonly present. [11].

When external factors consistently expose their surfaces to composite materials, they demonstrate significant wear resistance, effectively resisting abrasion and degradation. In applications that demand high friction resistance, it is common to prefer carbon fiber-reinforced composites and ceramic matrix composites. Carbon fiber-reinforced composites provide exceptional stiffness and friction resistance while maintaining a lightweight profile. Ceramic matrix composites demonstrate remarkable durability against high temperatures and frictional forces. Consequently, composites find extensive application in scenarios where friction is persistent, such as brake discs, bearings, and industrial machinery [12].

Composite materials play a significant role in the field of engineering, particularly because of their thermal and acoustic properties. Composites exhibit effective thermal insulation properties attributed to their low thermal conductivity when analyzed from a thermal perspective. This property provides diverse applications, including construction and aerospace, focused on enhancing energy efficiency and optimizing thermal regulation. The multilayered and porous structure of the composites exhibits acoustic properties that facilitate the absorption or reflection of sound waves, thereby contributing to a reduction in noise levels. Polymer matrix composites exhibit notable thermal and acoustic insulation properties, rendering them advantageous for a variety of applications, including automotive cabins, train carriages, and aircraft fuselages [13, 14].

Composite materials possess extensive uses in engineering, owing to their versatility in surface adaptability. Surfaces with flat, inclined, or intricate geometries can advantageously utilize these materials, which readily mold with various matrix configurations and reinforcement types. Polymer-based kinds are particularly notable in surface coating, protective layer creation, and structural reinforcement because of their low viscosity and malleability. The versatility of this application offers essential features such as corrosion protection, waterproofing, and abrasion resistance, thereby enhancing durability in both industrial and structural domains. [15].

Composite materials present a range of benefits, yet they also come with certain drawbacks. Composites are favored in numerous industrial applications because of their outstanding properties; however, they, like

all materials, possess certain limitations. The following points outline these disadvantages.

- High manufacturing knowledge requirement,
- Directional mechanical properties,
- Delamination issues,
- Difficulty in repair and recycling.

Composite material manufacture calls for in-depth engineering and advanced manufacturing expertise. Careful consideration of the matrix and reinforcement component combinations is required throughout the design and processing of these materials. The manufacturing techniques utilized have a direct impact on the performance of the materials and include intricate operations. Techniques like resin infusion, autoclave curing, and filament winding, to name a few, call for expert-level understanding. Consequently, comprehensive knowledge of complex designs and manufacturing procedures is essential for the effective manufacture of composites, in addition to specialized equipment. Because of this, producing composites is more complicated and expensive than generating other, more conventional materials [16].

Composite materials exhibit distinct directional mechanical properties. The material demonstrates elevated strength and rigidity along the specified direction while exhibiting reduced performance in alternative directions, attributable to the orientation of fibers or reinforcement elements in that particular alignment. This scenario results in possible vulnerabilities when subjected to multiaxial loading conditions. During the design phase of composites, it is crucial to ensure the proper orientation of the fibers and to accurately calculate load distribution. In carbon fiber-reinforced polymers, the orientation of the fibers contributes to improved strength performance while simultaneously presenting a potential risk of reduced strength in alternative directions [17].

Delamination, a notable weakness of composite materials, is characterized by the separation that occurs between the layers of the material, potentially compromising the structural integrity of composites. Impacts, cyclic loading, or manufacturing defects typically cause this condition, which significantly reduces the material's strength. Delamination formation adversely impacts the mechanical performance and load-bearing capacity of composites, leading to safety risks in high-performance applications, including aviation, automotive, and wind turbines. To prevent delamination, it is essential to

optimize material design and manufacturing techniques meticulously to achieve more effective bonding between the fibers and the matrix [18].

A significant drawback of composite materials lies in the challenges associated with their repair and recycling. The structural complexity and multilayered nature of these materials result in more intricate and expensive repair processes when damage occurs, in contrast to traditional materials. Particularly in instances of delamination or cracks, the repair processes necessitate specialized equipment and a high level of technical expertise. Along the same lines, recycling composites is very hard because separating the matrix and reinforcement parts and making them usable again usually requires very complicated and energy-intensive methods. Consequently, it is essential to implement sophisticated mechanical and chemical methods in the recycling of composites [19].

3. Application Areas of Composite Materials

The progress in composite material technology has resulted in a growing application of these materials in various industrial and technological fields. Scientific inquiry into composites is intensifying in the aviation sector, as they gain popularity across various fields. The adaptable design capabilities of composites provide a notable benefit for the distinct needs and anticipations of various sectors. The significance of these materials extends beyond their function as raw materials in diverse fields; they also serve as essential auxiliary equipment in production processes. The following sectors frequently utilize composites:

- Technology related to outer space,
- Military and aerospace sectors,
- Sector focused on construction and building,
- Automotive industry,
- Industry focused on chemicals,
- Production of medical instruments,
- The maritime industry,
- Robotics technology,
- Electrical electronics,
- Musical instruments,
- Sector focused on food and agriculture,

- Production of athletic gear.

Composite materials are essential in the aviation industry because of their advantageous characteristics, including low weight, high strength, and resistance to corrosion. Numerous components, such as the aircraft fuselage, wings, various tail sections, and interior structural elements, extensively utilize composite materials (Figure 1). Carbon fiber-reinforced polymers are the predominant composite materials utilized in commercial and military aircraft, mostly owing to their exceptional strength-to-weight ratio. These materials enhance airplane fuel efficiency and decrease operational expenses while ensuring sustained performance. The increasing utilization of composites in aviation has facilitated enhanced efficiency and reliability objectives in engineering design [20].

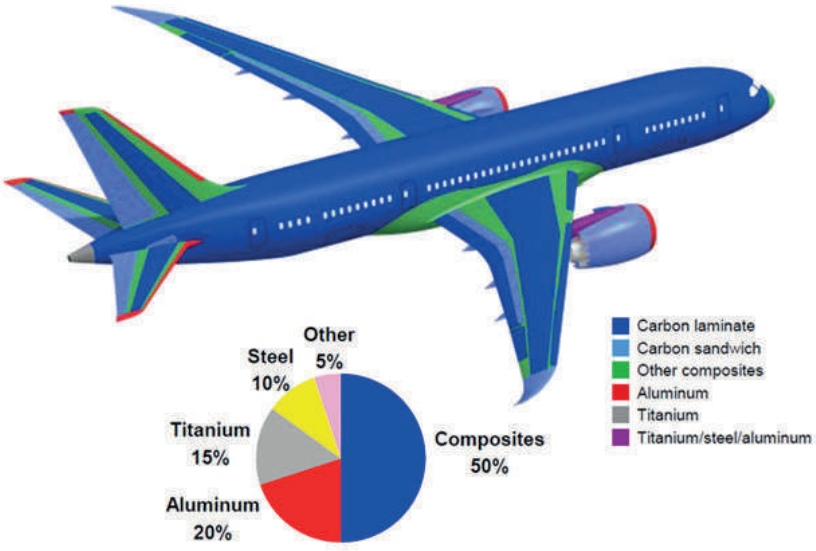

Figure 1. Composite structure content on the Boeing 787 [21]

Composite materials substantially contribute to the car industry's objectives of weight reduction, fuel efficiency, and performance improvement. The high strength-to-weight ratio, corrosion resistance, and design flexibility of composites render them advantageous for diverse automotive applications, including vehicle structural components, body panels, bumpers, and chassis parts. Carbon fiber reinforced polymers are commonly utilized in the body panels and chassis components of luxury and sports vehicles, thereby diminishing the overall weight of the vehicle and improving acceleration,

handling, and energy economy. Glass fiber reinforced polymers are extensively utilized in many automotive components due to their corrosion resistance and cost-effectiveness [22].

The chemical industry relies heavily on composite materials because of their exceptional durability and resilience to harsh chemicals, abrasive materials, and high temperatures. Composites based on vinylester and glass fiber are extensively utilized in a variety of equipment, including storage tanks, pipelines, heat exchangers, reactor linings, and reactors. These materials not only save maintenance costs and downtime, but they also offer corrosion resistance. Composites' lightweight structure and high strength enable easier transportation and assembly of equipment. Composites have several uses in the chemical industry because of the many benefits they provide, including reduced costs and increased durability [23].

Composite materials find extensive applications in the construction and building sector, including exterior and interior facade cladding, decorative applications, roofing sheets and roof detail profiles, load-bearing profiles, rainwater drainage systems, various insulation works, concrete molds, prefabricated buildings, and bridges (Figure 2). People commonly use glass fiber-reinforced polymers to enhance the earthquake resistance of structures and boost the load-bearing capacity of bridges. The materials provide a sustainable solution by enhancing the durability of structures, owing to their resistance to environmental conditions and their capacity to lower maintenance expenses [24].

Figure 2. Architecture of family house, made of prefabricated elements [25]

The maritime sector extensively uses composite materials, particularly in various structural components. Ship hulls and boat coverings frequently utilize composite materials, particularly glass fiber reinforced polymers (GFRP) and carbon fiber reinforced polymers (CFRP), due to their lightweight and durable properties. Propellers and shafts use composites to meet high

strength and low weight criteria, which enhances fuel efficiency and speed performance. Ballast tanks, underwater pipelines, and diving equipment use composites due to their chemical and corrosion resistance properties. Specialized applications commonly use them, such as deck materials, masts, underwater structural components, and windsurfing boards [26].

4. Components and Classification of Composite Materials

The composite structure is composed of two distinct materials referred to as "matrix" and "reinforcement." The matrix constitutes the primary component of the composite, whereas the reinforcement element acts as a more robust material that enhances the strength of the matrix.

The matrix serves as one of the two primary components of the composite material, establishing the fundamental structure and offering several key contributions to the material's performance:

- Facilitating the transmission of forces to the fibers and ensuring their even distribution,
- Safeguarding the fibers against environmental influences and mechanical impacts,
- Enhancing the toughness of the composite,
- Mitigating crack initiation and inhibiting the advancement of pre-existing cracks within the composite.

Composite materials can be categorized based on the type of matrix material, resulting in distinct groups that exhibit varying performance characteristics and application domains. The classification can be organized in the following manner:

- Polymer Matrix Composites
- Metal Matrix Composites
- Ceramic Matrix Composites

Composite materials can be categorized based on the configuration and arrangement of reinforcement elements, leading to distinct classifications that influence the mechanical properties and performance characteristics of the material. The classification can be established according to the orientation, size, and distribution of the reinforcing elements as outlined below:

- Particle-Reinforced Composites
- Fiber-Reinforced Composites

- Layered (Laminar) Composites
- Combined (Hybrid) Composites

4.1. Polymer Matrix Composites

Polymerization is the process in which small molecules known as monomers, influenced by temperature, pressure, and various chemicals, join to create long chains termed polymers. The polymerization process transforms ethylene into polyethylene, propylene into polypropylene, and styrene into polystyrene, so producing polymers. Polymers (plastics) are extensively utilized across several sectors owing to their economical manufacture, malleability, and capacity for customization to specific features. Approximately 90% of composites are derived from polymer-based matrices, leading to their designation as reinforced plastics [27].

Polymers are materials extensively utilized across various industries attributed to their distinct physical and chemical properties (Table 1). We can structure polymers in various configurations based on their classification as thermoplastic or thermoset types, offering a diverse array of benefits. We categorize the properties of polymers as follows:

- Various chain structures can be formed;
- Properties can be modified via the polymerization process;
- Production can occur at varying density levels;
- Customization with additives is possible;
- They are sourced from petroleum derivatives.

Thermoset plastics, referred to as thermosetting plastics, exhibit a highly rigid structure due to their three-dimensional cross-linking through covalent bonds. The materials in question undergo hardening via cross-linking and exhibit no dissolution or melting upon exposure to heat. Specific chemical reactions produce thermoset plastics in their liquid state through the lateral bonding of monomer molecules. The irreversible polymerization reaction during production prevents heating from softening and reshaping thermoset plastics. Unlike thermoplastics, thermosets are not reusable, but they can undergo recycling. During production and storage, it is essential to keep them in freezers to avoid hardening. The shelf life varies between 6 and 18 months. Upon removal from the freezer and exposure to room temperature for a duration of 1–4 weeks, the items undergo hardening, resulting in a loss of formability. Thermoset resins exhibit resistance to chemical effects and do not dissolve. Common materials within this category encompass polyester,

epoxy, high-temperature resins, phenolic, silicone, polyimide, polyurethane, and cyanate esters [28].

Table 1. Polymer Matrix Properties [29]

Polymer	**Density (g/cm³)**	**Mechanical Strength (MPa)**	**Heat Resistance (°C)**	**Applications**
Epoxy	1.2-1.3	60-80	150-250	Aerospace, automotive, electronics
Polyurethane	1.1-1.2	40-60	120-150	Insulation, furniture, sports equipment
Polyethylene (PE)	0.91-0.96	10-30	80-110	Pipe systems, packaging
Polypropylene (PP)	0.90-0.91	20-40	100-130	Automotive parts, household items
Polyamide (Nylon)	1.1-1.2	50-100	200-250	Textiles, engineering parts
Polyketone	1.3-1.4	70-100	200-260	High-performance engineering applications
Polyvinyl Chloride (PVC)	1.3-1.4	30-50	80-120	Pipes, coatings, electrical insulations
Polyarylate	1.2-1.4	80-120	250-300	Aerospace and defense industries

Thermoplastic materials, commonly referred to as "thermoplastic resins," find extensive application in the automotive and aerospace sectors. Their distinctive characteristic is the capacity to become pliable upon heating and revert to a solid state upon cooling. Thermoplastics exhibit a thermal expansion coefficient that is roughly five times greater than that of metals. Their specific heat values can attain levels up to four times those of ceramics. Additionally, the thermal conductivity of thermoplastics is three times lower than that of metals. These materials are typically manufactured through injection and extrusion molding techniques, utilized in the fabrication of pressable glass fiber reinforced thermoplastics. Their shelf life is extended, and they are equipped with recycling capabilities. The materials exhibit high elongation rates of 1500% and demonstrate superior impact toughness. They also perform effectively regarding impact resistance and electrical insulation properties. These items can be maintained at ambient temperature without the necessity for refrigeration and can be reconfigured through reheating following processing. Thermoplastics present certain drawbacks as well. The materials exhibit low strength, particularly in terms of tensile

strength, as well as low hardness and rigidity, which are identified as their weaknesses. Their application as a matrix in the production of composite materials presents challenges and incurs high costs, with certain types necessitating solvents to attain the specified shape. Thermoplastics include a variety of materials such as acetals (POM), polyethylene (PE), polymethyl methacrylate (PMMA), polyamides (PA), acrylonitrile butadiene styrene (ABS), polypropylene (PP), polytetrafluoroethylene (PTFE), polyvinyl chloride (PVC), polyether sulfone (PES), polyether imide (PEI), polyamide imide (PAI), polyphenylene sulfide (PPS), polyether ether ketone (PEEK), and polystyrene (PS) [30].

Elastomers are made up of cross-linked long-chain molecules, which are similar to thermosets. They can change shape a lot when little forces act on them. Certain elastomers can demonstrate elastic deformation levels reaching up to 500%. Rubber, the most well-known elastomer, falls into two primary categories: Specific plants source natural rubber, while analogous polymerization processes manufacture synthetic rubber for use in thermoset and thermoplastic polymers [31].

4.2. Metal Matrix Composites

Metal matrix composites (MMCs) are sophisticated materials formed by embedding ceramic or metal reinforcement components within a metal matrix, providing enhanced mechanical and thermal characteristics. The characteristics of MMCs are as follows:

• These materials find extensive applications in high-performance industries, including automotive, aerospace, and aviation.

• They enhance the mechanical properties of composite materials by providing superior strength, rigidity, and toughness relative to plastic matrices.

• A good composite structure is not achievable with all types of fibers.

• The inability to establish compatible interfaces with all fiber types can lead to complexities and increased costs in composite production. This scenario represents a major drawback associated with metal matrix composites. Light metals, including aluminum, magnesium, nickel, titanium, copper, zinc, and their respective alloys, are frequently selected as metal matrix materials.

Aluminum and its alloys are significant among the frequently utilized metal matrix materials. Examples of materials in this group include 6061 and 2024 aluminum alloys, along with 1010 pure aluminum. Composite materials are manufactured through the hot-pressing technique, operating

within a temperature range of 450-550°C. These materials are capable of retaining their properties at temperatures up to 300°C. Aluminum alloys are capable of forming composites with carbon fiber. In this combination, it is essential to coat the fiber surface with nickel or silver to mitigate corrosion risks. Furthermore, these materials are favored in scenarios that necessitate electrical conductivity. Aluminum alloys incorporate alloying elements, including Mg, Mn, Si, Cu, and Zn, utilized individually or in various combinations to attain desired properties. [32].

Magnesium and its alloys are favored in applications necessitating lightweight and robust materials, such as spacecraft, high-speed machinery, and transportation vehicles, owing to their low density (1.74 g/cm^3) and elevated specific strength. However, these materials have notable drawbacks such as limited corrosion resistance, insufficient stiffness, diminished fatigue strength, and inadequate wear resistance at elevated temperatures. Typically, alloys with aluminum and zinc utilize magnesium, which comes in both hardenable and non-hardenable varieties. Moreover, magnesium provides superior machinability in chip production relative to other metals [33].

The low melting point of 419 °C of zinc and its alloys makes them ideal casting materials. These characteristics facilitate the efficient fabrication of thin-walled (0.5 mm thick), intricately formed, and small-diameter apertures. Zinc alloys manufactured through die casting are known as Zamak, encompassing numerous varieties including Zamak 3, Zamak 5, Zamak 8, Zamak 15, and Zamak 27, which are also designated by codes such as Z33520 and Z35540. Coating zinc onto steel or cast-iron cathodes as an anode imparts corrosion resistance to these materials (zinc-coated steel: galvanized steel). Zinc alloys have a density of 7.13 g/cm^3 and have significant wear resistance at low-speed and high-load conditions. While they demonstrate commendable fatigue resistance at ambient temperatures, they display brittle characteristics at lower temperatures. Although their ductility enhances with extended usage, their mechanical strength diminishes slightly. The automotive industry extensively uses zinc alloys in the manufacturing of kitchenware and some precision components [34].

Titanium and its alloys possess one of the lowest coefficients of thermal expansion among metals and have superior strength and stiffness relative to aluminum. Furthermore, its exceptional corrosion resistance sets it apart. Typically, alloys of titanium include aluminum, manganese, silicon, and vanadium. Machine components, such as compressor blades and disks, extensively utilize titanium alloys due to their heat-resistant properties. We can integrate titanium alloys with boron carbide and silicon carbide (SiC)

fibers as matrix materials to create high-performance composites. These materials demonstrate exceptional performance at operation temperatures ranging from 420 to 550 °C. Their exceptional specific strength characteristics make them especially favored in crucial applications within the aerospace and aviation sectors [35].

4.3. Ceramic Matrix Composites

Ceramics are classified as high-temperature matrices and can be defined as earth materials subjected to elevated firing temperatures. Ceramics are defined as inorganic compounds that are produced through the sintering process, involving the combination of one or more metals with non-metallic elements. The fundamental components of ceramics include silicates, aluminates, water, metal oxides, and alkali and alkaline earth compounds. The structure of these materials exhibits high stability, attributed to the presence of both partially ionic and covalent bonds. Various sectors, including industrial furnaces, electronics, and optics, utilize ceramics, which possess either a crystalline or amorphous structure. Although these materials exhibit high strength, their hard and brittle structures contribute to fragility, thereby restricting their applications. Ceramics typically find use in high-temperature settings due to their elevated thermal resistance [36].

Overview of Ceramic Matrix Properties:

- **Structural Composition:** Made up of silicates, aluminates, metal oxides, alkali, and alkaline earth compounds.
- **Diversity**: This category encompasses oxides, nitrides, borides, carbides, silicates, and sulfides.
- **Bond Structure:** The presence of both partially ionic and covalent bonds contributes to a stable structural configuration.
- **Crysal and Amorphous Structures:** The material can display characteristics of both crystalline and amorphous structures.
- **Applications:** Frequently utilized in industrial furnaces, as well as in the electrical, electronic, and optical sectors.
- **Mechanical Properties:** The material exhibits high strength; however, it is characterized by brittleness owing to its hard and fragile structure.
- **Thermal Resistance:** This material exhibits resistance to elevated temperatures, making it suitable for applications in environments subjected to high thermal conditions.

•**Melting Temperature:** The melting temperatures of these materials are elevated; silica has a melting point of 1750°C, while alumina has a melting point of 2050°C.

•Isolation Properties: Delivers electrical and thermal insulation capabilities.

4.4. Particle Reinforced Composites

Particle reinforcement elements, which might be microscopic or macroscopic in size, typically show isotropic material qualities. Different methods allow large and small particles to carry loads in particle-reinforced composites. Large particles evenly distribute the load across the components, while small particles increase the material's strength by hindering dislocation movements. Ceramic materials like Al_2O_3 and SiC are frequently utilized in applications where the diameters of tiny particles are less than or equal to 1 μm [37].

Benefits and Drawbacks of Particle-Reinforced Composites:

• Economic Production: The production process for particle-reinforced composites is more cost-effective when compared to that of fiber-reinforced composites.

• Challenges in Achieving Homogeneous Distribution: In particle-reinforced composites created through casting processes, the ability to effectively wet the particles and attain a uniform distribution is hindered by the reduction in melt viscosity.

• Limited Mechanical Properties: Fiber-reinforced composites exhibit enhanced mechanical properties in comparison to those that are particle-reinforced.

4.5. Fiber-Reinforced Composites

Fiber-reinforced composites are sophisticated materials extensively utilized in contemporary engineering and technology, providing exceptional mechanical qualities. These composites are classified into two primary categories: discontinuous fibers and continuous fibers. Discontinuous fibers may possess diameters not exceeding several micrometers and range in length from a few millimeters to several centimeters. Continuous fibers serve as essential strength components of the composite construction, exhibiting advantageous characteristics including low density, high elastic modulus, elevated strength, and stiffness. Continuous fibers are essential, particularly

in the advancement of contemporary composites, and are generated by continuous manufacturing techniques like the wire wrapping method [38].

Overview of characteristics:

• **Exceptional Microstructural Characteristics:** Fibers reduce material imperfections owing to their reduced diameters and fine internal structural grains, resulting in elevated elasticity modulus and strength.

• **High Load Carrying Capacity:** The increased fiber length-to-diameter ratio enhances the load transfer from the matrix to the fiber, resulting in improved mechanical strength of the composite.

• **Types of Fiber Materials:** The primary categories of fibers utilized are glass fiber, carbon (graphite) fiber, aramid (Kevlar) fiber, boron fiber, oxide fiber, high-density polyethylene fiber, polyamide, polyester, and natural organic fibers. The most commonly utilized types of continuous fibers include glass, carbon, boron, and aramid fibers.

• **Production Costs:** The processes involved in the production of fiber-reinforced composites, particularly the continuous production and processing of continuous fibers, can incur significant expenses.

• **Brittleness:** Fiber-reinforced composites may demonstrate brittleness under specific conditions, even though they possess high strength.

• **Complex Manufacturing Processes:** Achieving a homogeneous distribution and appropriate orientation of fibers within the matrix necessitates intricate manufacturing processes.

Glass fiber is produced from materials including silica, colemanite, aluminum oxide, and soda, and is the predominant type of fiber utilized in the manufacturing of fiber-reinforced composites. The process of producing glass fiber involves the passage of molten glass through a specially engineered furnace equipped with small apertures at the base, utilizing pressure to facilitate the operation. Upon formation of the fiber, a coating process is implemented to improve its durability. Polymers that exhibit high solubility in water are typically favored prior to the production of composites for this coating. The bond between the fiber and the resin must be strong, as weak adhesion can lead to a reduction in the stiffness and strength of the composite material. To mitigate this limitation, glass fiber undergoes treatment with chemical coatings that improve adhesion properties [39].

People recognize carbon fiber for its exceptional mechanical properties, which include lightness, high strength, elastic modulus, and corrosion resistance. It serves as a crucial reinforcement material in high-performance

applications such as aircraft, space vehicles, and sports equipment. Advanced composite materials favor carbon fiber because it is lighter and more durable than glass fiber, offering high-temperature resistance and compatibility with all resins. Nonetheless, the expenses associated with production remain significant, and various types are perpetually under development [40].

Aramid fibers exemplify the dual role of polymers, serving effectively as both matrix materials and fiber reinforcements. Kevlar is a lightweight polymer fiber characterized by an aromatic polyamide structure, which imparts significant strength and rigidity to composite materials. Aramid fiber is widely recognized in commercial applications under the brand names Kevlar (DuPont) and Twaron (Akzo Nobel). Kevlar fibers are primarily categorized into two types: Kevlar 29 and Kevlar 49. Special properties of aramid fibers can be harnessed for various applications, and they typically exhibit a yellow hue [41].

4.6. Laminated Composites

Optimal performance of a layered composite is achieved by combining the mechanical properties of each layer, which are added in a specified order, to create an improved material. Composites like this are ideal for a wide range of commercial uses because of their strength, portability, and adaptability [42].

Fundamental Characteristics of Laminated Composites:

• **Adaptable Load-Bearing Capability:** The layers oriented in multiple directions offer resistance to diverse load types, improving the material's strength in various directions.

• **Lightness and High Strength:** Laminated composites present a remarkable combination of high strength and low weight, achieving an ideal equilibrium between mass and resilience.

• **Adaptability and Creative Potential:** The integration of diverse materials and fibers enables the attainment of various characteristics, facilitating designs tailored for particular uses.

• **Interlayer Bonding:** Robust adhesion among layers guarantees the composite's integrity, contributing to its long-lasting durability.

• **Fatigue and Wear Resistance:** Laminated structures demonstrate exceptional durability against fatigue and wear, ensuring prolonged functionality.

• **Thermal and Electrical Properties:** The performance of laminated composites in terms of thermal and electrical insulation is largely influenced by the selection of materials.

• **Fracture Resistance:** Layered structures exhibit significant resistance to targeted impacts and crack propagation, thus improving the material's dependability.

5. Conclusion

This study thoroughly investigates the fundamental properties, benefits, drawbacks, classifications, and types of matrix reinforcement in composite materials, highlighting their significance in engineering applications. Composite materials are essential in contemporary engineering, effectively addressing various requirements that traditional materials often cannot meet due to their enhanced mechanical, chemical, and physical properties. The properties of these materials, including low weight, high strength, design versatility, and durability, facilitate their use across various sectors, such as aviation, automotive, construction, medicine, and energy. Nonetheless, high production costs, intricate recycling processes, and restricted impact resistance in certain applications represent significant obstacles to the broad adoption of composites. The research showed that grouping things into categories based on matrix and reinforcement types gives us a lot of options for making composites work better in real life. The choice of polymer, metal, and ceramic as matrix materials, combined with fibers, particles, or plates as reinforcement elements, provides tailored solutions to meet specific mechanical and physical requirements. Expanding research on composite materials will address current challenges and facilitate the development of next-generation solutions that are more sustainable, economical, and high-performing. We expect composite materials to play a more significant role in future engineering applications.

References

1. Abanto, G.A., et al., *Thermal properties of adobe employed in Peruvian rural areas: Experimental results and numerical simulation of a traditional bio-composite material.* Case Studies in Construction Materials, 2017. **6**: p. 177-191.
2. Singh, S., M. Uddin, and C. Prakash, *Introduction, history, and origin of composite materials*, in *Fabrication and Machining of Advanced Materials and Composites*. 2022, CRC Press. p. 1-18.
3. Nagavally, R.R., *Composite materials-history, types, fabrication techniques, advantages, and applications.* Int. J. Mech. Prod. Eng, 2017. **5**(9): p. 82-87.
4. Cevahir, A., *Glass fibers*, in *Fiber technology for fiber-reinforced composites*. 2017, Elsevier. p. 99-121.
5. González, C., et al., *Structural composites for multifunctional applications: Current challenges and future trends.* Progress in Materials Science, 2017. **89**: p. 194-251.
6. Gururaja, M. and A.H. Rao, *A review on recent applications and future prospectus of hybrid composites.* International Journal of Soft Computing and Engineering, 2012. **1**(6): p. 352-355.
7. Gu, X. and F. Pierron, *Towards the design of a new standard for composite stiffness identification.* Composites Part A: Applied science and manufacturing, 2016. **91**: p. 448-460.
8. Radhamani, A., H.C. Lau, and S. Ramakrishna, *Nanocomposite coatings on steel for enhancing the corrosion resistance: A review.* Journal of Composite Materials, 2020. **54**(5): p. 681-701.
9. Shanmugasundram, H.P.P.V., E. Jayamani, and K.H. Soon, *A comprehensive review on dielectric composites: Classification of dielectric composites.* Renewable and Sustainable Energy Reviews, 2022. **157**: p. 112075.
10. Ma, L., et al., *Diversifying composition leads to hierarchical composites with design flexibility and structural fidelity.* ACS nano, 2021. **15**(9): p. 14095-14104.
11. Zuo, P., D.V. Srinivasan, and A.P. Vassilopoulos, *Review of hybrid composites fatigue.* Composite Structures, 2021. **274**: p. 114358.
12. Aramide, B., et al., *Wear-resistant metals and composites.* Handbook of Nanomaterials and Nanocomposites for Energy and Environmental Applications, 2021: p. 731-755.
13. Burger, N., et al., *Review of thermal conductivity in composites: Mechanisms, parameters and theory.* Progress in Polymer Science, 2016. **61**: p. 1-28.

14. Das, P.P., et al., *Acoustic performance of natural fiber reinforced polymer composites: Influencing factors, future scope, challenges, and applications*. Polymer Composites, 2022. **43**(3): p. 1221-1237.
15. Allcock, B. and P. Lavin, *Novel composite coating technology in primary and conversion industry applications*. Surface and Coatings Technology, 2003. **163**: p. 62-66.
16. Hoa, S.V., *Principles of the manufacturing of composite materials*. 2009: DEStech Publications, Inc.
17. Vasiliev, V.V. and E.V. Morozov, *Advanced mechanics of composite materials and structures*. 2018: Elsevier.
18. Babu, J., et al., *Assessment of delamination in composite materials: a review*. Proceedings of the Institution of Mechanical Engineers, Part B: Journal of Engineering Manufacture, 2016. **230**(11): p. 1990-2003.
19. Yang, Y., et al., *Recycling of composite materials*. Chemical Engineering and Processing: Process Intensification, 2012. **51**: p. 53-68.
20. Kesarwani, S., *Polymer composites in aviation sector.* Int. J. Eng. Res, 2017. **6**(10).
21. Loukil, M.S., *Experimental and numerical studies of intralaminar cracking in high performance composites*. 2013, Luleå tekniska universitet.
22. Hovorun, T.P., et al., *Modern materials for automotive industry.* 2017.
23. La Mantia, F. and M. Morreale, *Green composites: A brief review.* Composites Part A: Applied Science and Manufacturing, 2011. **42**(6): p. 579-588.
24. Mosallam, A.S., *Composites in construction*. Handbook of materials selection, 2002: p. 1369-1420.
25. Tažiková, A., J. Talian, and J. Galla, *Analysis of prefabricated systems in the construction of family houses*. TEM Journal, 2020. **9**(3): p. 959.
26. Rubino, F., et al., *Marine application of fiber reinforced composites: a review.* Journal of Marine Science and Engineering, 2020. **8**(1): p. 26.
27. Wang, R.-M., S.-R. Zheng, and Y.G. Zheng, *Polymer matrix composites and technology*. 2011: Elsevier.
28. Chaudhary, V. and F. Ahmad, *A review on plant fiber reinforced thermoset polymers for structural and frictional composites*. Polymer Testing, 2020. **91**: p. 106792.
29. Huang, S., et al., *Characterization of interfacial properties between fibre and polymer matrix in composite materials–A critical review.* journal of materials research and technology, 2021. **13**: p. 1441-1484.
30. Grigore, M.E., *Methods of recycling, properties and applications of recycled thermoplastic polymers*. Recycling, 2017. **2**(4): p. 24.

31. Patil, A.O. and T.S. Coolbaugh, *Elastomers: A literature review with emphasis on oil resistance*. Rubber Chemistry and Technology, 2005. **78**(3): p. 516-535.
32. Chak, V., H. Chattopadhyay, and T. Dora, *A review on fabrication methods, reinforcements and mechanical properties of aluminum matrix composites*. Journal of manufacturing processes, 2020. **56**: p. 1059-1074.
33. Yang, H., et al., *Microstructures and mechanical properties of titanium-reinforced magnesium matrix composites: review and perspective*. Journal of Magnesium and Alloys, 2022. **10**(9): p. 2311-2333.
34. Singh, P., et al., *Mechanical and tribological properties of zinc-aluminium (ZA-27) metal matrix composites: a review*. Advances in Materials and Processing Technologies, 2024: p. 1-19.
35. Ammisetti, D.K. and S.H. Kruthiventi, *Recent trends on titanium metal matrix composites: A review*. Materials Today: Proceedings, 2021. **46**: p. 9730-9735.
36. Binner, J., et al., *Selection, processing, properties and applications of ultra-high temperature ceramic matrix composites, UHTCMCs–a review*. International Materials Reviews, 2020. **65**(7): p. 389-444.
37. Zhou, D., et al., *Manufacture of nano-sized particle-reinforced metal matrix composites: a review*. Acta Metallurgica Sinica (English Letters), 2014. **27**: p. 798-805.
38. Yang, G., M. Park, and S.-J. Park, *Recent progresses of fabrication and characterization of fibers-reinforced composites: A review*. Composites Communications, 2019. **14**: p. 34-42.
39. Sathishkumar, T., S. Satheeshkumar, and J. Naveen, *Glass fiber-reinforced polymer composites–a review*. Journal of reinforced plastics and composites, 2014. **33**(13): p. 1258-1275.
40. Zheng, H., et al., *Recent advances of interphases in carbon fiber-reinforced polymer composites: A review*. Composites Part B: Engineering, 2022. **233**: p. 109639.
41. Dharmavarapu, P. and S.R. MBS, *Aramid fibre as potential reinforcement for polymer matrix composites: a review*. Emergent materials, 2022. **5**(5): p. 1561-1578.
42. Zhang, X., et al., *Progress on the layer-by-layer assembly of multilayered polymer composites: Strategy, structural control and applications*. Progress in Polymer Science, 2019. **89**: p. 76-107.

Chapter 6

A Single-Phase Tubular Flux-Switching Generator Analysis for Generating Electrical Energy from Walkways

Serdal Arslan[1]

Abstract

Today, alternative methods are being sought for obtaining electrical energy via harvesters. One of these methods is the use of small powerful energy harvesters on walking paths, which has been an important research topic in recent years. For example, these harvesters can be used to obtain electrical energy from both daily walking and sports activities. Piezoelectric material systems generally used to obtain electrical energy from walking paths. Although their power values are in nano or micro values, it can be predicted that significant electrical energy will be gained during use. Electrical energy can also be obtained from systems integrated with linear generators positioned on the walking path. For these applications, both the single-phase model of the linear flux switched generator internal and external moving models have been compared.

1. INTRODUCTION

In our daily lives, the energy we expend because of our physical movements is going to waste. This has led to the search for systems that can generate electrical energy on a mini and micro scale for the recovery of expended energy. In other words, systems referred to as energy harvesting systems can meet our instantaneous energy needs. It is not expected that energy harvesting technologies alone will meet countries' increasing energy demands. However, they can meet the requirements of existing energy-consuming sensor systems. Considering that harvesting technology is relatively new, innovative applications for various fields are on the rise [1,2]. Energy harvesting from a biomechanical perspective in humans has been

1 Doç.Dr., Harran Üniversitesi Organize Sanayi Bölgesi M.Y.O. Elektrik Programı, serdalarslan@harran.edu.tr, 0000-0002-1187-5633

https://doi.org/10.58830/ozgur.pub575.c2604

classified as piezoelectric, triboelectric, electromagnetic, and electrostatic [3]. Particularly, piezoelectric and thermoelectric systems can be used for energy harvesting when implanted in the body [4]. The daily power generation from human movements (hand, arm, or foot) of approximately 20-70W is noteworthy [5]. Portable, wearable, and even implantable harvesters are limited in terms of power, and power generated from the foot is quite high [5]. Integration of energy harvesting systems into transportation (road, rail, air, sea) systems is particularly interesting. Some key studies for these applications related to small-scale energy harvesting technologies can be summarized [6]:

- The installation of solar panels on highways to generate electrical energy [7]. Currently, there are issues related to installation and durability [6,8]. However, by using durable materials, warning LEDs can be powered to ensure the attention of vehicles in areas with pedestrian crossings [7].
- It is possible to generate electricity from wind energy in areas with heavy vehicle traffic [9].
- In hot climates, electricity can be generated through Thermoelectric Generators (TEGs) [6,8].
- Despite not being satisfactory in terms of output power, it is possible to generate energy from noise in places with high sound sources.
- There are extensive studies on energy harvesting using piezoelectric technology, primarily through vibrations. The power that can be obtained from this system is in the micro or milli range [1-8,10].
- Applications for energy harvesting systems can be diversified through electromechanical systems. Models in this field have mostly focused on energy production from mechanical systems or piezoelectric systems. It is possible to generate sufficient power for sensors and charging systems from these systems [1-8,10].

The Dutch start-up Energy Floors can be cited as the pioneer in this field. In 2008, they implemented the first application of converting kinetic energy from dancers into electricity at Club Watt, a sustainable dance club in Rotterdam [11]. Later, in 2014, they focused on electricity generation from a pedestrian floor that converts solar energy, known as the Smart Energy Floor [11]. These applications have become widespread at festivals, fairs, educational institutions, public transportation, and globally. In fact, these systems offer a new application area known as "Smart or Sustainable Floors." Additionally, they can be designed for on-grid use, but these systems are often

used as off-grid interactive LED lighting or power sources. The harvested electrical energy from the system is used to power the electronic card, which includes sensors, motion detectors, and a charging control system.

One of their applications, "The Gamer," focuses on promoting physical exercise in game parks through a solar-powered floor while simultaneously generating electrical energy [11]. Another company, Pavegen, founded in 2009, has a focus on interactive data collection as a "Smart or Sustainable Floor" [11]. They use this data to establish meaningful connections with individuals and companies. For instance, it's possible to convert the data from smart footsteps into digital currency or brand-based discounts. Figure 1 provides simulations of a solar panel-based and an electromechanical energy-harvesting pedestrian pathway.

(a) *(b)*

Figure 1. (a) Photovoltaic-based pedestrian pathway floor application[2], (b) Electromechanical-based pedestrian pathway floor application[3] [12]

Most of these studies are aimed at meeting the energy needs of sensor systems. In this study, unlike other harvesting concepts (such as photovoltaic, wind, piezoelectric, electromagnetic, etc.), designs of linear generators driven by a moving mechanism have been considered. These systems typically generate electricity through walking, running, climbing, hand-arm

2 [2]The images shown here are artificial intelligence-generated visuals related to energy harvesting from pedestrian pathways.

3 [3]The images shown here are artificial intelligence-generated visuals related to energy harvesting from pedestrian pathways.

coordination, or forward-backward hand movements. Handheld harvesters (such as battery-less flashlights, etc.) or energy harvesting from natural walking or daily physical activities of humans are commonly preferred. For example, a mechanical system placed in a backpack for carrying loads generated 7.4W of power [13]. A controlled sliding system was proposed as a new harvester design [14]. Acceleration data at 3km/s for the sole of the foot, toe, and heel were examined. Additionally, five different linear generator designs were studied to obtain micro power for shoes [15]. For the shoe application, the pole ratio, shape ratio, inner and outer diameter ratios of the linear generator were parametrically examined, and suitable models were tested [16-17]. Sajwani et. al. [18] proposed a Halbach-arrayed linear generator as the harvester. Studies discussed in the literature have focused on portable, implantable, and wearable harvesting systems. However, the system considered in this article is based on energy generation through a generator that can be integrated into a pedestrian pathway. Electric power can be generated through a linear generator driven by a mechanical system depending on motion.

Linear generators can come in various types, including induction, permanent magnet, switched reluctance, and more [19]. Especially, permanent magnet generators are known for their high efficiency and power density, leading to increased research on machines based on permanent magnets and their variations. Based on magnet arrangement, they can be classified as Halbach arrayed, axial flux, and radial flux [20]. The Halbach arrangement increases the magnetic flux in the air gap and allows for smoother sinusoidal voltage output. Halbach arrangement consists of axial and radial flux magnets. Continuous magnet linear generators can be evaluated based on their moving parts, construction, and magnetic flux direction dependency [21]. The moving part can be composed of steel material, magnets, windings, or various combinations thereof. Depending on the condition of the stator and the moving part, it can be categorized as short or long stroke. It can also be classified as transverse or longitudinal according to the magnetic flux direction. Single-sided/double-sided construction has been studied for suspension systems [22], but more research has been conducted on the tubular structure due to its advantages (zero net radial forces, absence of end winding effects, etc.). The core structure of the stator or moving part can be made of iron or air. Iron core provides more power compared to air-core [23,24]. Flux-switching machines feature windings, magnets, and steel materials in the stator structure, while the moving part consists solely of steel material. This allows for mechanical robustness and cooling in the moving part [25]. A comparison has been made between the Halbach

arrayed tubular linear generator with a 9/10 slot/pole combination and the flux-switching tubular linear generator (FSTLG) [26], and the FSTLG with 12 slots/10 poles and 12 slots/14 poles structures has been examined [27]. The stator and moving steel materials of the FSTLG can be made of the same or different materials [28]. In another study, 6 slots/5 poles and 6 slots/7 poles FSTLGs have been investigated [29].

The selected linear generator topology should have a short stroke, occupy minimal space, be lightweight, provide good mechanical damping [30], and offer high output performance depending on speed changes [30], especially tailored to the intended use, the speed-frequency profile, and force values of the system may vary.

2. FSTLG STRUCTURE AND MODEL

This study considers the dimensional specifications of a multi-pole, three-phase tubular flux-switching generator that has been previously designed and implemented [31] (Table 1). Figure 3 shows a single-phase tubular flux-switching generator. Using one phase of the three-phase generator as a reference, inner runner and outer runner models have been created (Figure 2).

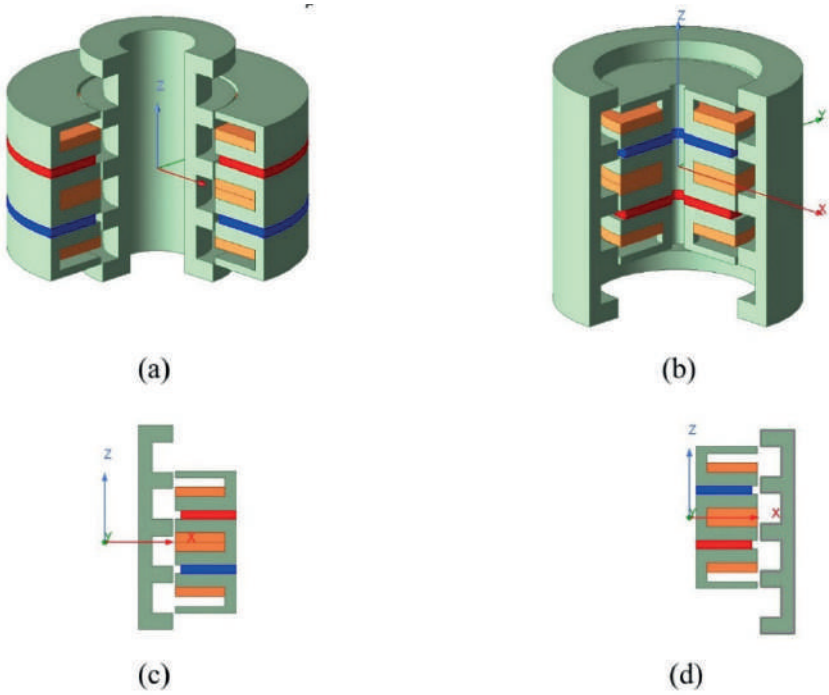

Figure 2. Flux-switching tubular linear generator models; a) 3D model of inner runner, b) 3D of outer runner, c) 2D-rz of inner runner, d) 2D-rz of outer runner

Figure 3 represents geometrical sizing of inner runner flux-switching tubular linear generator in rz coordinate system. Taking the inner radius into account, the outer runner model in Figure 2 was created. The primary and secondary dimensions of both models were taken equal.

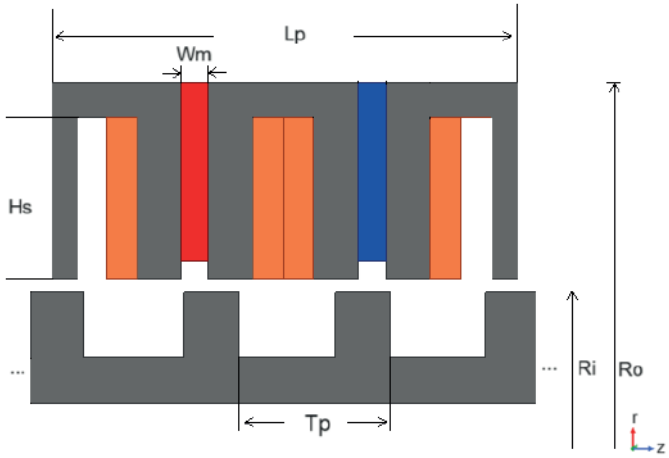

Figure 3. 2D representation of geometrical sizing of flux-switching tubular linear generator in rz coordinate system

Information about the dimensional parameters shown in Figure 3 is provided in Table 1.

Table 1. Characteristics of the tubular linear generator geometric

Geometric	Values (mm)	Geometric	Definitions and Values (mm)
Primer length (Lp)	51.4	Primary and Secondary Steel Material	M43_29G
Pole pitch (Tp)	17	Permanent Magnet (PM) Type	NdFe35
Height slot (Hs)	18	Inner diameter to outer diameter ratio for tubular type	0.53
Magnet width (Wm)	3	Inner radius (Ri)	25.5mm
Winding Type	Double Layer	Air-gap length (g)	1mm

3. FINITE ELEMENT ANALYSIS RESULTS AND EVALUATION

For numerical analyses, the commercial software ANSYS Maxwell was used due to its wide-ranging capabilities, solver infrastructure, and established validity in the literature. Solving electromagnetic problems using the finite element method offers both high accuracy and time efficiency. The models presented in Figure 2c and Figure 2d were analysed using this software through numerical simulations. The analyses were performed on a computer with the following specifications: 12th Gen Intel(R) Core (TM) i7-12700H 2.30 GHz processor and 16GB of RAM. The mesh numbers for inner runner, outer runner models are listed as 59,400 and 630,592, respectively. The magnetic flux density distribution for magnetostatic analysis is shown in Figure 4.

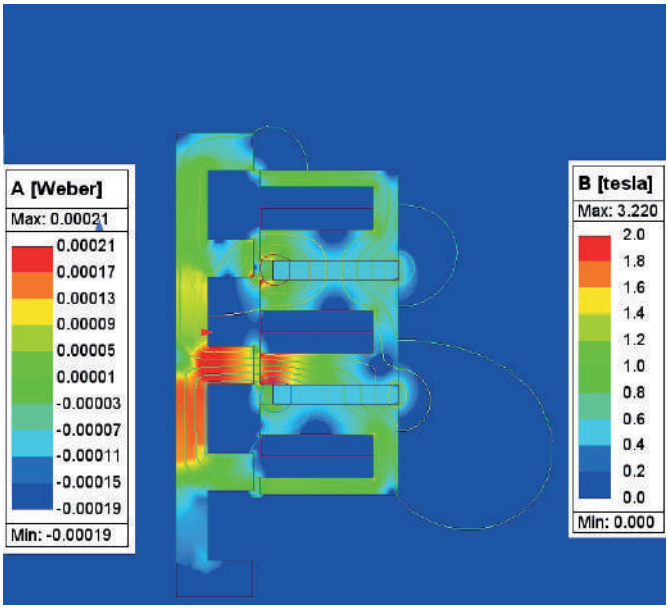

(a)

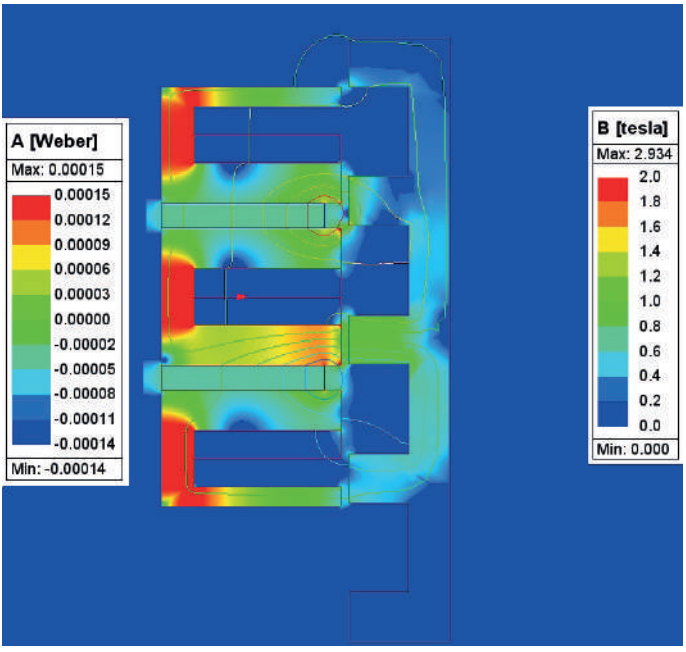

(b)

Figure 4. Magnetic flux density distribution, (a) Inner runner, (b)Outer runner

Here, similar changes in magnetic flux density were observed between the secondary teeth and magnet for both inner runner and outer runner models. However, in the inner runner model, an increase in magnetic flux density was observed in the moving steel compared to the outer runner model. Additionally, there is leakage flux at the upper and lower points of the magnet in all models, and these regions should be considered. Partial demagnetization can be occurred. In Figure 5, the flux density distribution in the air gap is similar for both models. However, it is observed that the inner runner model has a higher flux density. The flux density at 37.5 mm is 43% higher than the outer runner model.

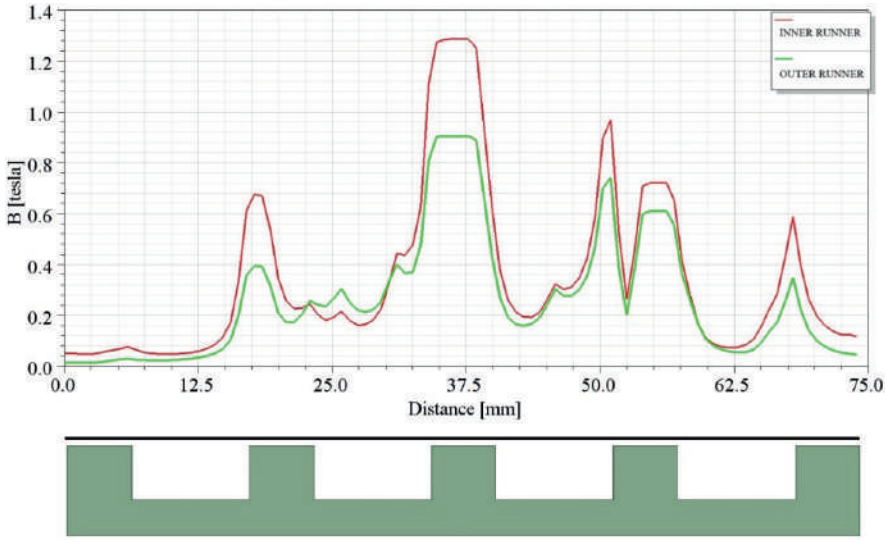

Figure 5. Magnetic field change along the in the middle of the gap

Transient analysis was performed for both models. In previous studies [32], the induced voltage increased as the speed increased. In this respect, no comparison was performed for variable velocities. In this context, the moving speed was taken as 1m/s. The inner radius was increased parametrically while keeping the velocity constant. The voltage induced in a phase winding was compared with the no-load operation (Figure 6).

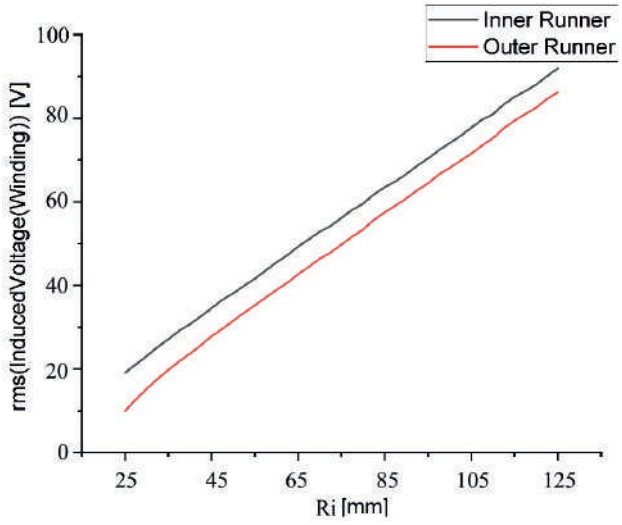

Figure 6. Induced voltage in the winding with Ri.

As the radius increases, the voltage induced in the winding increases linearly. While the V/mm ratio increases at the same rate, there is a difference in the induced voltage of approximately 7.4V.

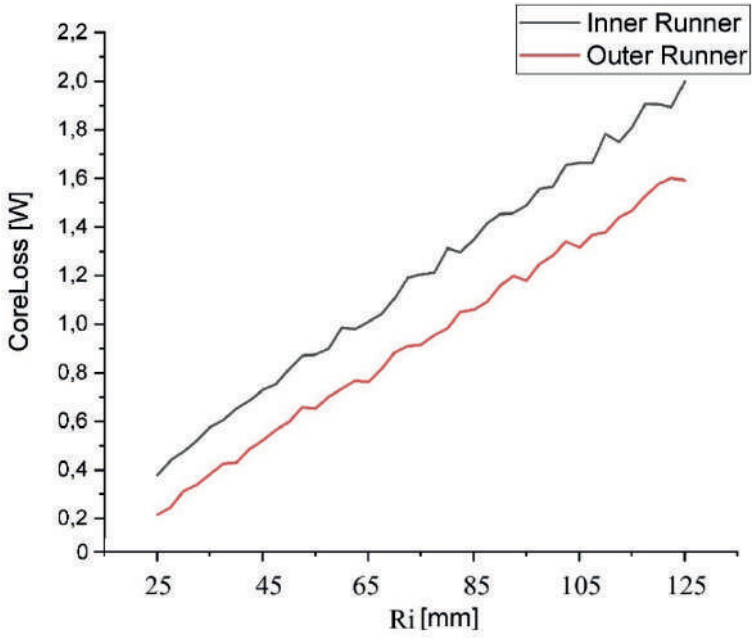

Figure 7. The core losses versus Ri

As the radius increases, iron loss increases. The internal moving (inner runner) model has more iron loss than the external moving (outer runner) one. This is due to the flux density. Although the air gap diameter of both models is equal, the phase resistance is not equal at the same number of turns. The internal moving model was loaded with a resistive load of 28.27 ohms and the external moving model with a resistive load of 14.13 ohms. Figure 8 was obtained according to the average value of the output power.

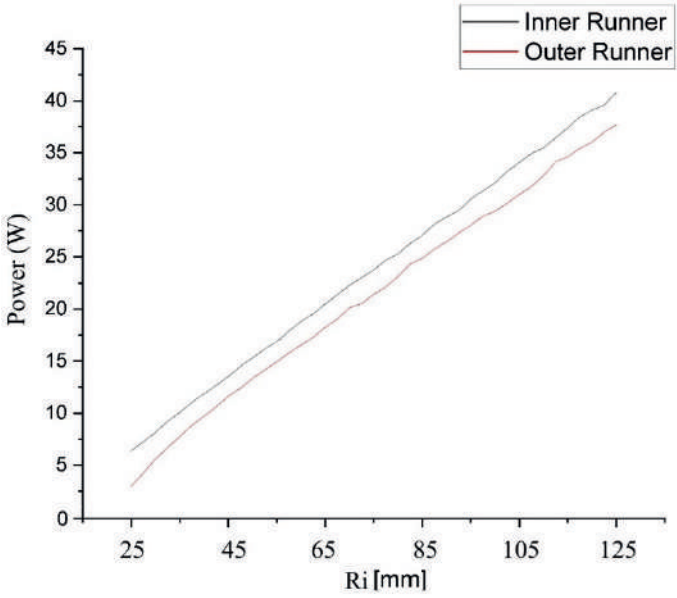

Figure 8. The power versus Ri

The unit cost values taken are 2.12 USD/kg for steel material, 14.85 USD/kg for copper material, and 84.87 USD/kg for magnet material (NdFeB) respectively [33]. The cost calculation presented in Table 2 does not include machine body and labor costs. Here, the primary steel density is taken as 7700 kg/m³, copper winding density as 8933 kg/m³, magnet density as 7400 kg/m³, and secondary steel density as 7700 kg/m³. Table 2 was prepared based on the data in Table 1.

Table 2. Material costs and mass of models

Models	Primary Iron Mass (kg)	Secondary Iron Mass (kg)	PM Mass (kg)	Cooper Mass (kg)	Total Mass (kg)	Total Cost (USD)
Inner Runner	1.150	0.483	0.209	0.474	2.316	28.23
Outer Runner	0.376	0.939	0.0697	0.212	1.596	11.851

When Table 2 is examined, the externally driven model is 31% less in terms of mass. Similarly, it is 58% less costly.

4. CONCLUSION

In this study, single-phase tubular flux-switching generator models for pedestrian walkways were analyzed. Simulation studies were conducted considering the single-phase condition of the three-phase generator subjected to tests. Analysing with the same dimensional parameters, the results showed that as the inner radius increased, the induced voltage in the winding also increased. In terms of core loss variation, inner runner showed higher variations compared to the outer runner model. However, the power exhibited only slight increments for inner runner. Although there is no significant difference in output power between the two models, it can be said that the externally driven model is the more suitable model in terms of cost and total weight.

Future work will involve multiphysics analyses of the designed models, followed by prototype manufacturing of the selected model. Experimental results will be obtained from the walking platform prepared for this purpose. This will enable the utilization of energy generated from activities such as walking, social activities, and playgrounds for local lighting and sensor systems.

Acknowledgment

The author would like to thank Ulupars Ltd. Şti. for financial support during the design and testing processes.

References

1. E. M. Nia, N. A. W. A. Zawawi, and B. S. M. Singh, "A review of walking energy harvesting using piezoelectric materials." IOP Conference Series: Materials Science and Engineering, IOP Publishing, 291, 1, 2017.
2. H. Akinaga, "Recent advances and future prospects in energy harvesting technologies," Japanese Journal of Applied Physics, 59,11, 2020.
3. I. Sobianin, S. D. Psoma, and A. Tourlidakis, "Recent Advances in Energy Harvesting from the Human Body for Biomedical Applications," Energies, 15,21, 2022.
4. T. M. Nidal, et al, "Recent Techniques for Harvesting Energy from the Human Body," Comput. Syst. Sci. Eng., vol. 40, 1, pp.167-177, 2022
5. H. Shi, Z. Liu, and X. Mei, "Overview of human walking induced energy harvesting technologies and its possibility for walking robotics," Energies, vol. 13, 1, 2019.
6. (2023) The Onio website. [Online]. Available: https://www.onio.com/article/energy-harvesting-higway-roads.html
7. Md. F. T. Hossain, et al, "Harvesting solar energy from asphalt pavement," Sustainability, vol. 13, 22, 2021.
8. E. H. H. Al-Qadami, Z. Mustaffa, and M.E. Al-Atroush, "Evaluation of the pavement geothermal energy harvesting technologies towards sustainability and renewable energy," Energies, vol. 15, 3, 2022.
9. (2023) The Elektrik Elektronik Egitimi website. [Online]. Available: https://elektrikelektronikegitimi.blogspot.com/2018/06/istanbulda-metrobus-ruzgarndan-elektrik.html
10. R. Riemer, and A. Shapiro, "Biomechanical energy harvesting from human motion: theory, state of the art, design guidelines, and future directions," Journal of neuroengineering and rehabilitation, vol. 8, pp.1-13, 2011.
11. (2023) The Whatdesigncando website. [Online]. Available: https://www.whatdesigncando.com/stories/why-not-use-our-pavements-and-roads-to-generate-energy/
12. (2023) The Openai website. [Online]. Available: https://openai.com/dall-e-3
13. R. C. Lawrence, et al, "Generating electricity while walking with loads," Science, vol.309, pp.1725-1728, 2005.
14. H. Xia, et al, "Controlled slip" energy harvesting while walking," IEEE Transactions on Neural Systems and Rehabilitation Engineering, vol. 28, 2, pp.437-443, 2019.
15. P. Gui, et al, "Micro linear generator for harvesting mechanical energy from the human gait," Energy, vol.154 pp. 365-373, 2018.

16. J.-X. Shen, et al, "A shoe-equipped linear generator for energy harvesting," IEEE Transactions on Industry Applications, vol.49, 2, pp. 990-996, 2013.
17. CF. Wang, et al, "A shoe-equipped linear generator for energy harvesting," IEEE International Conference on Sustainable Energy Technologies (ICSET), 2010, p.1-6.
18. S.H., et al, "Hallbach array-based linear generator for human motion energy harvesting," International Conference on Electrical and Computing Technologies and Applications (ICECTA), 2017, p.1-6.
19. S. Arslan, and O. Gurdal, "Polygonal tubular linear permanent magnet generator analysis and experimental test," Scientia Iranica, vol.29, 1, pp. 168-182, 2022.
20. A.S. Jalal, N. J. Baker, and D. Wu, "Design of tubular moving magnet linear alternator for use with an external combustion-free piston engine, vol. 6-6, 2016.
21. S. Arslan, "Overview of Generating Electricity from Wave Energy Systems and Investigation of Generator Topologies Used in Archimedes Wave Swing Systems," International Conference on Natural Science and Engineering (ICNASE'16), 2016.
22. O. Shunsuke, "Basic characteristics of the linear synchronous generator using mechanical vibration of the automobile," International Conference on Electrical Machines and Systems, 2010, p. 1550-1554.
23. H. Li, and P. Pillay, "A methodology to design linear generators for energy conversion of ambient vibration," IEEE Transactions on Industry Applications, vol.47, pp.2445-2452, 2011.
24. B. LJ Gysen, et al, "Design aspects of an active electromagnetic suspension system for automotive applications," IEEE transactions on industry applications vol. 45, pp.1589-1597, 2009.
25. M. Kang, et al., "A new tubular fault-tolerant permanent-magnet motor for active vehicle suspension," IECON 2012-38th Annual Conference on IEEE Industrial Electronics Society, 2012, p. 4082-4086.
26. J. Wang, et al., "Comparative studies of linear permanent magnet motor topologies for active vehicle suspension," IEEE Vehicle Power and Propulsion Conference, 2008, p. 1-6.
27. J. Wang, et al., "Design considerations for tubular flux-switching permanent magnet machines," IEEE Transactions on Magnetics, vol. 44, pp.4026-4032, 2008.
28. Y. Putgul, and D. Altiparmak, "Vehicle Suspension System Types and Their Effects on Front Axle Geometry," Journal of Polytechnic-Politeknik Dergisi, vol.19, 2, 2016.

29. I. Martins, et al., "Permanent-magnets linear actuators applicability in automobile active suspensions," IEEE Transactions on vehicular technology, vol.55, pp.86-94, 2006.
30. B. Ebrahimi, "Development of hybrid electromagnetic dampers for vehicle suspension systems," Doctoral Thesis, Mechanical and Mechatronics Engineering, University of Waterloo, Canada, 2009.
31. S. Arslan, "Optimizasyon vasıtasıyla tüp tipi akı anahtarlamalı doğrusal jeneratörün vuruntu kuvveti azaltımı," Academic Perspective Procedia, vol.2, pp.668-676, 2019.
32. S. Arslan, Developing a Tubular Type Flux-Switching Permanent Magnet Linear Machine for a Semi-active Suspension Systems. International Journal of Automotive Technology, 1-14, 2024.
33. G. Du, et al., "Comprehensive Comparative Study on Permanent-Magnet-Assisted Synchronous Reluctance Motors and Other Types of Motor," Applied Sciences, vol.13, 14, 2023.

Bölüm 7

Serbest Pistonlu Dıştan Yanmalı Motorlar için Tüp Tipi Doğrusal Jeneratör Analizi

Serdal Arslan[1]

Özet

Son yıllarda güneş enerjisinden elektrik enerjisi elde etmeye yönelik Stirling Çanağı tasarımları ve uygulamaları dikkat çekmektedir. Bu sistemde ek bir mekaniksel dönüşüme gerek duymadan doğrudan elektrik enerjisi elde edilebilmektedir. Serbest piston mekanizmasına doğrusal jeneratör yerleştirilerek sağlanabilmektedir. Güç yoğunluğu açısından sürekli mıknatıslı tüp tipi jeneratörler bu uygulamalar için tercih edilmektedir. Literatürde bu çalışma alanı üzerine gerçekleştirilen çalışmalar genel hatlarıyla incelenmiştir. Analitik tasarımı gerçekleştirilmiş olan tüp tipi doğrusal jeneratörün sayısal analizi ele alınmıştır. Sayısal analizler Ansys Maxwell yazılımı kullanılarak gerçekleştirilmiştir. Jeneratöre ait çıkış verilerinin elde edilmesinin yanı sıra maliyet analizi de gerçekleştirilmiştir. Farklı çalışma frekans değerliliklerindeki analiz sonuçları da incelenmiştir.

1. Giriş

Fosil kaynakların giderek tükenmesi enerji üretimi üzerine gerçekleştirilen çalışmaları yenilenebilir enerji kaynaklarının kullanımı üzerine yöneltmiştir. Özellikle güneş enerjisi üzerine gerçekleştirilen çalışmalar güneş paneli üzerine elektrik üretimini oluşturmasına karşın odaklamalı güç sistemlerinden de elektrik üretimi giderek artmaktadır. Ayrıca fotovoltaik panellerin verimini arttırıcı malzeme materyaldeki gelişmelere nazaran; kirlenme, panel sıcaklığı gibi verim düşüren faktörler bulunmaktadır. Sınırlı verimliliklerinden dolayı fotovoltaik panellere nazaran yoğunlaştırılmış güneş enerjilerinden elektrik üretimi son yıllarda ilgi çekici hale gelmiştir. Güneş enerjisi odaklama sistemleri sırasıyla Parabolik oluk (Parabolic through), güç kulesi (Power tower), doğrusal fresnel (Lineer fresnel), Stirling Çanağı (Dish Stirling)

1 Doç.Dr., Harran Üniversitesi Organize Sanayi Bölgesi M.Y.O. Elektrik Programı, serdalarslan@harran.edu.tr, 0000-0002-1187-5633

https://doi.org/10.58830/ozgur.pub575.c2693

olarak verilebilir [1]. Ayna, fresnel lens ve odaklayıcı sistem ile güneş enerjisi yoğunlaştırılabilmektedir ancak güneş ışınlarının gün içindeki geliş açısındaki değişim önemli sorun olarak görülmesine rağmen güneş takip mekanizması ile bu sorun çözülebilir [2]. Bu sistem özelinde gerçekleştirilen çalışmalar dıştan yanmalı motordan hareket enerjisi eldesine kadar dayanmaktadır. Dıştan yanmalı motor olarak çalışan Strling motoru adını 1816 yılında Robert Stirling'ten almaktadır [3]. Isı enerjisinden elde edilen dairesel hareket kimi zaman bir aracı, gemiyi vb. tahrik etmesine rağmen içten yanmalı motorun icadı ile dıştan yanmalı motorlar üzerine çalışmalar sınırlı kalmıştır. Stirling motorun harici ısı kaynakları kullanımı, tasarımları, gerçekleştirilen çalışmalarla zaman içerisinde değişiklik göstermiştir. Ancak son yıllarda Parabolik çanak- Strling motor kullanan sistemden elektrik enerjisi üretimi dikkat çekici hale gelmiştir. Bu sistemde güneş ışınlarını yansıtılıp odak noktasında toplanmaktadır, alıcı tarafından ısı soğurulur. Stirling motorları alfa (α), beta (β) ve gama (γ) olmak üzere üç mekanik düzen sınıfında değerlendirilirler [3].

Tablo 1. Bazı Stirling Motor Çalışmaları: Basınç, sıcaklık değerlerine göre güç değerlikleri

Referanslar	Stirling Motor Tipi	Sıcaklık (°C)	Şarj Basıncı (bar)	Güç (W)
[3,4]	V tipi bir Stirling motoru	1100	2,5	65
[3,5,6]	Gama tipi bir Stirling motoru	1000	2	21,46
[3,7,6]	Çift yer değiştirme pistonuna sahip bir Stirling motoru	1000	1,5	65
[3,8,6]	Beta tipi bir Stirling motoru	1000	3,5	83,12
[3,9]	Gama tipi bir Stirling motoru	1000	4	128,3
[3,10]	Beta tipi bir Stirling motoru	1000	-	5,98
[3,11,12]	Beta tipi bir Stirling motoru	200	2,8	51,93
[3,13]	Beta tipi bir Stirling motoru	185 ±5	4,7	22,01
[3,14]	Scotch yoke hareket iletim mekanizmalı Beta tipi bir Stirling motoru	500	7	95,4
[3, 6,15]	Rhombic hareket mekanizmalı beta tipi bir Stirling motoru	450	2	95,77
[3,16]	Beta tipi bir Stirling motoru	850	8	390
[3,17]	Gama tipi bir Stirling motoru	500	10	570
[3,6,18]	Beta tipi bir Stirling motoru	600	15	288
[19,20]	Rhombic hareket mekanizmalı bir Stirling motoru	700 ±5	3	244
[21-23]	Scotch Yoke hareket mekanizmalı bir Stirling motoru	700	8	74
[6,24,25]	Krank biyel hareket iletim mekanizmalı Beta tipi bir Stirling motoru	1000	2,5	14

[24,26]	Rhombic hareket iletim mekanizmalı bir Stirling Motor	850	9	1358
[6,27]	Beta tipi rhombic hareket mekanizmalı bir Stirling motoru	-	3	221,77

Stirling motorun hareket mekanizması doğrusal veya dairesel olabilir (Şekil 1). Yer değiştirme pistonu ile güç pistonu arasındaki mekanik bağlantı çıkartılarak düzenlendiğinde serbest pistonlu Stirling motorlarına dönüştürülebilir. Bu motorlar serbestçe ileri-geri hareket edebilme kabiliyeti, daha az mekanik aşıntı, düşük maliyet, nispeten yüksek verim sunması gibi avantajları dikkat çekicidir [3].

Şekil 1a'da görüldüğü üzere Stirling motorun ısı aktarma organı üzerinden mekanik enerji üretilmektedir. Elde edilen bu dönme hareketi doğrudan jeneratörü tahrik edebilmektedir. Dairesel hareketten elektrik enerjisi üreten sistemler, dönme hareketini elektromanyetik indüksiyon yoluyla elektrik enerjisine dönüştürmektedir. Şekil 1b'de görüldüğü üzere ek mekanik bileşenlerin (krank-biyel) kaldırılarak serbest pistonlu modeli verilmiştir. Stirling motor çevrimi serbest pistonlu hareket çevrimi birbirine benzer hareket profili sergilemektedir [34]. Böylece Şekil 1c'de görüldüğü üzere serbest piston mekanizması üzerine yerleştirilecek doğrusal jeneratörden elektrik enerjisi elde edilebilir.

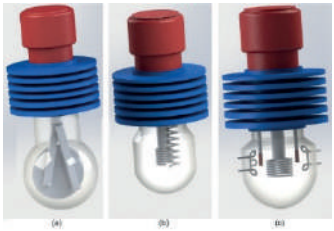

Şekil 1. (a) Krank ve biyel kol Mekanizmalı, (b) Serbest Piston Mekanizması, (c) Serbest Pistonlu Doğrusal Jeneratör [34].

2. Doğrusal Jeneratörler ve Tasarım Modeli

Doğrusal hareketli mekanizma üzerine yerleştirilen jeneratörden elektrik üretimi sağlanır. Bu jeneratörler asenkron [28] veya senkron [29] tipte olabilir. Ancak sürekli mıknatıslı modelin yüksek verim ve güç yoğunluğu sayesinde yaygın olarak tercih edilmektedir. Bu jeneratörlerin modelleri sargı yapısı, hareketli yapısı, mıknatıslı yapısı vb. çeşitlerde farklılaşmaktadır

ve farklı uygulama alanları için kullanılmaktadır [30-34]. Tüp tipi oyuksuz doğrusal jeneratör tasarımı ve uygulaması gerçekleştirmiştir [35-38]. Dört yanlı [39-41], iki yanlı oluksuz [42,43], iki yanlı oluklu [44], tek yanlı dış [45] ve sekizgen şeklindeki çok yanlı doğrusal jeneratör tasarımı gerçekleştirilmiştir [46,47]. Ayrıca iki primer bir sekonder tüp tipi [48,49], tüp tipi eksenel akılı mıknatıslı hava nüveli [50,51], yüzey yerleştirmeli oyuklu tip iç hareketli [52-54], yüzey yerleştirmeli oyuklu tip dış hareketli [55-57] çalışmaları da dikkat çekicidir. Mıknatıs dizimi açısından radyal, eksenel ve Halbach olan tüp tipi jeneratör karşılaştırmıştır [58,59]. Sürekli mıknatıslı doğrusal jeneratör çeşitlerine ait ağaç grafiği Şekil 2'de verilmiştir.

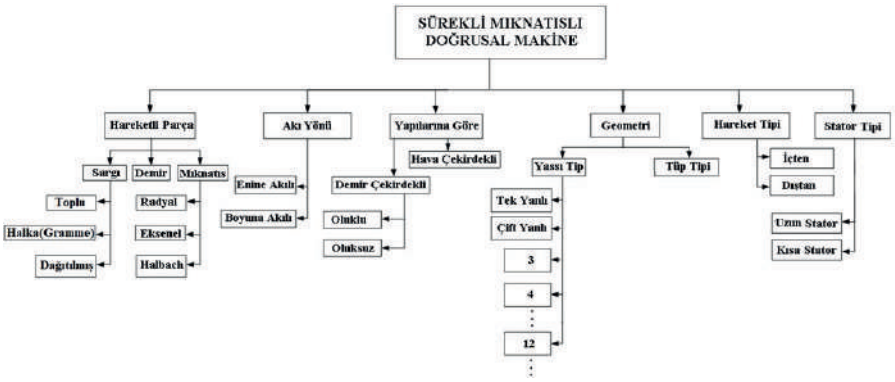

Şekil 2. Doğrusal jeneratör çeşitlerine yönelik sınıflandırma [30]

Farklı sabit mıknatıslı makineler incelendiğinde çift primerli akı anahtarlamalı, tek akı anahtarlamalı ve radyal mıknatıs dizilimli jeneratörleri karşılaştırmıştır [60]. Enine akılı tüp tipi jeneratör tasarım ve optimizasyonunu gerçekleştirmiştir [61]. Sargılar açısından süper iletkenli doğrusal jeneratör çalışması dikkat çekmektedir [62]. Ayrıca ele alınan elektrik makinesinin akı yolu dikkate de alınmalıdır. Burada ele alınan jeneratör boyuna akılıdır. Boyuna akılı makineler için hem iki boyutlu hem de üç boyutlu analiz tercih edilebilir. Enine akılı makineler için üç boyutlu analiz dikkate alınırken Eksenel akılı makineler için üç boyutlu tercih edilir ancak iki boyutta ele alınacak yöntemlerle de (quasi static, 2,5D) analiz yapılabilir.

Daha önceki çalışmamızda benzer topolojideki [30-34], 3 fazlı bu modelin tasarım, analiz ve optimizasyon çalışmaları gerçekleştirilmiştir. Çalışmadaki deney seti üzerinden üç fazlı modelin deneyleri gerçekleştirilerek nümerik analizde elde edilen veriler karşılaştırılmıştır. Elde edilen deneysel verilerin analiz verileri ile oldukça uyumlu olduğu görülmüştür. Bu çalışmada ise

13mm strok boyu için farklı oluk-kutup oranlı jeneratör incelenmiştir. Parabolik çanak veya Stirling Çanağı olarak adlandırılan sistem için daha yüksek güçlü jeneratör analizini içermektedir.

2.1. Tasarım Modeli

Ansys Maxwell; literatürde yaygın tercih edilen elektromanyetik problemlerin çözümü için kullanılan yazılımdır. Elektrik makinelerinin modellenmesinde kullanılan bu yazılım; modele ait elektriksel parametreleri (indüktans değeri, akım yoğunluğu, manyetik alan şiddeti, manyetik akı yoğunluğu vb.) elde edilebilir [34,63]. Yazılım; elektrik makinasının 3 boyutlu modelini 2 boyutlu xy veya rz düzlemlerinde modellenmesine imkân tanır. Ancak asimetrik modellerin çözülmesi için 3 boyutlu çözücü modülleri seçilmesi gerekir. Doğrusal jeneratör modeli 3 boyutlu simetrik yapıda olduğundan dolayı 2 boyutlu rz geçici hal analiz ve sürekli hal analiz çözücüleri tercih edilmiştir. Modelin anlaşılabilmesi için 3 boyutlu modelden ¼'lük kısmı çıkartılarak modelin parçaları ve iç yapısı Şekil 3'te verilmiştir.

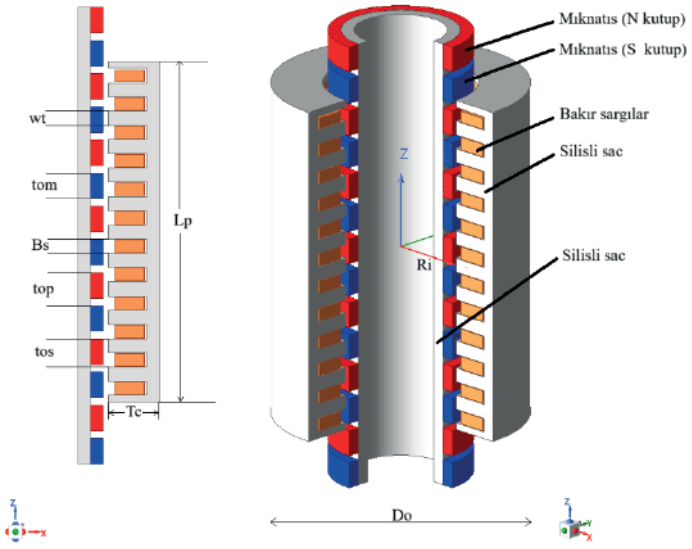

Şekil 3. Tasarlanan tüp tipi doğrusal jeneratör

Şekil 3'te verilen boyutlandırma parametrelerin büyüklükleri Tablo 2'de verilmiştir. Modelin içteki hareketli (çelik ve mıknatısları içeren) kısmının tamamına sekonder, dışta sargıların bulunduğu duran kısmına ise primer olarak adlandırılmaktadır. Primer, daha iyi performans sağlayan silisli sacın paketlenmesinden ya da üretim kolaylığı sağlayan yumuşak manyetik

malzemeden meydana gelebilir [64]. Sekonder (Hareketli kısım) ise primer çelik malzemesi kullanılabilir. Oluk-Kutup değişimine bağlı olarak özellikle vuruntu kuvveti olmak üzere; demir, bakır kaybı, verim ve güç yoğunluğu değerleri değişiklik göstermektedir [65].

Tablo 2. Tüp tipi jeneratörün boyutlandırma büyüklükleri

Tasarım Parametreleri ve birimleri	Değerler	Tasarım Parametreleri	Değerler
Do (mm)	100	Alfa (tom/top)	0,775
Di (mm)	60	Beta (Bs/Tos)	0,5
Lp (mm)	133,87	Gama (Di/Do)	0,6
Top (mm)	13	Çelik malzeme	M19_24G
Tc (mm)	20	Mıknatıs	NdFe 35
Tos (mm)	11,15	Hava aralığı (mm)	2

2.2. Sürekli Hal Analizi

2 boyutlu analiz 12th Gen Intel(R) Çekirdekli (TM) i7-12700H 2.30 GHz işlemcili ve 16GB RAM özellikli bilgisayar ile çözüm gerçekleştirilmiştir. 0,5 hata enerji hata değerine karşılık ağ sayısı 17942 olarak atandığı görülmüştür. Manyetik akı dağılımı Şekil 4'te görülmektedir.

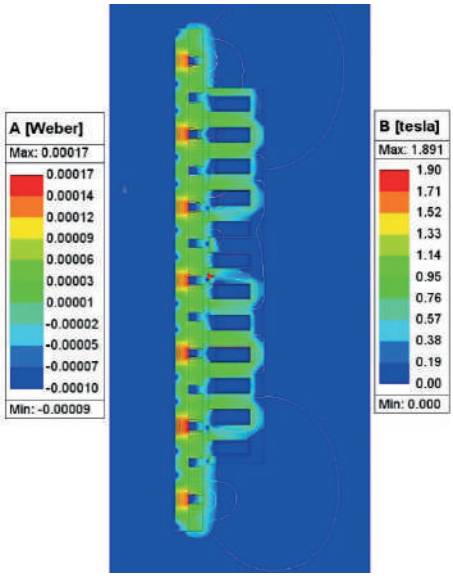

Şekil 4. Manyetik akı yoğunluğu değişimi

Hava aralığı imalat nedenlerinden dolayı 2 mm alınarak gerçekleştirilmiştir. Hava aralığının artışı toplam akı miktarını azaltacaktır. Ancak Şekil 4'te sekonder üzerindeki manyetik akı yoğunluğu da yüksektir. Özellikle mıknatıs-mıknatıs arası kaçak akılar olmasına karşın akının büyük bölümü primer üzerinden devresini tamamlamaktadır.

2.3. Geçici Hal Analizi

Geçici hal analizi modelin sürekli hal durumuna geçinceye kadar ya da anlık belirlenen zaman aralıklarında elektromanyetik problemi incelemek için kullanılabilir. Hem 2 hem de 3 boyutlu analize imkân vermektedir. Daha önce de bahsedildiği gibi Stirling motor çevrimi serbest pistonlu hareket çevrimi birbirine benzer hareket profili sergilediğinden dolayı hız değişimi sinusoidal biçimde tanımlanmıştır. Eşitlik 1'de maksimum hız değerinin Lstr (Strok boyu) ve f (Frekans) ilişkisi verilmiştir. Hız zamana bağlı değişiminden dolayı Eşitlik 2'de hız sinüs fonksiyonu olarak verilmiştir [34].

$$v_m = 2\pi L_{str} f \tag{1}$$

$$v\,(t) = v_m \sin(2\pi f t) \tag{2}$$

Vuruş boyu (strok mesafesi) sabit kalma koşuluyla frekans değeri 10 Hz'den başlayarak 50 Hz değerine kadar arttırılmıştır (Şekil 5).

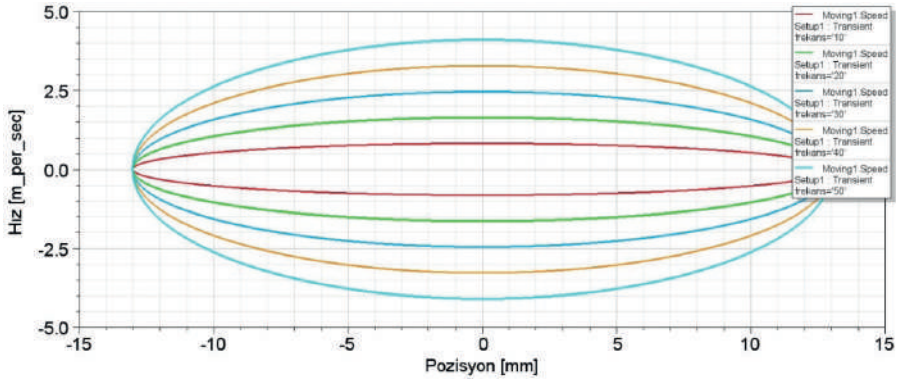

Şekil 5. Doğrusal hareketli pozisyonu-hız profili

Boş çalışma durumunda 3 faz sargılardan elde edilen gerilimin frekansa bağlı olarak değişimi Şekil 6'da verilmiştir. Burada çalışma frekansı arttıkça

gerilim doğrusal olarak artmıştır. Çünkü çalışma frekansı ile hız orantılıdır (bakınız Eşitlik 1).

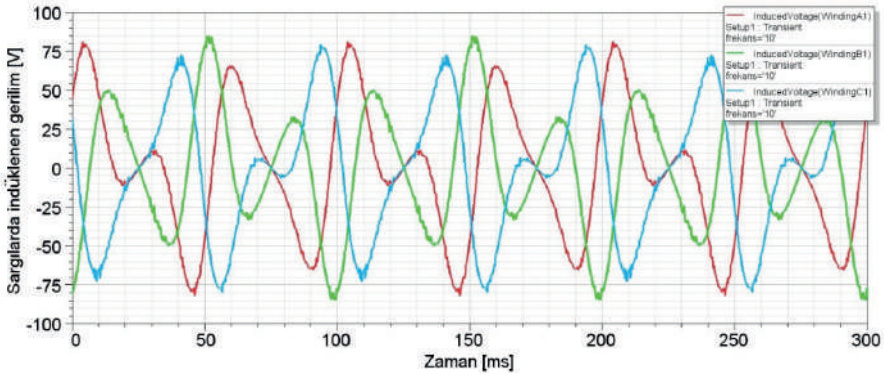

(a)

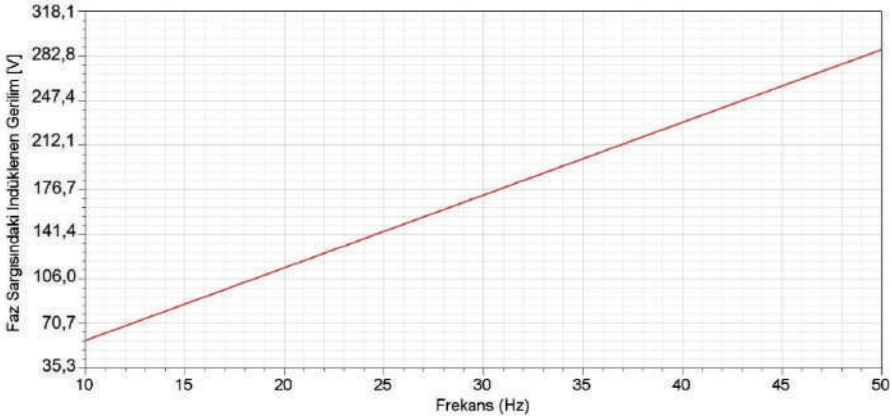

(b)

Şekil 6. 10Hz'deki sargılarda indüklenen üç faz gerilim değişimi (a), Frekans değişimine göre bir faz sargısında indüklenen gerilim değeri (b)

Demir kaybının hesaplanabilmesi için hem primer hem de sekonder çelik malzemesi M19-24G seçilmiştir.

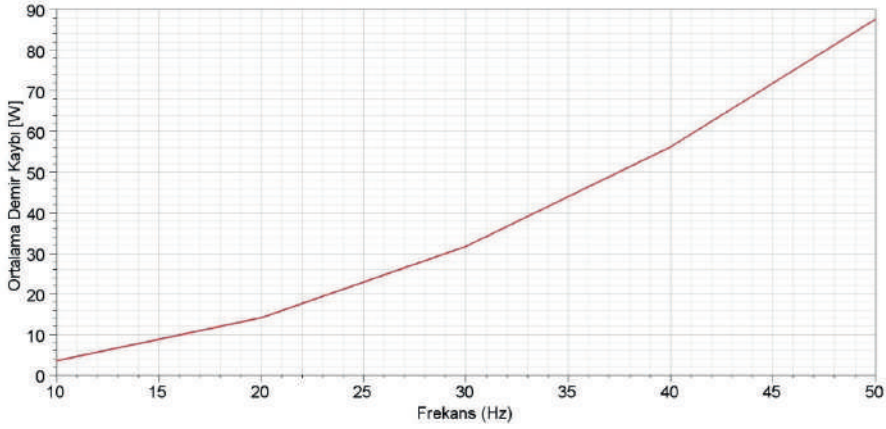

Şekil 7. Frekans değişimine göre demir kaybı değişimi

Çalışma frekansı arttıkça jeneratörün demir kaybı artmaktadır. Bu artışın doğrusal olmadığı Şekil 7'den anlaşılmaktadır. 10Hz değerindeki kayıp değeri 3,5W iken 50Hz değerindeki kayıp değeri 87,5W'tır. Şekil 8'de farklı frekans değerlikleri için çıkış gücü değişimi verilmiştir.

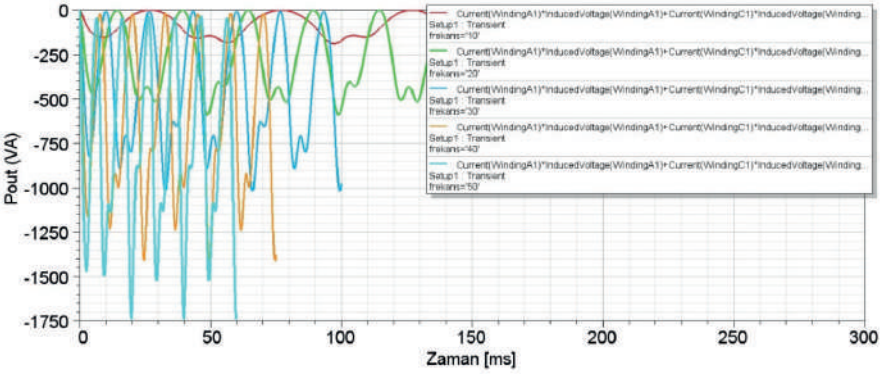

(a)

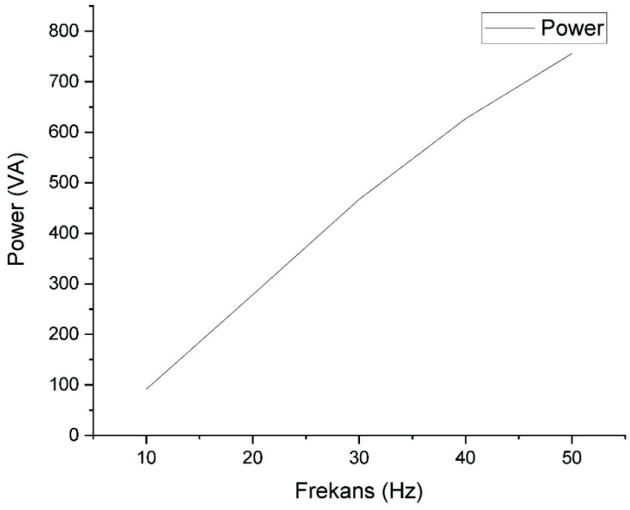

(b)

Şekil 8. Farklı frekans değerliklerine göre çıkış gücü (a), Frekans değişimine göre çıkış gücü değişimi (b)

Şekil 8'den anlaşılacağı üzere frekans arttıkça çıkış gücü artmaktadır. 10Hz'de ortalama 91,71 VA, 50Hz'de ise yaklaşık 756VA güç alınmaktadır.

2.4. Maliyet Analizi

Çelik, bakır ve mıknatıs malzemelerinin kg başına fiyatı 2.12 USD/kg, 14.85 USD/kg, 84.87 USD/kg olarak sıralanabilir [66]. Torna, CNC vb. işçilik giderleri ihmal edilerek Tablo 3'te yaklaşık maliyet hesaplanmıştır. Hesaplamalar için çelik, bakır ve mıknatıs malzemelerinin özkütleleri sırasıyla 7650 kg/m³, 8933 kg/m³, 7400 kg/m³ olarak alınmıştır.

Tablo 3. Toplam kütle ve maliyet

Toplam Mıknatıs Kütlesi (Kg)	Toplam Bakır Kütlesi (Kg)	Primer Çelik Kütlesi (Kg)	Sekonder Toplam Kütle (Kg)	Toplam Kütle (Kg)	Toplam Maliyet ($)
0,837	1,523	3,33	1,72	6,57	102,57

3. Sonuç

Ülkemizde incelenen lisansüstü çalışmalar daha çok Strling motoru tasarımı, analizi üzerine yapılmıştır. Ancak doğrusal jeneratör üzerine gerçekleştirilen çalışmalar oldukça sınırlı kalmıştır. Bu çalışmada Stirling

Çanağı'ndan elektrik enerjisi üretmeye yönelik tasarlanan jeneratörün sayısal analizi yapılmıştır. Strok mesafesinin kısa olması güç değerini sınırlandırmıştır. Ancak çıkış gücü bu uygulamalar için yeterlidir. Özellikle sabit vuruş mesafesinde çalışma frekansındaki artış gücü arttırmaktadır. Hareketlinin sabit hız değeri için gerilimin sinüzoidal değişmesi beklenir. Ancak hareketli parçanın hız profili sinüzoidal olduğundan dolayı indüklenen gerilim değişimi Şekil 6a'daki gibi olur. Hızlanma ve yavaşlama kısımlarında gerilimde artış ve azalış şeklinde görülür. Toplam hareketli kütlesini azaltmaya yönelik optimizasyon çalışmaları gerçekleştirilebilir. İlerleyen çalışmalarda vuruntu kuvveti analizi prototip imalat gerçekleştirilecektir.

4. Kaynakça

1. Azanpa, M., "Stirling Motoru Hacim Optimizasyonu ve Kontrolü", Yüksek lisans tezi, Yıldız Teknik Üniversitesi Fen Bilimleri Enstitüsü, Mekatronik Mühendisliği, 2020.
2. Alahmad, A., "Güneş Takip Sistemi ve Stirling Motor Kullanarak Elektrik Üretimi", Yüksek lisans tezi, Kilis 7 Aralık Üniversitesi Fen Bilimleri Enstitüsü, Elektrik Elektronik Mühendisliği, 2018.
3. Arslan T. A., "Rhombıc Mekanizmalı Beta Tipi Bir Stirling Motorunda Sıkıştırma Oranının Motor Performansına Etkilerinin Sayısal Olarak İncelenmesi", Yüksek lisans tezi, Gazi Üniversitesi Fen Bilimleri Enstitüsü, Otomotiv Mühendisliği, 2021
4. Karabulut, H., Yücesu, H. S. and Koca, A. (2000). Manufacturing and testing of a Vtype stirling engine Turkish Journal of Engineering and Environmental Sciences, 24(2), 71-76.
5. Demiralp, M. (2000). Gama Tipi Bir Stirling Motorunun Tasarımı ve İmalatı. Doktora Tezi, Gazi Üniversitesi Fen Bilimleri Enstitüsü, Ankara, 6-60.
6. Eroğlu H. İ., "Rhombic Hareket Mekanizmalı Stirling Motorunun Halojen Lamba ile Performans Testleri", Yüksek lisans tezi Afyon Kocatepe Üniversitesi Fen Bilimleri Enstitüsü, Makine Mühendisliği, 2018
7. Üstün, S. (2000). Çift Yer Değiştirme Pistonlu V Tipi Küçük Güçlü Bir Stirling Motorunun Tasarım ve İmali. Doktora Tezi, Gazi Üniversitesi Fen Bilimleri Enstitüsü, Ankara, 1-37.
8. Özgören, Y.Ö. (2005). Stirling Motorunda Termal Bariyer Kaplamanın Motor Performansına Etkilerinin Deneysel Olarak İncelenmesi. Selçuk Üniversitesi Teknik Bilimler Meslek Yüksekokulu Teknik-Online Dergisi, 4: 122-133.
9. Çınar, C. and Karabulut, H. (2005). Manufacturing and testing of a gamma type Stirling engine. Renewable Energy, 30(1), 57-66.
10. Çınar, C., Yücesu, S., Topgül, T. and Okur, M. (2005). Beta-type Stirling engine operating at atmospheric pressure. Applied Energy, 81, 351-357.
11. Karabulut, H., Yücesu, H. S., Çınar, C. and Aksoy, F. (2009). An experimental study on the development of a b-type Stirling engine for low and moderate temperature heat sources. Applied Energy, 86, 68–73.
12. Önder, M. (2012). Stirling Motoru İçin Borulu Tip Isı Değiştiricisi Tasarımı ve CFD Analizi (Doctoral dissertation, Doktora Tezi, Gazi Üniversitesitesi Fen Bilimleri Enstitüsü, Ankara).
13. Karabulut, H. ve Aksoy, F. (2011). Güneş Enerjisi ile Çalışan Bir Stirling Motorunun Performans Testleri. Makine Teknolojileri Elektronik Dergisi, 8, 55-62.

14. Sripakagorn, A. and Srikam, C. (2011). Design and Performance of a Moderate Temperature Difference Stirling Engine. Renewable Energy, 36, 1728-1733
15. Çınar, C., Aksoy, F. ve Okur, M. (2013). Design, manufacturing and performance tests of a stirling engine with rhombic drive mechanism. Journal of the Faculty of Engineering and Architecture of Gazi University, 28, 795-801.
16. Cheng, C. H., Yang, H. S. and Keong, L. (2013). Theoretical and experimental study of a 300-W beta-type Stirling engine. Energy, 59, 590-599.
17. Hachem, H., Gheith, R., Aloui, F. and Nasrallah, S. B. (2015). Numerical characterization of a γ-Stirling engine considering losses and interaction between functioning parameters. Energy Conversion and Management, 96, 532-543.
18. Duan, C., Sun, C., Shu, S., Ding, G., Jing, C. and Chang, J. (2015). Similarity design and experimental investigation of a beta-type Stirling engine with a rhombic drive mechanism. International Journal of Energy Research, 39, 191–201.
19. Zencirkıran, M. (2021). Stırlıng motorlarında ısı transfer yüzey alanının artırılmasının motor performasına etkisi (Master's thesis, Fen Bilimleri Enstitüsü).
20. Akyel E, "Rhombic Hareket Mekanizmalı Bir Stirling Motorunun Tasarımı ve Performans Analizi", Yüksek Lisans Tezi, Afyon Kocatepe Üniversitesi, Fen Bilimleri Enstitüsü, 90s, Afyonkarahisar, 2015.
21. Eroğlu, S. B. (2020). Beta tipi stirling motorları için hareket mekanizması optimizasyonu (Master's thesis, Pamukkale Üniversitesi Fen Bilimleri Enstitüsü).
22. Hirata, K., Iwamoto, S., Toda, F. and Hamaguchi K., "Performance Evaluation for a 100W Stirling Engine" Proceeding of 8th International Stirling Engine, Conference, 19-28, (1997).
23. Hirata, K., (1999). Development of a small 50W class Stirling engine. Sixth International Symposium on Marine Engineering, p. 235-240.
24. Erol, Derviş. (2020). Beta tipi bir Stirling motorunun tasarımı imalatı ve performans analizleri. (Yayınlanmamış Doktora Tezi). Hitit Üniversitesi, Fen Bilimleri Enstitüsü, Makine Mühendisliği Anabilim Dalı
25. Çınar, C., Topgül, T., Yücesu, H. S., (2007). Stirling çevrimi ile çalışan beta tipi bir motorun imali ve performans testleri. Gazi Üniversitesi, Mühendislik Mimarlık Fakültesi Dergisi, 22(2), p. 411-415.
26. Yang, H. S., Cheng, C. H., Huang, S. T. (2018). A complete model for dynamic simulation of a 1-kW class beta-type Stirling engine with rhombicdrive mechanism. Energy, 161, p. 892-906.

27. Karabulut, H., Çınar, C., Aksoy, F., Solmaz, H., Özgören Y.Ö., Arslan, M., Aysal, F.E. (2015). Beta Tipi Rhombic Hareket Mekanizmalı Bir Stirling Motorunun İmalatı ve Testleri. International Symposium on Innovative Technologies in Engineering and Science (ISITES), 2129-2136.

28. Dang, T. T., Ruellan, M., Ahmed, H. B., Prevond, L., & Multon, B. (2014, June). Sizing optimization of tubular linear induction generator for a new stirling micro-cogenerator system. In Power Electronics, Electrical Drives, Automation and Motion (SPEEDAM), 2014 International Symposium on (pp. 1362-1367). IEEE.

29. Sui, Y., Liu, Y., Cheng, L., Liu, J., & Zheng, P. (2017). A tubular hybrid Halbach/axially-magnetized permanent-magnet linear machine. AIP Advances, 7(5), 056629.

30. Arslan, S., Gurdal, O. (2022). Polygonal tubular linear permanent magnet generator analysis and experimental test. Scientia Iranica, 29(1), 168-182. doi: 10.24200/sci.2019.50094.2739

31. Arslan, S., & Oy, S. A. (2017). Design and Optimization of Tube Type Interior Permanent Magnets Generator for Free Piston Applications.

32. Arslan, S., & Mellah, H. (2023). Analysis and testing of internal combustion engine driven linear alternator. Electrical Engineering & Electromechanics, (1), 3–9. doi:10.20998/2074-272X.2023.1.01

33. Arslan, S., Gurdal, O., Akkaya Oy, S. (2020). Design and optimization of tubular linear permanent-magnet generator with performance improvement using response surface methodology and multi-objective genetic algorithm. Scientia Iranica, 27(6), 3053-3065. doi: 10.24200/sci.2018.50093.1506

34. Arslan, S., Akkaya Oy, S.: Linear generator design for concentrating solar power technologies: Optimization and prototype development. IET Renew. Power Gener. 1–12 (2023). https://doi.org/10.1049/rpg2.12881

35. Rhinefrank, K., Agamloh, E. B., von Jouanne, A., Wallace, A. K., Prudell, J., Kimble, K., ... & Schacher, A. (2006). Novel ocean energy permanent magnet linear generator buoy. Renewable Energy, 31(9), 1279-1298.

36. Ribeiro, J., & Martins, I., Development of a low speed linear generator for use in a wave energy converter. In Proceedings of the International Conference on Renewable Energies and Power Quality, Granada (Spain), 23th to 25th March, 2010.pp. 252-257.

37. Parel, Thomas, Rotaru, Mihai, Sykulski, Jan and Hearn, Grant, Design study of a tubular linear machine with permanent magnets for wave power generation. Electromagnetic Phenomena in Nonlinear Circuits EPNC2010, Dortmund and Essen, Germany. 29 Jun - 02 Jul 2010. pp. 143-144.

38. Bracco, G., Giorcelli, E., Mattiazzo, G., Marignetti, F., Carbone, S., & Attaianese, C. (2011, September). Design and experiments of linear tubular generators for the Inertial Sea Wave Energy Converter. In Energy Conversion Congress and Exposition (ECCE), 2011 IEEE (pp. 3864-3871). IEEE.

39. Kimoulakis, N. M., Kladas, A. G., & Tegopoulos, J. A. (2009). Cogging force minimization in a coupled permanent magnet linear generator for sea wave energy extraction applications. IEEE Transactions on Magnetics, 45(3), 1246-1249.

40. Parthasarathy, R. (2012). Linear PM Generator for wave energy conversion (Doctoral dissertation, Faculty of the Louisiana State University and Agricultural and Mechanical College in partial fulfillment of the requirements for the degree of Master of Science in Electrical Engineering in The Department of Electrical and Computer Engineering by Rajkumar Parthasarathy Bachelor of Engineering, Anna University).

41. Bai, B., Lu, J., & Xu, B. (2011, August). The research of external buoy wave permanent magnet linear generator's design. In Electrical Machines and Systems (ICEMS), 2011 International Conference on (pp. 1-5). IEEE

42. Mueller, M., McDonald, A., Ochije, K., & Jeffrey, J. (2007, September). A novel lightweight permanent magnet generator for direct drive power take off in marine renewable energy converters. In Proceedings of the 7th European Wave and Tidal Energy Conference.

43. Nilsson, K., Danielsson, O., & Leijon, M. (2006). Electromagnetic forces in the air gap of a permanent magnet linear generator at no load. Journal of Applied Physics, 99(3), 034505.

44. Crozier, R., & Mueller, M. (2012). Integrated structural and electromagnetic design of direct-drive linear machines for wave energy. IET Renewable Power Generation, 6(3), 137-148.

45. Gargov, N., & Zobaa, A. F. (2011, September). Multiphase tubular permanent magnet linear generator for wave energy converters. In Renewable Power Generation (RPG 2011), IET Conference On (pp. 1-5). IET.

46. Ivanova, I. A., Agren, O., Bernhoff, H., & Leijon, M. (2005). Simulation of wave-energy converter with octagonal linear generator. IEEE Journal of Oceanic Engineering, 30(3), 619-629.

47. Ivanova, I. A., Agren, O., Bernhoff, H., & Leijon, M. (2004, April). Simulation of cogging in a 100 kW permanent magnet octagonal linear generator for ocean wave conversion. In Underwater Technology, 2004. UT'04. 2004 International Symposium on (pp. 345-348). IEEE.

48. Schmulian, R. (2013). Reduction of cogging forces in a double sided tubular linear permanent magnet generator used for ocean wave energy conversion (Doctoral dissertation).

49. Joseph, D. M. (2010). A double-sided tubular linear synchronous generator for wave-energy conversion (Doctoral dissertation, Faculty of Engineering and the Built Environment, University of the Witwatersrand, Johannesburg).

50. Baker, N. J., Mueller, M. A., Ran, L., Tavner, P. J., & McDonald, S. (2007). Development of a linear test rig for electrical power take off from waves. Journal of Marine Engineering & Technology, 6(2), 3-15.

51. Vermaak, R. (2013). Development of a novel air-cored permanent magnet linear generator for direct drive ocean wave energy converters (Doctoral dissertation, Stellenbosch: Stellenbosch University).

52. Szabo, L., Oprea, C., Viorel, I. A., & Biró, K. Á. (2007, May). Novel permanent magnet tubular linear generator for wave energy converters. In Electric Machines & Drives Conference, 2007. IEMDC'07. IEEE International (Vol. 2, pp. 983-987). IEEE.

53. Danielsson, O., Eriksson, M., & Leijon, M. (2006). Study of a longitudinal flux permanent magnet linear generator for wave energy converters. International Journal of Energy Research, 30(14), 1130-1145.

54. Li, W., Chau, K. T., & Jiang, J. Z. (2011). Application of linear magnetic gears for pseudo-direct-drive oceanic wave energy harvesting. IEEE Transactions on Magnetics, 47(10), 2624-2627.

55. Prudell, J., Stoddard, M., Amon, E., Brekken, T. K., & von Jouanne, A. (2010). A permanent-magnet tubular linear generator for ocean wave energy conversion. IEEE Transactions on Industry Applications, 46(6), 2392-2400.

56. Prudell, J., Stoddard, M., Brekken, T. K., & von Jouanne, A. (2009, September). A novel permanent magnet tubular linear generator for ocean wave energy. In Energy Conversion Congress and Exposition, 2009. ECCE 2009. IEEE (pp. 3641-3646). IEEE.

57. Si, J., Feng, H., Su, P., & Zhang, L. (2014). Design and analysis of tubular permanent magnet linear wave generator. The Scientific World Journal, 2014.

58. Sui, Y., Zheng, P., Cheng, L., Wang, W., & Liu, J. (2017). A single-phase axially-magnetized permanent-magnet oscillating machine for miniature aerospace power sources. AIP Advances, 7(5), 056659.

59. Zheng, P., Sui, Y., Tong, C., Bai, J., Yu, B., & Lin, F. (2014). A novel single-phase flux-switching permanent magnet linear generator used for free-piston Stirling engine. Journal of Applied Physics, 115(17), 17E711.

60. Sui, Y., Zheng, P., Tong, C., Yu, B., Zhu, S., & Zhu, J. (2015). Investigation of a tubular dual-stator flux-switching permanent-magnet linear generator for free-piston energy converter. Journal of Applied Physics, 117(17), 17B519.

61. Joubert, L. H., Schutte, J., Strauss, J. M., & Dobson, R. T. (2012, September). Design optimisation of a transverse flux, short stroke, linear generator. In Electrical Machines (ICEM), 2012 XXth International Conference on (pp. 640-646). IEEE.

62. Wu, Z. H., & Jin, J. X. (2014). Novel concept of dish Stirling solar power generation designed with a HTS linear generator. IEEE Transactions on Applied Superconductivity, 24(5), 1-5.

63. Fenercioğlu, A., and Tarimer, I., Solution Processes of a Magnetic System's Magnetostatic Analysis wıth Maxwell 3D Field Simulator. Selçuk Teknik Dergisi, 2007. 6(3): p. 221-240.

64. Wang, J., and Howe, D. (2005). Influence of soft magnetic materials on the design and performance of tubular permanent magnet machines. IEEE Transactions on Magnetics, 41(10), 4057-4059.

65. Chen, A., Arshad, W. M., Thelin, P., and Zheng, P. (2004). Analysis and optimization of a longitudinal flux linear actuator for hybrid electric vehicle applications. IEEE Symp. Vehicle Power and Propulsion

66. G. Du, et al., "Comprehensive Comparative Study on Permanent-Magnet-Assisted Synchronous Reluctance Motors and Other Types of Motor" Applied Sciences, vol.13, 14, 2023.

Interdisciplinary Studies on Contemporary Research Practices in Engineering- VII

Editor:
Assist. Prof. Dr. Murat Metehan TÜRKOĞLU

ÖZGÜR PRESS

ISBN 978-625-95522-9-3